Dissertations   **Theses and Dissertations**

Fall 1997

Analysis of safe separation distances from natural gas transmission pipelines

James Stephen Haklar
New Jersey Institute of Technology

ABSTRACT

ANALYSIS OF SAFE SEPARATION DISTANCES
FROM
NATURAL GAS TRANSMISSION PIPELINES

by
James Stephen Haklar

Accidental rupture of natural gas transmission pipelines with subsequent ignition of the escaping gas can result in the loss of life and property. In the United States, current means of protecting both the pipeline and the public include the establishment of class locations, in which specific pipeline design, construction and operation requirements must be attained. In addition, distances at which the pipelines can be safely set back from the community, called safe separation distances, have been developed in some European countries (e.g., Great Britain, the Netherlands) through use of risk assessment principles. However, to date there has been no simple, consistent method for determining these distances.

A method for evaluating safe separation distances is proposed herein, in which the point source method for determining heat flux is coupled with relationships for predicting both the mass release rate from the rupture and the flame height of the ignited gas. The method is utilized to develop charts for predicting safe separation distances based on pipeline operating pressure and nominal pipeline diameter. The method is compared to information from both actual pipeline accidents reported upon by the National Transportation Safety Board and from the work of prior researchers utilizing other methodologies. The comparisons reveal that the method proposed in this thesis can produce results that are consistent with the above sets of data tested.

Blank Page

ANALYSIS OF SAFE SEPARATION DISTANCES
FROM
NATURAL GAS TRANSMISSION PIPELINES

by
James Stephen Haklar

A Dissertation
Submitted to the Faculty of
New Jersey Institute of Technology
in Partial Fulfillment of the Requirements for the Degree of
Doctor of Philosophy

Department of Civil and Environmental Engineering

October 1997

APPROVAL PAGE

ANALYSIS OF SAFE SEPARATION DISTANCES
FROM
NATURAL GAS TRANSMISSION PIPELINES

James Stephen Haklar

Dr. Robert Dresnack, Dissertation Advisor   Date
Professor of Civil and Environmental Engineering, NJIT, Newark, N.J.

Dr. Paul C. Chan, Professor of Civil and Environmental   Date
Engineering, NJIT, Newark, N.J.

Dr. Su Ling Cheng, Professor of Civil and Environmental   Date
Engineering, NJIT, Newark, N.J.

Dr. Eugene B. Golub, Professor of Civil and Environmental   Date
Engineering, NJIT, Newark, N.J.

Dr. Robert P. Kirchner, Professor of Mechanical   Date
Engineering, NJIT, Newark, N.J.

BIOGRAPHICAL SKETCH

Author: James Stephen Haklar

Degree: Doctor of Philosophy

Date: October 1997

Date of Birth:

Place of Birth:

Undergraduate and Graduate Education:

- Doctor of Philosophy in Civil Engineering,
  New Jersey Institute of Technology, Newark, NJ, 1997

- Master of Science in Environmental Engineering,
  New Jersey Institute of Technology, Newark, NJ, 1989

- Bachelor of Science in Chemical Engineering,
  New Jersey Institute of Technology, Newark, NJ, 1984

Major: Civil Engineering

Professional Experience:

- United States Environmental Protection Agency,
  290 Broadway, New York, NY, 1985 - Present

Title: Environmental Engineer

To my wife, my parents, and my sister

ACKNOWLEDGMENT

TABLE OF CONTENTS

TABLE OF CONTENTS
(Continued)

Chapter   Page

TABLE OF CONTENTS
(Continued)

Chapter   Page

TABLE OF CONTENTS
(Continued)

LIST OF TABLES

LIST OF TABLES
(Continued)

LIST OF FIGURES

LIST OF FIGURES
(Continued)

LIST OF ABBREVIATIONS AND SYMBOLS

Abbreviations

A	cross-sectional area of pipeline
A_2	area of minimum cross-section of a puncture or nozzle
a	ambient air condition
ALOHA	Aeral Locations of Hazardous Atmospheres
API	American Petroleum Institute
atm	atmosphere
BLEVE	Boiling Liquid Expanding Vapor Explosion
BR	burn radius
Btu	British thermal unit
$\bar{C}_L$	lean limit concentration
c	critical conditions
CCPS	Center for Chemical Process Safety
CFR	Code of Federal Regulations
cm	centimeter
C_p	heat capacity at constant pressure
C_T	mol fraction of nozzle fluid in unreacted stoichiometric mixture
C.W.	crosswind
C_v	heat capacity at constant volume
D_s	burner source diameter
D	diameter, distance from flame center to observer
d	pipeline diameter
d_j	jet diameter, diameter of flare stack
D.W.	downwind
E	longitudinal joint factor, surface emissive power of a flame
E_{bb}	equivalent blackbody emissive power
EGIG	European Gas Pipeline Incident Data Group
F	design factor, geometric view factor, fraction of total heat radiated
f	friction factor
^oF	degrees Fahrenheit
FLACS	Flame Acceleration Simulator
ft	foot
H	flame height
h	hour, height of flare stack
hr	hour
HACS	Hazard Assessment Computer System
HSE	Health and Safety Executive
I	thermal radiation intensity

LIST OF ABBREVIATIONS AND SYMBOLS
(Continued)

Abbreviations

j	discharge condition
K	degrees Kelvin, radiant heat flux, constant
k	gas specific heat ratio, extinction coefficient
kPa	kilopascal
kW	kilowatt
L	length
L_B	distance from burner exit to flame tip
L_{BV}	vertical length of flame tip from the plane of the burner
l	distance between upstream and downstream locations
lb	pound
M	Mach number, mass
M_1	upstream Mach number
M_2	downstream Mach number
M_a	molecular weight of air
M_f	molecular weight of fuel
M_N	molecular weight of nozzle fluid
M_S	molecular weight of surrounding fluid
m^*	mass flow rate
m^*_e	mass release rate of gas at time = t
m^*_{oe}	initial mass release rate
m	meter
Mcf	thousand cubic feet
MIACC	Major Industrial Co-ordinating Council of Canada
mm	millimeter
NFPA	National Fire Protection Association
NGL	natural gas liquids
NJIT	New Jersey Institute of Technology
NPS	nominal pipe size
NTSB	National Transportation Safety Board
P	design pressure, incident operating pressure
P'	gauge operating pressure
P_1	absolute pressure near the opening
p_1	absolute vessel pressure, upstream pressure, operating pressure at rupture
p_2	absolute pressure in the minimum cross-section, downstream pressure
PAR	pipeline accident report
psi	pounds per square inch
psia	pounds per square inch absolute

LIST OF ABBREVIATIONS AND SYMBOLS
(Continued)

Abbreviations

psig	pounds per square inch gauge
Q	total heat content of flared gas, volumetric gas flow rate
q	radiant heat flux, thermal radiation at receptor
q"	incident radiant flux
q_2	average heat flux
r	relative humidity
R	gas constant, velocity ratio equal to crosswind speed (U)/ jet velocity (U_j)
^{o}R	degrees Rankine
ROW	right-of-way
RPA	Response Planning Area
S	yield strength, curvilinear coordinate
$\bar{S}_0$	curvilinear distance
s, sec.	second
scf	standard cubic foot
SFPE	Society of Fire Protection Engineers
SAFEMODE	Safety Assessment for Effective Management of Dangerous Events
T	temperature derating factor, temperature
T_1	gas temperature
T_0	seawater temperature
T_F	adiabatic flame temperature
T_N	temperature of nozzle fluid
t	wall thickness, time, end of flame axis
t_c	duration of exposure
TSB	Transportation Safety Board (of Canada)
u	gas velocity, velocity
u_j	velocity of gas jet
u_w	velocity of wind
U.W.	upwind
V"	volumetric gas flow rate
V_{AVG}	average gas flow rate
V_{CALC}	maximum gas flow rate
W_0	total mass of gas in pipeline
W_1	flame base width
W_2	flame tip width
WHAZAN	World Bank Hazard Analysis
X	x-coordinate of flame tip

LIST OF ABBREVIATIONS AND SYMBOLS
(Continued)

Abbreviations

$\bar{x}$ x-coordinate of receptor

$\bar{X}_o$ dimensionless coordinate

yr   year
Z   z-coordinate of flame tip
z   cross-stream distance

$\bar{z}$ z-coordinate of receptor

$\bar{Z}_o$ dimensionless rise

Symbols

α $W_o/[\beta m^*_{oe}]$, angle subtended by flame with respect to vertical
α_B angle subtended by burner tip and tip of flame with respect to vertical
α_T mols reactants/mols products for the stoichiometric mixture
β final release time constant
d differential (i.e., derivative) operator
∂ partial differential (i.e., partial derivative) operator
θ angle between normal to surface receiving thermal radiation and line of sight from flame center
ρ gas density
ρ_1 density of gas inside vessel
ρ_a density of air
ρ_j density of jet
τ atmospheric transmissivity

LIST OF CONVERSIONS

Area

1 Acre = 43,560 ft^2

Heat Transfer

1 Btu/h ft^2 = 3.1546 W/m^2
1 Btu/h = 0.29307 W
1 calorie/h = 1.1622 x 10^{-3} W

Length

1 in. = 2.540 cm
100 cm = 1 m
1 m = 3.2808 ft = 39.37 in.
5,280 ft = 1 mile

Pressure

1 atm = 14.696 psia = 1.01325 bar
1 bar = 1 x 10^5 Pa
gauge pressure = absolute pressure - 1 atm

Temperature

T (Celsius) = K - 273.15
1.8 $^{\circ}$F = K = 1°C

Note: All conversions with the exception of the conversion for Area are from
Geankoplis, C.J., *Transport Processes and Unit Operations.* Boston, MA: Allyn
and Bacon, Inc. (1983). The conversion for Area is from *Webster's Ninth New
Collegiate Dictionary.* Springfield, MA: Merriam Webster, Inc. (1991).

CHAPTER 1

INTRODUCTION

Natural gas is most commonly transported between collection and distribution points

through a series of interstate pipelines called transmission pipelines. According to the

Transportation Research Board of the National Research Council, there are approximately

271,000 miles of natural gas transmission lines in the United States. The lines are

typically constructed of steel, operate between 400 and 1,500 pounds per square inch

(psi) of pressure and are buried under 2.5 feet to 3 feet or more of cover (1).

Increased development of formerly sparsely populated areas has resulted in

instances of encroachment of transmission pipeline rights-of-way (ROWs). Accidental

ruptures of these pipelines with subsequent ignition of the escaping gas can result in the

loss of life and property near these lines.

A description of the effects of such accidents can be found in the pipeline accident

reports prepared by the National Transportation Safety Board (NTSB). The NTSB is an

independent Federal agency that investigates pipeline accidents occurring in the United

States. It is worth noting that the Canadian government has established a similar agency,

called the Transportation Safety Board of Canada (TSB). The TSB's functions are

similar to those of the NTSB, in that the NTSB also investigates transportation accidents.

One example of the destructive effects of pipeline ruptures was the rupture and

resultant fire occurring at Beaumont Kentucky, on April 27, 1985 involving a 30-inch

diameter natural gas line operating at 992 pounds per square inch gauge (psig). This

accident killed 5 persons, injured 3 and, excluding the pipeline, resulted in one million

1

dollars worth of damage (2). More recently, a 36-inch pipeline operating at a pressure of 970 psig exploded in Edison, New Jersey. This accident occurred on March 23, 1994 and severely affected a nearby apartment complex. The apartment complex sustained $12.4 million in damages, which includes the loss of eight apartment buildings, severe damage to six buildings and minor damage to several other buildings (3). These two examples serve to illustrate the importance of determining the proximity at which pipelines can be safely sited near a community. These distances are called "safe separation distances."

In the United States, pipelines are regulated by the U.S. Department of Transportation pursuant to the statutory authority of the Natural Gas Pipeline Safety Act of 1968. The implementing regulations can be found in Parts 191 and 192 of the Code of Federal Regulations (CFR). The regulations establish a series of four class locations, within which specific design, construction and operational requirements must be met. Class locations extend 220 yards on either side of the centerline of any 1 mile length of pipeline, and are differentiated as follows (4):

Class 1 Location: Has 10 or less buildings intended for human occupancy.

Class 2 Location: Has more than 10 but less than 46 buildings intended for human occupancy.

Class 3 Location: Has 46 or more buildings intended for human occupancy; or an area where the pipeline lies within 100 yards of either a building or a small, well defined outside area (such as a playground, recreation area, outdoor theater, or other place of public assembly) that is occupied by 20 or more persons on at least 5 days a week for 10 weeks in any 12 month period.

Class 4 Location: Where buildings with four or more stories above ground are prevalent.

It should be noted that each separate living unit in a multiple unit building is counted as a separate building intended for human occupancy.

As indicated above, each class location has specific requirements that pertain to the design, construction and operation of a pipeline. For example, the regulations specify that the design pressure for steel pipe be determined in accordance with the following equation:

$$P=(2St/D)xFxExT$$

In the above equation, P represents the design pressure (psig); S is the yield strength (psi); D is the outside diameter (inches); t is the wall thickness (inches); and F, E and T are, respectively, the design factor, longitudinal joint factor and temperature derating factor (all dimensionless). As indicated in the regulations (5), the pressure design factors for steel pipe can vary from 0.72 to 0.40 as the Class Location varies from 1 to 4. The United States regulations, however, do not specify required separation distances between a natural gas pipeline and buildings in proximity to the pipeline.

Other countries have likewise established regulations for natural gas pipelines (5). Canada has developed a four class location system which is almost identical to the system used in the United States. The German regulations establish separation distances which are dependent on the diameter of the pipe. However, the regulations indicate that the right of way "is to protect the pipeline" (as opposed to protecting the community). Australia's regulations provide for six class locations, but (as with the United States and Canadian regulations) do not specify minimum separation distances between pipelines

and neighboring structures. While the Japanese regulations specify minimum separation distance requirements from select receptors (such as schools, theaters, train stations, etc.), these requirements apply to above-ground pipelines only.

The United Kingdom has developed 3 classifications, with the separation distances to existing occupied structures being a function of the specific classification, the operating pressure and the outside diameter of the pipe. However, the minimum separation distance requirements decrease with increased population density (which allows for siting of pipelines in heavily populated areas).

Since 1972, the Health and Safety Executive (HSE) of Great Britain has been providing advice to planning authorities concerning the potential risks and effects of hazards to neighboring populations. However, HSE guidance for construction near pipelines is still under development (6).

As described in information provided by Hans van Poelje of N.V. Nederlandse Gasunie (personal communication, November 30, 1995), the Dutch have established four area classes, and have identified two separation distances - effect and building distances. The Dutch zoning guidelines recommend building outside of the effect distance if possible, and it is the area inside the effect distance that is actually classified from 1 (low population density) to 4 (high density). The effect and building distances depend on the diameter and pressure of the pipe, and are based on calculated contours of individual risk

(which vary from 10^{-8} to 10^{-6}). Individual risk is defined by the Dutch (H. van Poelje: personal communication, September 30, 1996) as being the probability per year of the death of a person who stands 24 hours a day undressed at a certain distance from the pipeline.

In general, both the United States and foreign countries address the establishment of separation distances either directly, or indirectly through the designation of various location or population classes. In those instances where a defined allowable ROW has been established, the width of the ROW from the pipe centerline is relatively small (less than 100 feet) and is generally intended to protect the pipe rather than the public. Separation distances have also been developed by some countries based on the concept of risk assessment. This dissertation describes the development of a methodology to estimate actual separation distances required, based upon the effects of a rupture of a natural gas transmission pipeline of a specified diameter and operating pressure. The methodology is developed, in part, with data collected from prior investigations of actual natural gas transmission pipeline accidents.

The dissertation is presented in seven chapters. Chapter 1 is an introduction. Chapter 2 discusses the literature review that has been performed; Chapter 3 provides the objective of the dissertation. Chapter 4 develops a new methodology by which safe separation distances can be determined. This technique is then compared, in Chapter 5, to actual pipeline accident data, and to the work of previous researchers. The results of the dissertation are presented and discussed in Chapter 6, while Chapter 7 provides conclusions and recommendations for future work.

CHAPTER 2

LITERATURE REVIEW

The purpose of the literature review was to gain an understanding of prior research concerning both natural gas pipeline accidents and the determination of safe separation distances from natural gas transmission pipelines. The literature review consisted of the following activities:

-   Review of NTSB files in Washington, DC;

-   Review of Commodity Pipeline Occurrence Reports, prepared by the Canadian TSB;

-   Review of databases compiled by the New Jersey Institute of Technology's (NJIT's) Institute for Transportation containing relevant citations of pipeline accidents and safe separation distances;

-   Correspondence with the European Gas Pipeline Incident Data Group located in the Netherlands;

-   Review of various texts pertaining to pipelines, hazard assessment, heat transfer and fluid flow;

-   Review of technical journals of the oil and gas pipeline industry; and

-   Discussions with the NTSB, the Canadian TSB, the Canadian National Energy Board, the United States Environmental Protection Agency, the American Gas Association, the Research and Special Programs Administration, the Gas Research Institute, and the Township of Edison regarding pipeline accidents and safe separation distances.

In general, the literature review revealed that there has been limited studies to date concerning the determination of safe separation distances. Before discussing the prior research, however, the properties of natural gas and the principles of fluid flow are discussed below.

2.1 Natural Gas and its Properties

Natural gas is composed primarily of methane. A typical commercial field gas has the following molar composition (7):

Table 2.1
Composition of Natural Gas

Component	Mole Percent
Oxygen	0.0008
Nitrogen	1.498
Carbon Dioxide	1.073
Methane	83.266
Ethane	9.608
Propane	3.597
Isobutane	0.3414
Normal Butane	0.4581
Isopentane	0.0403
Normal Pentane	0.0342
Hexane	0.0046
Heptane	0.0003
Octane	0.0001
Toluene	0.0002

Natural gas generally has a gross heat content of 1,000 Btu/ft^3 measured dry at 60° F and 30 inches (or one atmosphere) of mercury (8). Since 60° F and 1 atmosphere are considered to be respectively the standard conditions for temperature and pressure in the gas industry (NTSB: personal communication, February 23, 1996), the heat content can be expressed as 1,000 Btu per standard cubic foot (scf).

Since methane is the primary constituent of natural gas, the gas mixture will exhibit physical properties similar to the properties for pure methane. At 1 atmosphere, methane has a freezing point in air of -296.46° F and a boiling point of -258.68° F (8). Therefore, at standard conditions, methane exists as a gas. Thermodynamically, the ratio of heat capacity at constant pressure (Cp) to heat capacity at constant volume (Cv) for methane varies from 1.39 at -150° F to 1.25 at 150° F (8).

Methane is a combustible gas, and has a lower flammability limit of approximately 5% by volume (8). The upper flammability limit is approximately 15% by volume (8). This implies that mixtures of methane and air will burn if the mixture contains between 5% and 15% (by volume) of methane. Outside of this range, the mixture is either too lean or too rich to burn.

Natural gas containing hydrogen sulfide is called sour gas. An example of a sour

gas mixture (9) is presented in Table 2.2:

Table 2.2
Composition of Sour Gas

Component	Mole Percent
Nitrogen	2.3046
Carbon Dioxide	1.1616
Hydrogen Sulfide	9.0791
Methane	58.7939
Ethane	12.7407
Propane	10.3420
Isobutane	1.1425
Normal Butane	3.0209
Isopentane	0.6091
Normal Pentane	0.5910
Hexane	0.1217
Other Components	0.0929

Gases (including natural gas) are considered compressible fluids. Therefore, the

following discussion will present the mathematical relationships that describe

compressible fluid flow.

2.2 Compressible Fluid Flow

2.2.1 Choked Conditions

When a vessel such as a tank is accidentally punctured (resulting in a small hole) or

intentionally blown down (through a nozzle), the gas (provided that it is at a sufficient

pressure) may leave the vessel at its sonic velocity. The sonic velocity is the speed of

sound in the gas, and is the maximum possible speed through the puncture or nozzle. A

"choked" condition is established if the gas leaves the vessel at a velocity equal to the sonic velocity. In order for choked flow to occur, the following criterion (assuming an ideal gas) must be satisfied (10):

$$(p_2/p_1)_c = (2/(k+1))^{k/(k-1)} \tag{2-3}$$

where:

p_1 = Absolute vessel pressure (slug/ft s^2)
p_2 = Absolute pressure in the minimum section (slug/ft s^2)
k = Gas specific heat ratio, Cp/Cv
c = Critical conditions

If the pressure ratio p_2'/p_1 (absolute pressure outside of the vessel to inside the vessel) is greater than the critical ratio and isentropic conditions are assumed (i.e., frictionless conditions where there is no exchange of heat), then the mass flow rate out of the vessel can be calculated as follows (10):

$$m^* = A_2\{(2k/(k-1))p_1(\rho_1)((p_2/p_1)^{2/k} - (p_2/p_1)^{(k+1)/k})\}^{1/2} \tag{2-4}$$

where:

A_2 = Area of minimum section of the puncture or nozzle (ft^2)
ρ_1 = Density of gas inside vessel (slug/ft^3)
m^* = Mass flow rate (slug/s)

If the pressure ratio p_2'/p_1 is less than the critical ratio, then the mass flow rate is found from (16):

$$m^* = (A_2p_1/(T_1)^{1/2})\{(k/R)(2/k+1)^{(k+1)/(k-1)}\}^{1/2} \tag{2-5}$$

where

R = Gas constant (5.98 ft lb/slug $^\circ$R)
T_1 = Gas temperature ($^\circ$R)

2.2.2 Isothermal Pipe Flow

Gas flow in pipelines can be isothermal. For isothermal conditions to exist (i.e., the gas temperature is constant), the heat transferred from the gas through the pipe walls is balanced by the heat generated by friction (10). Such conditions can occur in uninsulated pipes where velocities are much less than sonic and where the temperatures inside and outside the pipeline are of the same order.

The following equation relates upstream and downstream pressures for isothermal flow (16):

$$p_1{}^2 - p_2{}^2 = (m^{*2} RT/A^2)(2\ln(p_1/p_2) + f(l/d)) \tag{2-6}$$

where:

p_1 = Upstream pressure (slug/ft s^2)
p_2 = Downstream pressure, (slug/ft s^2)
A = Cross-sectional area of pipeline (ft^2)
T = Gas temperature ($^\circ$R)
R = Gas constant (5.98 ft lb/slug $^\circ$R)
m^* = Mass flow rate (slug/s)
f = Moody friction factor
l = Distance between upstream and downstream locations (ft)
d = Pipeline diameter (ft)

The above equation can also be written in terms of k (heat capacity ratio) and the upstream and downstream Mach numbers (M_1, M_2 respectively, where M is the ratio of the gas velocity to the sonic velocity) (10):

$$(M_1{}^2/M_2{}^2) = 1 - kM_1{}^2(2\ln(M_2/M_1) + f(l/d)) \tag{2-7}$$

These equations are applicable only for the range

$$M_1 < M_2 \leq (1/k)^{1/2} \tag{2-8}$$

2.2.3 Adiabatic Pipe Flow

As described by Vennard & Street (10), adiabatic conditions (i.e., conditions in which there is no heat transfer) can occur in pipes that are either insulated or of short length. Under these conditions, the Mach number increases downstream in subsonic flow, but decreases downstream in supersonic flow. In both subsonic and supersonic flow, the Mach number tends toward unity, with M =1 being the limiting condition. Given an upstream condition, the distance "l" downstream of that location can be increased until M=1 at the discharge location. Any further increases in "l" cannot be made without altering the upstream conditions or creating a shock wave. The relevant equation used for performing calculations is:

$$(dM^2/M^2) = kM^2\{(1+((k-1)/2)M^2)/(1-M^2)\}f\,(dl/d) \qquad (2\text{-}9)$$

With this understanding of natural gas properties and compressible flow, the work of several investigators regarding pipeline blowdown can be discussed.

2.3 Prior Research Pertaining to Pipeline Blowdown

2.3.1 Wilson

In his 1979 study for Alberta Environment, Wilson (11) developed a method for evaluating ground-level transient gas releases for the purpose of assessing risks from sour gas pipeline ruptures. As described by Wilson, automatic block valves are used to isolate the ruptured pipeline segment. Furthermore, during blowdown, the following time periods exist:

-      Soon after the rupture, an expansion wave moves down the pipeline at a velocity equal to the speed of sound. The exiting mass flow can be thought of as an emission from a source of gas at the initial temperature and pressure of the pipeline. Additionally, the gas is considered to flow through a pipe length which increases with time at a rate equal to the speed of sound.

-      Once the wave reaches the end of the pipe, the system will behave as a gas source of constant size which exits through a hole at one end.

Wilson performs both adiabatic and isothermal analyses of the initial moving wave transient. Furthermore, the author also performs an analysis for an isothermal release during the subsequent condition of constant length. An assumption is made that the system is quasi-steady state, which means that fluid acceleration forces are small as compared to pressure forces. The author concludes that the mass release rate models developed through these analyses are difficult to use, and recommends using the following double exponential model developed by R. P. Bell:

$$m^*_e = (m^*_{oe}/(1+\alpha))[\exp(-t/(\alpha^2 \beta)) + \alpha \exp(-t/\beta)] \tag{2-10}$$

where, in dimensions of mass (M), length (L) and time (t), the terms are:

m^*_e = Mass release rate of gas at time t (M/t)

m^*_{oe} = Initial mass release rate calculated using Eq. 2-5 (M/t)

$\alpha = W_o/[\beta \, m^*_{oe}]$ (dimensionless)

W_o = Total mass of gas in pipeline (M)

β = Final release time constant (t)

In his later work (12), Wilson describes the initial mass release rate as a fraction

of the value obtained by Equation 2-5:

$$m^*_{oe} = K(m^*_{oe} \text{ found using Eq. 2-5}) \qquad (2\text{-}11)$$

Where K = equals a constant less than 1, which accounts for the resistance to flow caused

by the overlying soil resting on the pipe. Wilson compares the results from two full scale

pipe rupture tests, and concludes that a K value of 0.5 provides the best fit of the double

exponential model.

In a later work concerning the risk of exposure concentrations in fluctuating

plumes (13), Wilson states that "predicting the behavior of a toxic gas plume from a

pipeline rupture is one of the most complex and difficult problems in atmospheric

diffusion." He cites complicating factors including the high pipeline pressures which

make the exiting gas supersonic and which results in large changes in gas temperature

and density. Furthermore, he indicates that the plume is sensitive to changes in terrain,

downwind obstacles and atmospheric stability. He also mentions that a "saving grace in

this messy problem" is that the release will be of short duration (30 minutes or less).

2.3.2 Groves, Bishnoi and Wallbridge

The authors (7) discuss the calculation of wave velocity in a ruptured pipeline. As

previously mentioned, the rupture of a high pressure gas pipeline results in the creation of

an expansion (or decompression) wave. This wave moves away from the rupture as the

gas flows toward it. Since natural gas is actually a mixture of condensible gases, decompression can result in condensation of individual compounds. Several of the assumptions that the authors make include the following:

- The flow is isentropic and nonviscous;

- The rupture is instantaneous and over the full cross-section of the pipe;

- Condensation occurs at constant temperature and pressure;

- After condensation, the liquid mixture is in equilibrium with the gas mixture; and

- The gas mixture is described by the Soave-Redlich-Kwong equation of state, which is referenced in the authors' document.

The authors present an iterative procedure to find the wave velocity, and compare theoretical predictions to experimental data for pure methane, argon and a natural gas mixture. The authors conclude by stating that it is possible to calculate the decompression wave behavior from pipeline ruptures containing pure gases or gas mixtures.

2.3.3 Fannelop and Ryhming

The work presented by these authors (14) involves the sudden and complete break of a high-capacity gas transmission line. The case which is used is an underwater pipeline 90 miles long, 36 inches in diameter, with inlet and outlet pressures of 133 atm and 55 atm, respectively. The ambient pressure outside the pipeline is 6 atm, and the line contains

7,000 tons of gas. Isothermal flow of a perfect (i.e., ideal) gas is assumed, with the flow also being one-dimensional, unsteady, compressible and with friction. The following equations are then presented:

Continuity:

$$\partial\rho/\partial t + (\partial/\partial x)\rho u = 0 \tag{2-12}$$

Momentum:

$$\partial u/\partial t + u(\partial u/\partial x) + (1/\rho)(\partial p/\partial x) + 2fu^2/D = 0 \tag{2-13}$$

Equation of state:

$$p = \rho R T_o \tag{2-14}$$

where, in dimensions of mass (M), length (L), time (t) and temperature (T), the various terms are:

ρ = gas density (M/L^3)
R = gas constant (L^2/Tt^2)
p = pressure (M/Lt^2)
t = time (t)
u = gas velocity (L/t)
x = length coordinate (L)
f = friction factor (f= 0.002)
D = pipeline diameter (L)
T_o = seawater temperature (T)

The authors describe different time regimes following the rupture, which require different methods of solution. The "early time" regime begins with an inviscid regime followed by a viscous expansion process. This early time regime lasts from the time of rupture until approximately 25 seconds or the waves penetrate 10,000 meters of pipeline. The "intermediate-time" regime lasts from approximately 25 seconds until the pressure

peak has moved to the closed end of the pipeline, at which time the "late-time" regime begins. When considering the low pressure end of the rupture, an intermediate region is not considered (since the pressure decreases monotonically toward the open end).

The authors acknowledge that a general solution of the above nonlinear partial differential equations is too complicated for routine engineering applications. They present an integral method which can be used to find the solution for the late time regime (which represents most of the outflow from the broken end). The authors also indicate that this method can be used (with modification) for the intermediate regime.

2.3.4 Flatt

In his 1985 work, Flatt (15) provided a second-order algorithm which is applicable to the inverse marching method of characteristics. This algorithm can be used to solve unsteady compressible one-dimensional flows in which the momentum equation has a high f(L/D) value and where the flow is in the high subsonic range. The author indicates that the method involves only one iteration.

Flatt acknowledges in another study (16) that the rupture problem is highly non-linear, making the finding of analytical solutions unlikely. He applies the inverse marching method of characteristics to the pipeline rupture presented in (14). The author assumes that initial conditions are of isothermal flow, while the unsteady flow generated after the rupture is adiabatic and one-dimensional. Additionally, the gas is considered perfect.

2.3.5 Lang and Fannelop

The pipeline rupture described in previously noted studies (14, 16) is again analyzed in a subsequent study (17). The partial differential equations are reduced by the authors to a set of ordinary differential equations by procedures used in the Method of Weighted Residuals. The reduced equations are then integrated using various numerical methods (Finite Element, Spectral Galerkin and Spectral Collocation). The authors assume the flow to be one-dimensional, compressible, viscous and isothermal, with the conditions of primary interest being those in the pipeline segment associated with the high pressure end. The authors state that the best results in terms of stability, accuracy and computing time are obtained using the Spectral Collocation Method.

2.3.6 Ryhming

The author considers the early time regime associated with a pipeline rupture (18). Specifically, the process of the expansion wave imparting motion to the gas particles against wall friction is studied. The governing equations are those provided in (14), and are solved using a matched asymptotic expansion procedure. The author also assumes isothermal flow conditions and a perfect gas.

While the author acknowledges that numerically correct solutions are obtained by considering the full adiabatic process, the isothermal assumption results in simpler equations and very little is lost in terms of the gas acceleration process.

2.3.7 Picard and Bishnoi

The authors use a real-fluid nonisentropic decompression model to evaluate the rupture of a sour gas pipeline (9). This model is used for two-phase (gas-liquid) multi component mixtures, and is based on unsteady nonisentropic one-dimensional compressible fluid flow. The model consists of characteristic and compatibility equations that are solved numerically using an explicit inverse marching method. Real fluid behavior is modeled using the Peng and Robinson equation of state.

The pipeline considered is part of a gas gathering system. It is uninsulated, 168.3 mm diameter and buried 42 cm below the ground (ground temperature is 275 K). The pre-rupture temperature of the fluid is 303 K, while the corresponding pressure is 11,000 kPa. When the pipeline is ruptured, it is assumed that an upstream emergency valve closes, restricting the blowdown length to 1,000 m.

The authors compare the results with those obtained using the assumption of a perfect gas, and conclude that a perfect gas assumption will underestimate the release rate by 30 to 45% while the total amount of fluid released may be underestimated by 50%. Additionally, the authors point out that perfect gas theory does not consider the effects of condensation.

2.3.8 Olorunmaiye and Imide

The authors (19) model the flow in the underwater pipeline that has been described previously. They assume unsteady, one-dimensional isothermal flow. The non-dimensional forms of the partial differential equations provided above are solved using the method of characteristics. The authors indicate that the flow rate predicted at the broken end of the pipe is 18% lower than that predicted by adiabatic flow theory, but that the flow rate agrees with the results of Lang and Fannelop.

2.3.9 Other Work

The Pipe Line Rules of Thumb Handbook (8) provides the following equation to use when calculating the volume of gas lost through a puncture or blowdown:

$$Q = D^2 P_1 \qquad\qquad (2\text{-}15)$$

where:

Q = Volume of gas in Mcf/hr at a pressure of 14.9 psi, 60°F with a specific gravity of 0.60
D = Diameter of the nipple or orifice in inches
P_1 = Absolute pressure in psi at some nearby point upstream from the opening

2.4 Prior Research Pertaining to Turbulent Jet Flames and Flame Geometry

2.4.1 Turbulent Jet Flames

As described by the National Fire Protection Association and the Society of Fire Protection Engineers (20), turbulent jet flames can form as the result of either an accidental release of hydrocarbon vapors or the intentional burning of waste gases in a flare. The flame is called turbulent based on the Reynolds number of the gas jet. A jet

fuel is assumed to exit a nozzle that is pointed in an upward position. The fuel is discharged into a surrounding medium that contains an oxidant. Starting at a low flow rate, the flame height increases with increasing flow rate. As the flow is increased, a maximum height is reached and then shortens. However, before reaching the maximum height, the flame begins to flicker at the top. This point changes the flame from a laminar diffusion flame to a transition flame. As the flow rate is increased further, the flickering spreads down and stops several diameters from the burner. When this happens, the flame is said to be turbulent, and the flame height becomes independent of flow rate.

2.4.2 Flame Geometry

Two important flame characteristics are the flame height and the amount of flame tilt in a cross-wind. Hawthorne, Weddell and Hottel (21) have developed the following relationship to predict the height of a turbulent flame in still air:

$$L/D = (5.3/C_T)\{(T_F/(\alpha_T T_N))(C_T+(1-C_T)(M_S/M_N)\}^{1/2} \qquad (2\text{-}16)$$

where, in dimensions of mass (M), length (L), time (t) and temperature (T), the various terms are:

L = visible flame length (L)
D = nozzle diameter (L)
T_F = adiabatic flame temperature (absolute T)
T_N = temperature of nozzle fluid (absolute T)
M_S = molecular weight of surrounding fluid (dimensionless)
M_N = molecular weight of nozzle fluid (dimensionless)
C_T = mol fraction of nozzle fluid in the unreacted stoichiometric mixture (decimal)
α_T = mols of reactants/mols products for the stoichiometric mixture (decimal)

facing 22

Note: Illustration Based on Information Provided in References Numbered 20 and 22

S

Z (Direction of Jet)

X (Direction of Cross-wind)
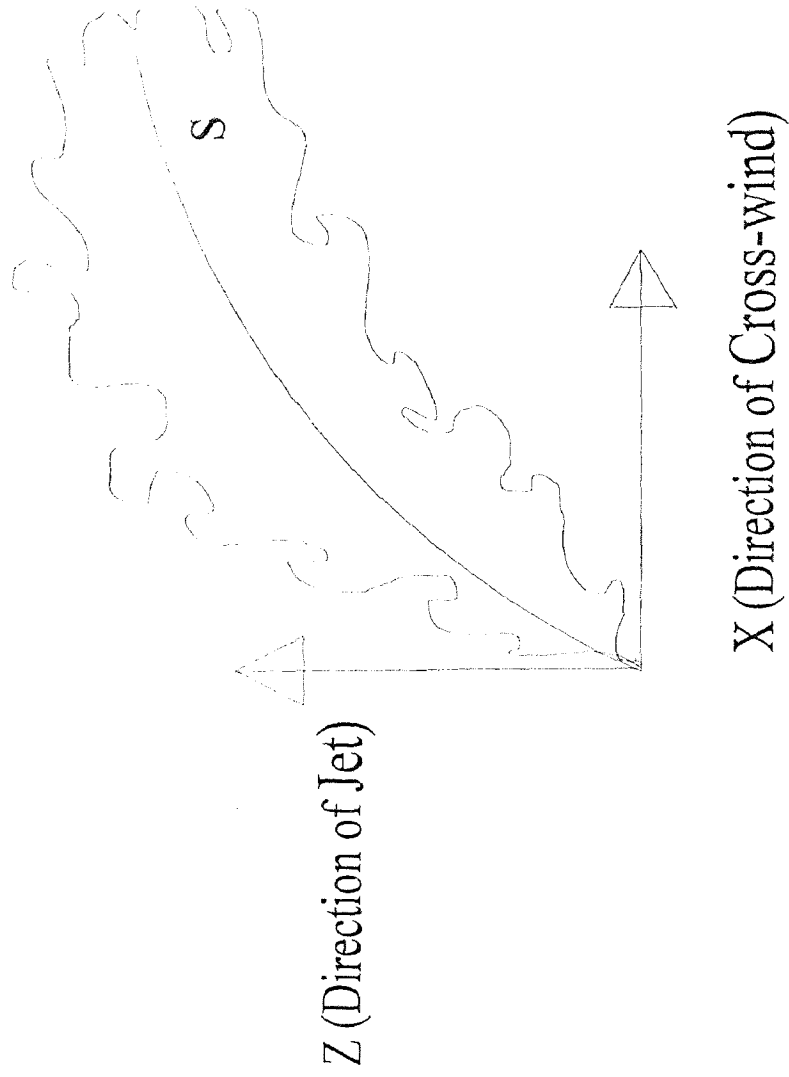
Figure 2.1 – Flame Shape with a Cross-wind

The work of Brzustowski, as presented in (20) and Gollahalli, et al (22) provides a procedure to determine flame shape with a cross-wind (see Figure 2.1). The procedure begins by calculating the dimensionless lean limit concentration:

$$\bar{C}_L = C_L (u_j/u_w)(M_f/M_a) \qquad (2\text{-}17)$$

where:

$\bar{C}_L$ = lean limit concentration (expressed as a decimal)
u_j = velocity of jet
u_w = velocity of wind
M_f = molecular weight of fuel
M_a = molecular weight of air

If $\bar{C}_L \leq 0.5$, the curvilinear distance $\bar{S}_L$ is determined from:

$$\bar{S}_L = 2.04\,(\bar{C}_L)^{-1.03} \qquad (2\text{-}18)$$

If $\bar{C}_L > 0.5$, then:

$$\bar{S}_L = 2.71\,(\bar{C}_L)^{-0.625} \qquad (2\text{-}19)$$

If $\bar{S}_L > 2.35$, then the dimensionless coordinate $\bar{X}_L$ is found from:

$$\bar{X}_L = \bar{S}_L - 1.65 \qquad (2\text{-}20)$$

If $\bar{S}_L < 2.35$, then $\bar{X}_L$ is determined from:

$$\bar{S}_L = 1.04\,\bar{X}_L^{\,2} + 2.05\,\bar{X}_L^{\,0.28} \qquad (2\text{-}21)$$

The dimensionless rise $\bar{Z}_L$ is calculated from:

$$\bar{Z}_L = 2.05\,(\bar{X}_L)^{0.28} \qquad (2\text{-}22)$$

The dimensional coordinates of the flame tip are then found from the following:

$$X = \bar{X}_L d_j\,(\rho_j/\rho_a)^{1/2}(u_j/u_w) \qquad (2\text{-}23)$$

$$Z = \bar{Z}_L d_j\,(\rho_j/\rho_a)^{1/2}(u_j/u_w) \qquad (2\text{-}24)$$

facing 23
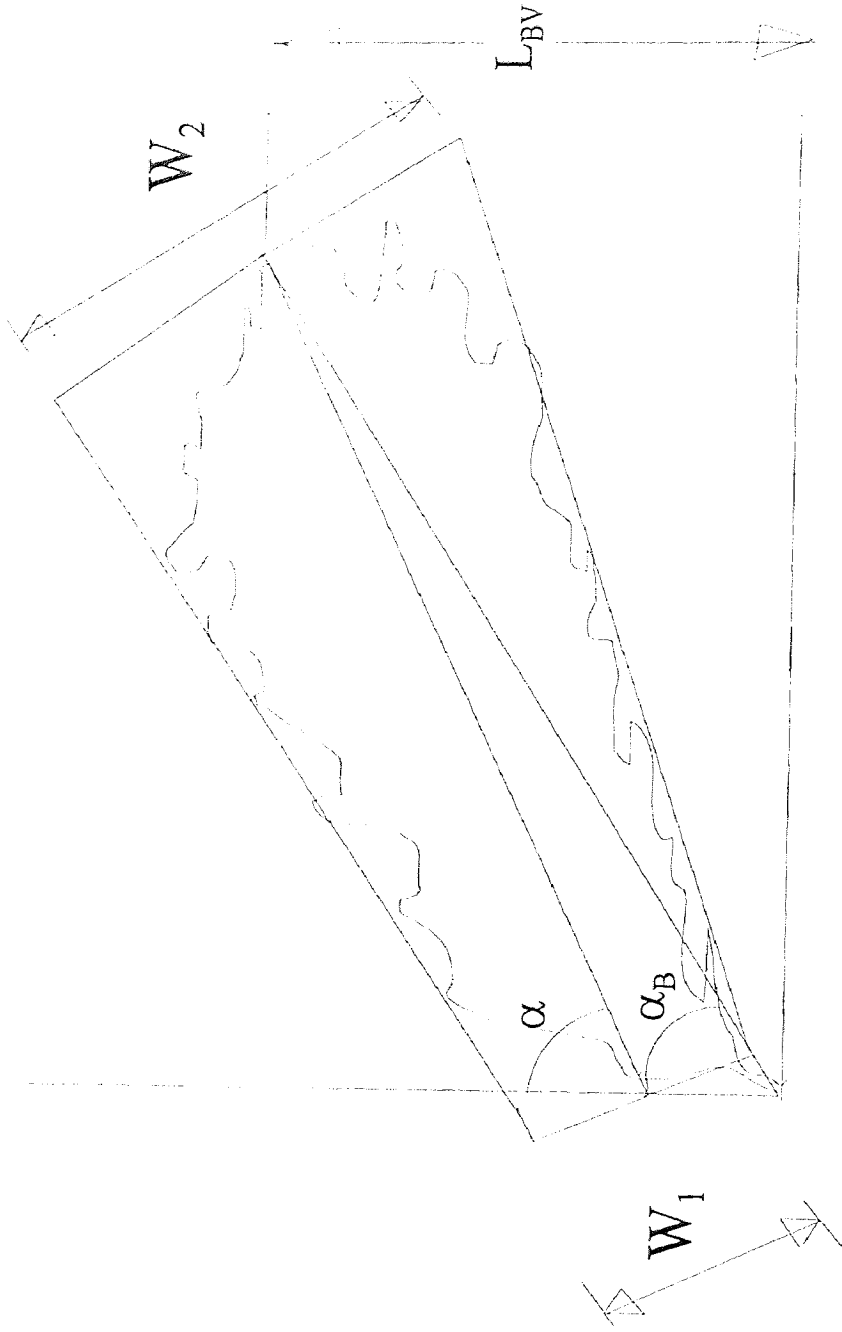
Note: Illustration Based on Information Provided in References Numbered 20 and 23

Figure 2.2 – Jet Flame Shape Parameters

where:

d_j = Jet diameter
ρ_j = Density of jet
ρ_a = Density of air

The work of Kalghatgi presented in (20) and (23) provides a means by which the

shape of a jet flame in a cross-wind can be described. He described the flame by a

frustum of a cone (see Figure 2.2) with the following parameters:

W_1 = flame base width
W_2 = flame tip width
L_{BV} = vertical length of the flame tip from the plane of the burner
α = angle subtended by the flame with respect to the vertical
α_B = angle subtended by the burner tip and the tip of the flame with respect to the
vertical

Kalghatgi also defined the burner source diameter as being

$$D_S = D(\rho_j/\rho_a)^{1/2} \tag{2-25}$$

where D is the actual burner diameter. A velocity ratio, R, is also defined as:

$$R = \text{cross-wind speed (U)/jet velocity (U}_j) \tag{2-26}$$

The following equations are then used to find the geometric parameters (for the

range 0.02 < R < 0.25):

$$\alpha_B = 94 - (1.6/R) - 35R \text{ (degrees)} \tag{2-27}$$

$$\alpha = 94 - (1.1/R) - 30R \text{ (degrees)} \tag{2-28}$$

$$(L_{BV}/D_S) = 6 + (2.35/R) + 20R \tag{2-29}$$

$$(W_2/D_S) = 80 - (0.57/R) - 570R + 1470R^2 \tag{2-30}$$

$$(W_1/D_S) = 49 - (0.22/R) - 380R + 950R^2 \tag{2-31}$$

facing 24

Note: Illustration Based on Information in Reference Number 20

Normal to Surface
Receiving Thermal
Radiation

Distance from Flame Center to Observer (D)

Θ

Flame

Observer
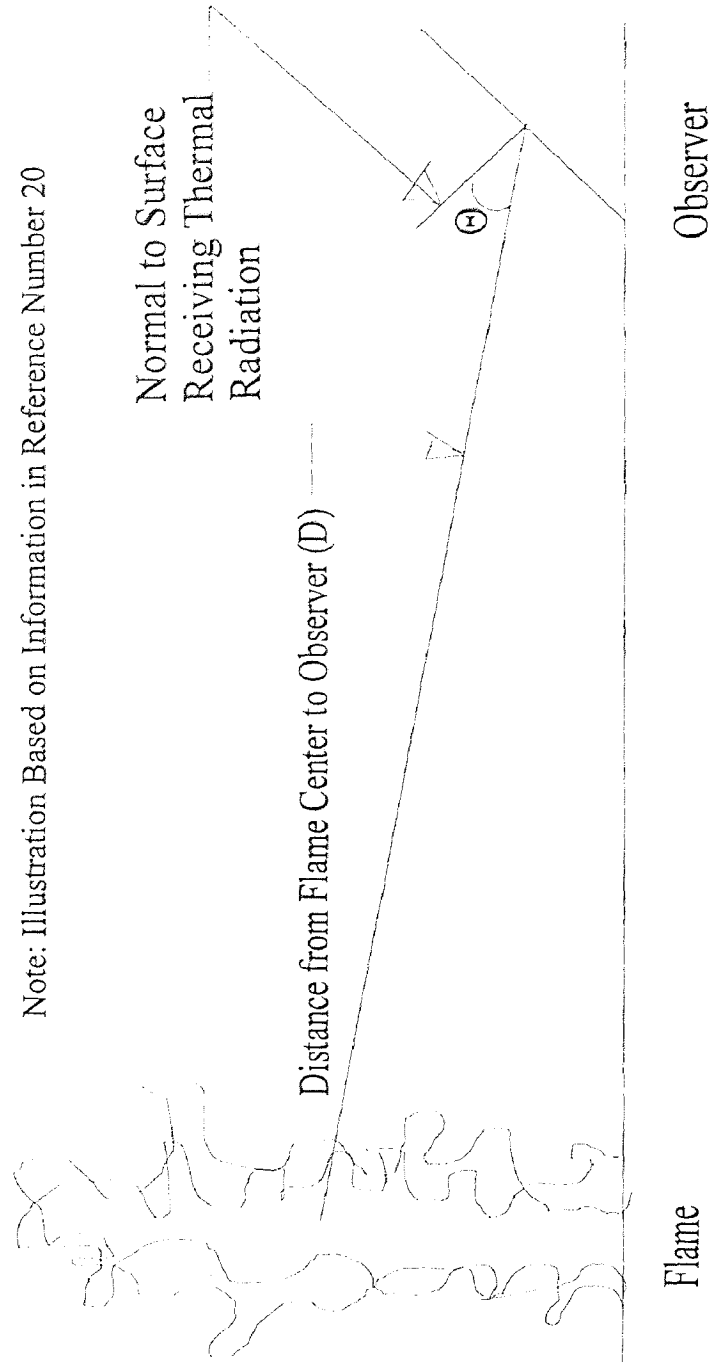
Figure 2.3 - Conceptual Illustration of the Point Source Model

2.4.3 Heat Transfer Models

The major source of damage or injury from large open hydrocarbon fires is from thermal radiation (20). The following discussion will present several models that can be used to predict the thermal radiation from jet flames.

2.4.3.1 Point Source Model: The point source model assumes that the source of radiant heat can be modeled by positioning a point source at the center of the flame (see Figure 2.3). The equation which is used to calculate the radiant heat flux is (20):

$$q'' = Fq_{rel}\cos\theta/(4\pi D^2) \qquad (2\text{-}32)$$

where:

q'' = incident radiant flux, kW/m^2 (or Btu/hr ft^2)
D = distance from flame center to observer, m (or ft)
q_{rel} = energy release rate, kW (or Btu/hr)
F = fraction of combustion energy resulting in radiation
θ = angle between normal to the surface receiving the thermal radiation and line of sight from flame center

Oenbring and Sifferman (24) provide the following form of the point source model to use when calculating radiant heat flux from a flare:

$$K = FQ/(4\pi D^2) \qquad (2\text{-}33)$$

where:

K = radiant heat flux from a flame (Btu/hr ft^2)
F = fraction of total heat radiated
Q = total heat content of flared gas (Btu/hr)

It can be seen from both forms of the model that the heat flux decreases with the square of the distance (i.e., there is an inverse square relationship).

Note: Ilustration Based on Information in Reference Number 25
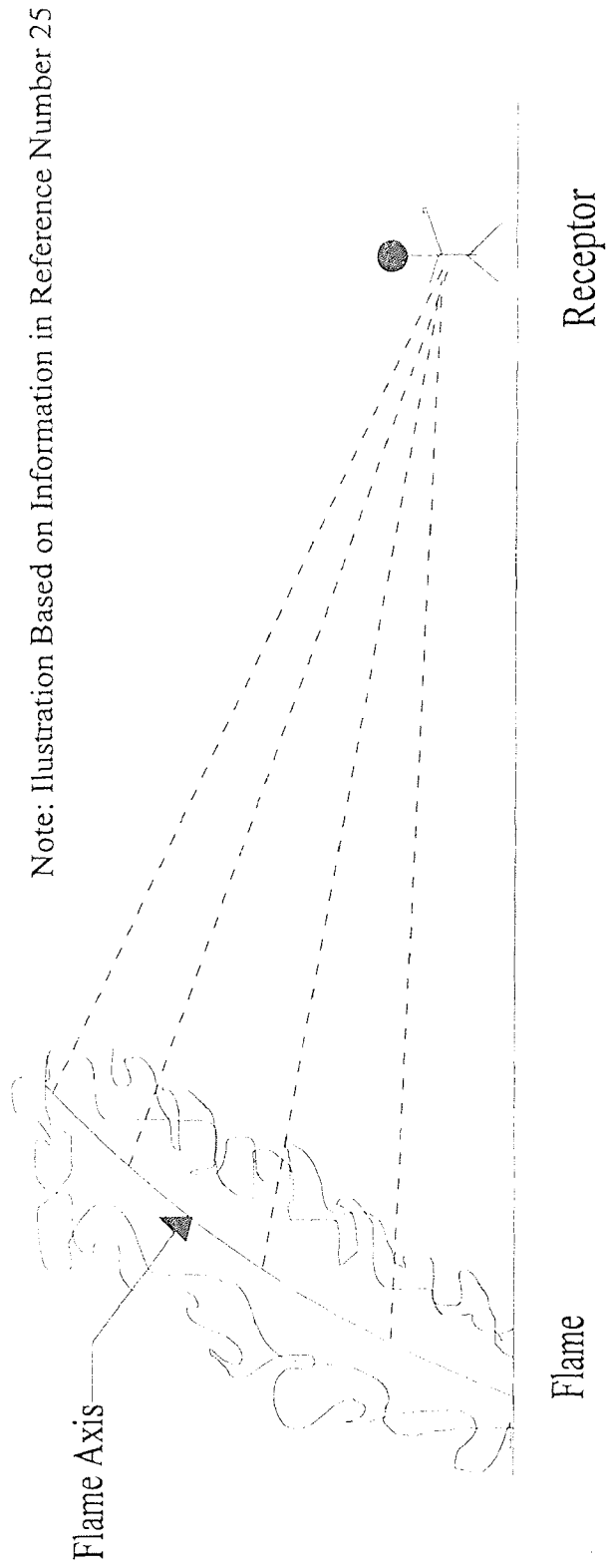
Figure 2.4 – Conceptual Illustration of the Line Source Model

2.4.3.2 Line Source Model: The NFPA and SFPE (20) explain that in the line source model, an elemental length of flame is assumed to radiate similar to a point source. The total radiant heat flux is calculated by integrating the flux from an elemental source over the length of the flame.

In addition, Fumarola, et al (25) have developed the following equation for use when the thermal radiation is evenly distributed along the flame axis:

$$q = 0.043 \ fQ \int [Ax^{0.36} + h - \bar{z}]/[x\{(Ax^{0.36} + h - \bar{z})^2 + (x - \bar{x})^2\}^{3/2}]dx \quad (2\text{-}34)$$

In Equation 2-34, A is equal to $3.1(d_j R)^{0.64}$, R is equal to $(u_j/u_a)(\rho_j/\rho_a)^{1/2}$, the limits of integration are from x equals zero to x equals x_t, and the following nomenclature is used:

d_j = diameter of flare stack, m
h = height of flare stack, m
f = fraction of radiant heat release
Q = total heat release, kcal/s
q = thermal radiation at receptor, kcal/s m^2
x = downstream distance, m
z = cross-stream distance, m

$\bar{x}$ = x-coordinate of receptor, m

$\bar{z}$ = z-coordinate of receptor, m

u = velocity, m/s
a = ambient air condition
j = discharge condition
t = end of the flame axis

A conceptual illustration of the line source model is provided in Figure 2.4.

2.4.3.3 Tilted Cylinder Model: While the point source model can be used to determine the thermal radiation from large turbulent flames, the model breaks down at locations close to the flame (20). Another model that can be used is the tilted cylinder model (20). This model approximates the flame by a cylindrical radiating surface. The radiant heat flux can be calculated from the following equation:

$$q = E\tau F \tag{2-35}$$

where:

E = surface emissive power of the flame, W/m^2 (or $Btu/hr\ ft^2$)
F = geometric view factor
τ = atmospheric transmissivity

The surface emissive power of the flame can be found from the equation:

$$E = E_{bb}(1-e^{-kL}) \tag{2-36}$$

where:

E_{bb} = equivalent blackbody emissive power (same units as E)
k = extinction coefficient, $1/m$ (or $1/ft$)
L = effective path length, m (or ft)

2.5 Prior Research in the Field of Hazard Analysis

2.5.1 Typical Models

There are numerous computer models that have been developed for use in the field of hazard analysis. These models are generally used to predict the fate and transport of hazardous materials that have been accidently released into the environment. Several of these models are described below.

ALOHA (Areal Locations of Hazardous Atmospheres) (26) was developed by the National Oceanic and Atmospheric Administration and the United States Environmental Protection Agency. The software is intended for use by emergency responders. ALOHA performs dispersion modeling for neutrally buoyant and heavy gases and (for a variety of chemicals) can model different sources such as tanks and pipes.

FLACS (Flame Acceleration Simulator) (27) has been used to predict gas explosions in complex geometries. The computer model can be used in the design of process areas (including offshore platforms). FLACS calculates parameters such as explosion pressure and flow characteristics as a function of time and space for different geometries and explosion situations.

SAFEMODE (Safety Assessment for Effective Management Of Dangerous Events) and *Micro HACS* (Hazard Assessment Computer System) were developed for the United States Coast Guard (28). This system can model releases from sources such as pressurized storage tanks, bulk storage tanks, barge, rail car and road transports) and predict fate and transport (such as explosion effects and pool fire thermal radiation) for over 1200 chemicals.

The *Hazard* model can be used with pipeline or tank storage failures (29). Predictions can be made of the specific locations of hazardous concentration limits (whether they are flammable or toxic limits) in the event of a release. The model treats gas pipeline failures using one-dimensional gas dynamics.

WHAZAN (World Bank Hazard Analysis) was developed by Technica International Ltd. in collaboration with the World Bank (30). The overall program is comprised of a series of consequence models. The models can predict the outflow of a chemical, its behavior immediately after release, its dispersion in the atmosphere, and fire or explosion events.

2.5.2 Research Performed by the European Gas Pipeline Incident Data Group

In Europe, there are 8 major natural gas transportation companies that are collectively called the European Gas Pipeline Incident Data Group (EGIG). In the 1960's and early 1970's, European governments based their regulatory actions on accident data from the United States. The European gas companies believed it was more appropriate to have their regulations based on European data, and so they decided to establish their own database. EGIG collects information on the technical conditions of the incident, such as the cause of the incident, incident frequencies, the diameter of the pipeline, the pipe wall thickness, and the thickness of the pipeline cover. The type of information that is collected is related to incident prevention, as opposed to collecting information on the effects of an incident once it occurs (H. van Poelje: personal communication, November 30, 1995).

Project management for EGIG is based in the Netherlands (at N.V. Nederlandse Gasunie), and so it is appropriate to further discuss the Dutch regulations. As explained in Chapter 1, the Dutch have established four area classes, with effect and building distances determined through a risk analysis. One of the possible ways in which risk

contours can be determined involves establishing the pipeline failure frequencies,

determining the probability of ignition and establishing the dose-effect relationship

(H. van Poelje: personal communication, September 30, 1996). It should be noted that

there is no internationally agreed method for risk calculation. While the Dutch definition

of individual risk is based on fatalities, this may not be the basis used by other countries.

Another basis which other countries use is casualties.

2.5.3 Research Performed by the British Health and Safety Executive

In their research report to the HSE, Hill and Catmur (31) compare individual and societal

risks for different high pressure pipelines including methane, oxygen, spiked crude oil,

NGL (natural gas liquids), gasoline, ethylene and ammonia. The authors define two

criteria for evaluating risk. "Fatality" is defined as an impact likely to cause death

immediately or after an extended duration, while "dangerous dose or worse" is defined to

include:

- Severe distress to many persons;

- A substantial proportion of persons affected require medical attention;

- Some persons are seriously injured, requiring prolonged treatment; and

- Any highly susceptible people might receive a fatal injury.

Individual risk transects and societal F/N curves were prepared. As defined in the report, The individual risk transects present the probability (at varying distances) that an individual could incur a fatal injury or dangerous dose due to an accidental release from a pipeline. F/N curves present societal risk as the probability of N or more fatalities due to a pipeline release.

The authors determine that all pipelines except oxygen and small diameter low pressure methane pipelines had individual risk levels greater than one in a million per year. Additionally, the greatest number of multiple fatalities were associated with methane, NGL and ethylene pipelines.

In a second research report prepared for the HSE, Hockey and Rew (32) review the factors that influence the response of humans to thermal radiation. The report also discusses and compares various methodologies for determining the effects of thermal radiation from process fires. The authors indicate that most risk assessment methodologies consider the speed of escape, delay before escape begins and the distance traveled to reach shelter as factors influencing the probability of fatality.

2.5.4 Research Performed in Canada

Based on information provided by the TSB of Canada (personal communication, February 28, 1997), a private company in Canada is developing, in coordination with the Major Industrial Co-ordinating Council of Canada (MIACC), a document intended for use by government officials during the planning of pipeline routes and development. The document defines a Response Planning Area (RPA) to be an area where public safety

31

issues (such as emergency response and preparedness) should be addressed. The RPA is

developed using consequence modeling, and is based on the following major factors:

- Source parameters (e.g., pipeline diameter and flow, and the properties of the transported material);

- Transport parameters which are used to evaluate the migration of material or energy from the pipeline; and

- Damage criteria

The RPAs are intended to be presented as graphs (for example, distance to a specified

damage criteria as a function of pipeline diameter and pressure).

In addition to the aforementioned information, the TSB of Canada likewise

provided (personal communication, February 28, 1997) information on guidelines,

developed by the Canadian Standards Association, for performing risk analyses on

pipelines in Canada. As stated in these guidelines, the intent is to:

"(a) identify the role of risk analysis within the context of an overall risk management process;

(b) set out standard terminology that is consistent with existing Canadian standards in the field of risk management;

(c) identify in general terms the components of the risk analysis process, the associated data requirements, and the requirements for documentation and records; and

(d) where applicable, provide reference to methodological guidelines for risk analysis".

2.5.5 Research Performed by NJIT

The NJIT Institute for Transportation (33) has reviewed NTSB Pipeline Accident Reports (PARs) for the purpose of determining the burn radius associated with natural gas pipeline failures involving fires. The authors acknowledge that there are many factors that contribute to the development of a burn radius (e.g., rupture geometry, wind conditions, terrain geometry, duration of release and quantity of material released, etc.). However, the authors maintain that it is still possible to determine an upper bound on the extent of the burn radius. The upper bound was found to be a 92 foot radius at an incident operating pressure of 260 psig, and a 610 foot radius at a pressure of 987 psig.

The authors also found a close correlation between the occurrence of a natural gas pipeline explosion and fire, and its resultant burn radii. Fire damage is a function of the radiant energy produced by a fire, and the authors indicate that after an explosion there is less natural gas available to produce radiant energy. Therefore, the authors conclude that the burn radius associated with explosions and fires is less than that associated with only fires for similar natural gas pipeline operating conditions.

2.6 Conclusions from Literature Review

The prior research reviewed and cited herein is predominantly concerned with predicting which sections of a pipeline are most vulnerable to damage and predicting the loss of product during an actual pipeline rupture (i.e., blowdown), rather than directed to concerns associated with establishment of adequate safe separation distances for the public.

The above research emphasis probably exists because the risk of injury and fatality to the general public related to natural gas pipeline ruptures has been documented by reviewing agencies to be minimal compared to other incidents which human beings may encounter (i.e., due to falls, drowning, poisoning, fires and burns, etc.) during their normal lifetime.

The modeling of product loss during a pipeline rupture, which is an important factor related to the establishment of a safe separation distance therefrom, is, as indicated in a number of research papers reviewed, difficult to simulate. This is due to disparity amongst researchers as to whether blowdown in the pipeline should be modeled as an adiabatic or isothermal condition; whether the fluid is viscous or nonviscous; whether the flow regime is isentropic or nonisentropic and consequently whether the natural gas should be treated as a perfect gas or a real fluid. Further, the prior research suggests that the gas may change from one physical state to another within the pipeline during the course of the same blowdown event.

In addition to the above-noted complexities in attempting to accurately simulate the fluid dynamics within a pipeline during a blowdown situation, there are a number of other factors which directly influence the required safe separation distance that should be established between a specific natural gas pipeline and its neighboring potentially impacted public at large. These factors include: the pipeline diameter; operating pressure; location of and time needed for emergency closure of the closest valves located upstream and downstream of the rupture; the interconnections (if any) with other pipelines in the vicinity of the rupture; the physical orientation (i.e., the nature and

location of the break) of the rupture; the depth of cover over the pipeline; and the atmospheric conditions (e.g. wind velocity, wind direction, etc.) in the immediate vicinity of the pipeline at the time of rupture. In attempting to predict, with the use of a generalized mathematical model, the impacts of all these variables both independently and jointly, it appears that an accurate single point estimate of associated safe separation distance would be exceedingly difficult if not impossible to develop.

The available hazard assessment models reviewed herein have been developed primarily for utilization by private industry and the Federal government, and are designed for generalized hazard assessment purposes. The models can be extremely expensive to purchase, and are, in many instances, proprietary in nature. Furthermore, specific documentation associated with the nature of the model development, such as the structure of the computer codes, is lacking in the published material associated with the above-noted models. As such, attempts to extract meaningful information related to this thesis have resulted in limited success.

The literature review also revealed that the available database of information associated with actual natural gas pipeline accident occurrences in the United States is limited. For example, it was previously indicated that the NTSB investigates and reports upon pipeline accidents in the United States. However, the NTSB does not investigate all pipeline accidents; the criteria that triggers an actual NTSB investigation relates to the extent of property damage and whether injuries or fatalities result from the accident. The results of the investigations that are performed are published as PARs. Also, a review of the available PARs by this author indicates that there is an inconsistency in the type of

information gathered by the NTSB for each accident. For example, the PARs do not consistently report the total volume of gas lost in an accident, nor the location of the closest valves upstream and downstream of the pipeline rupture. Furthermore, supporting information for the more dated PARs (in the PAR dockets in Washington, DC) is periodically destroyed.

The Commodity Pipeline Occurrence Reports prepared by the Canadian TSB are similar to the PARs in that there are also inconsistencies in the extent of information contained in these reports. Further, the Canadian TSB investigates an extremely small number of accidents (i.e., approximately one percent of all pipeline accidents in Canada).

Because of all the aforementioned reasons, it is concluded herein that an approach to advance the state-of-the-art in the discipline of pipeline risk analysis is to develop a reliable estimation technique to conservatively predict safe separation distances to be articulated between the public and the ruptured natural gas pipeline. To aid in this development, the literature review indicates that extensive work has been performed in determining turbulent jet flame characteristics. In addition, the previously noted point source model can be utilized to calculate the heat flux generated at various distances from industrial flares. As will be seen in the following chapters, this model can be applied to the evaluation of safe separation distances which can be considered by regulatory agencies to protect the quality of life of residents located in proximity to natural gas pipelines.

CHAPTER 3

OBJECTIVE OF THE DISSERTATION
AND
INTRODUCTION TO THE DISSERTATION RATIONALE

As noted in Chapter 2 in the literature search and the analysis thereof, there is

considerable complexity involved in attempting to mathematically model the dynamics

associated with a natural gas pipeline rupture. This complexity arises due to the

numerous variables involved in the process as well as the varying assumptions made by

previous investigators as to the nature of the physical state of the natural gas during a

rupture condition. In consideration of the above, proposed herein is a simplified

approach for estimating safe separation distances based upon assumptions that the

damage from a pipeline rupture is primarily due to the thermal radiation produced by the

ignited gas behaving like a vertical jet flame, and that the major variables associated with

the burn radii (i.e., impact area) resulting from a pipeline rupture are the size of the

pipeline and its operating pressure (which directly affects the mass flow rate in the

pipeline). The appropriateness of this approach in providing results of an accuracy

suitable for regulatory agencies to utilize for establishing zoning guidelines is confirmed

in this thesis by comparing results from the aforementioned model with actual burn radii

found in a limited number of accident investigations conducted by the NTSB in which

sufficient data was obtained to verify the subject model herein.

As indicated above, an assumption is made that the damage from a pipeline rupture is primarily due to the thermal radiation produced by the ignited gas. Therefore, a safe separation distance is defined as the distance beyond which a pre-established level of thermal radiation damage will not likely occur. Other damage (such as projectile damage from pipeline fragments or damage due to overpressures from explosions) is not considered. This assumption is consistent with the results from investigations of actual pipeline ruptures, in which damage was found to be caused primarily from the fire.

It was also previously mentioned that the escaping gas is assumed to behave, once ignited, like a vertical jet flame. A release from a pressurized system like a pipeline can produce other scenarios such as dispersion of the unignited gas, formation of a fireball, development of a flash fire or a vapor cloud explosion (20, 31, 34). Furthermore, the rupture orientation may be such that a flame jet, if it exists, may not be truly vertical.

Assuming that all of the above scenarios can occur increases the number of variables to be considered, in that the probabilities of each scenario happening (either alone or in combination with other scenarios) must then be determined. Furthermore, should these other scenarios occur, there is no certainty that they will contribute significantly to the overall thermal radiation damage. For example, the dispersion of unignited gas would not produce thermal radiation damage. Vapor cloud explosions can produce damage through the generation of pressure waves. However, according to the Center for Chemical Process Safety (CCPS), the following conditions need to be present for a vapor cloud explosion to occur (34):

- The released material must be flammable and at an appropriate temperature and pressure.

- A suitably-sized cloud of the escaping gas must be present before ignition. CCPS reports that ignition delays of 1 to 5 minutes are the most probable for generating clouds which can explode.

- A sufficient portion of the cloud must be within the flammable range of the material.

- The rate of flame propagation within the cloud determines the severity of blast effects. High flame speeds can produce high overpressures.

As indicated previously, thermal radiation is the primary cause of damage in natural gas pipeline ruptures. Since vapor cloud explosions are produced only under a set of very specific circumstances and since blast effects are not the primary cause of damage, this scenario is not expected to routinely occur.

With regard to the development of a flash fire, CCPS (34) indicates that very little information is currently available concerning the thermal radiation produced. CCPS also states that thermal radiation hazards from burning vapor clouds are considered less significant than blast effects, and that combustion associated with a flash fire lasts no more than a few tens of seconds. In addition, Hockey and Rew (32) indicate that for the

39

calculation of hazard ranges, it is assumed that people in contact with the flame are fatally

burned while those at a distance would not be seriously affected. It should be noted that

the fire dimensions will depend on the shape of the vapor cloud, which itself is dependent

upon many variables. Given these limitations, the modeling of flash fires for the

determination of safe separation distances is not considered in the dissertation.

Although fireballs are typically associated with BLEVEs (*B*oiling *L*iquid

*E*xpanding *V*apor *E*xplosions), they can also happen as a result of a pipeline rupture.

CCPS (34) lists the properties of fireballs which have the greatest influence on thermal

radiation. These include:

-      Fireball diameter as a function of time and maximum diameter;

-      Height of fireball center above its ignition position as a function of time elapsed

       after liftoff;

-      Fireball surface emissive power; and

-      Total combustion duration.

Although fireballs produce the highest radiation intensity, these events can be

assumed to last only 10-30 seconds (32). Formulas for fireball diameter, duration and

hazard distances have been published (34) which are functions of the mass of the fuel.

However, in the case of a pipeline rupture the mass of fuel involved in a fireball is

difficult to predict since the release rate varies with time. Due to the limitations and

numerous variables involved, fireball modeling is not attempted in the dissertation.

In order to model a vertical flame jet emanating from a pipeline rupture, the point source model will be used. As indicated previously, the point source model was used by Oenbring and Sifferman (24) to calculate the heat flux from a flare. Since the damage incurred by an object receiving radiant heat from a flame is dependent upon the heat flux, the point source model can be used to relate thermal radiation damage to the distance from the ruptured pipeline. The model is dependent upon the total heat content of the escaping gas (which is a function of the gas release rate) and the height of the flame (for location of the point source). Therefore, the following chapter of the dissertation will develop relationships for flow rate and flame height which will be used in conjunction with the point source method for predicting safe separation distances.

CHAPTER 4

DEVELOPMENT OF METHOD TO DETERMINE
SAFE SEPARATION DISTANCES

This chapter presents the methodology which is used to estimate safe separation distances based on pipeline diameter and incident operating pressure. The equations for determining heat flux, gas flow rate and flame height are presented and combined to produce a single safe separation distance equation. This equation is then used in the preparation of charts for predicting safe separation distances.

4.1 Calculation of Burn Radii

As indicated in Chapter 3, the majority of damage resulting from a pipeline rupture is caused by thermal radiation. Therefore, the safe separation distance from a pipeline can be defined in terms of the distance needed to protect against a specified heat flux. This specified heat flux will produce an area of thermal radiation damage in the vicinity of the pipeline which can be estimated by calculating the burn radius. In Chapter 3, the assumption was made that a pipeline rupture produces a vertical jet flame. An assumption is now made that this vertical flame will radiate equivalently in all directions so that the burn area will be symmetric about the rupture. The burn area can then be described by a circle, with the radius of the circle being the burn radius. The following section describes how the burn radius can be determined using the point source method.

4.1.1 Use of the Point Source Method

As explained in Chapter 3, the point source method forms the basis for the estimation of

safe separation distances. In Chapter 2, the following equation was presented from the

work of Oenbring and Siffferman (24):

$$K = FQ/(4\pi D^2) \qquad (2\text{-}33)$$

where

K = Radiation heat flux from a flame (Btu/hr ft^2)
F = Fraction of total heat radiated
Q = Total heat content of the flared gas (Btu/hr)
D = Distance from point source to receptor (ft)

The authors provide the source for Equation 2-33 as being the American Petroleum

Institute (API) document API RP-521. In a later version of this document (35), API

provides the revised equation:

$$D = (\tau FQ/(4\pi K))^{1/2} \qquad (4\text{-}1)$$

where

τ = the fraction of thermal radiation transmitted through the atmosphere

Application of the point source method is shown in Figure 4.1, where ignition of

escaping gas from a pipeline rupture results in a flame of height " H". The point source is

placed in the center of the flame at H/2, and the burn radius (BR) is found from the

Pythagorean Theorem:

$$BR = \{D^2 - (H/2)^2\}^{1/2} \qquad (4\text{-}2)$$

By inserting Equation 4-1 into Equation 4-2, the following relationship is obtained:

$$BR = \{(\tau FQ/(4\pi K)) - (H/2)^2\}^{1/2} \qquad (4\text{-}3)$$

This is the basic form of the burn radius equation. The burn radius is function of the transmissivity of the thermal radiation through the atmosphere, the fraction of total heat radiated, the heat content of the escaping gas and the specified heat flux (or level of damage).

Based on information provided by various researchers for methane (20), the value of F can be reasonably estimated to be 0.2. Furthermore, API (35) discusses the work of Brzustowsi and Sommer (36) for calculating transmissivity of thermal radiation through the atmosphere. The authors indicate that τ can be found from the following equation:

$$\tau = 0.79(100/r)^{1/16}(100/D)^{1/16} \qquad (4\text{-}4)$$

where

r = relative humidity, %
D = distance to flame, feet

The authors caution that Equation 4-4 is "strictly applicable" when the flame is radiating at a temperature of 2240° F, relative humidity is greater than 10%, dry bulb temperature is 80° F and the distance from the flame is greater than 100 feet but less than 500 feet. However, the authors indicate that an "order of magnitude" estimate can be made under a wider range of conditions. Since the results from pipeline accident investigations typically show damage extending several hundred feet from the rupture, an estimate for τ is found by assuming a relative humidity of 50% and a distance to the flame of 500 feet (both of which are reasonable values):

$$\tau = 0.79(100/50)^{1/16}(100/500)^{1/16} = 0.746$$

Inserting the values of τ and F into Equation 4-3, the equation for the burn radius becomes:

$$BR = \{(0.746(0.2)Q/(4\pi K)) - (H/2)^2\}^{1/2}$$

$$= \{(0.011873Q/K) - (H/2)^2\}^{1/2} \tag{4-5}$$

The total heat content of the escaping gas (Q) in Btu/hr can be found by multiplying the

heat content of natural gas (1,000 Btu/scf) by the volumetric flow rate of the escaping gas

(scf/hr):

$$Q=1,000(V') \tag{4-6}$$

where

V' = Volumetric flow rate (scf/hr)

If Equation 4-6 is combined with Equation 4-5, the expression for the burn radius

becomes:

$$BR = \{(11.873(V')/K) - (H/2)^2\}^{1/2} \tag{4-7}$$

The following sections of this chapter will provide discussions of the three variables in

equation 4-7: heat flux (K); gas flow rate (V'); and flame height (H).

4.1.2 Heat Flux Values

Examples of heat flux values corresponding to specific consequences are provided in

Table 4.1. These values were obtained from a review of the literature. A comprehensive

listing of heat flux values can be found in Appendix A.

Table 4.1

Heat Flux Values

Heat Flux		Reference	
Btu/hr ft^2	kW/m^2	Number	Consequence
222**	0.7	37	Unprotected skin becomes red and burns with prolonged exposure.
317	1	34	Solar heat flux during a hot summer day.
555**	1.75	37	Threshold of pain reached after 60 second exposure.
634**	2.0	37	Damage to PVC - insulated cables.
2,000	6.5	38	Maximum tolerable heat flux for short-term (i.e., 20 seconds) exposure for people.
3,994**	12.6	39	Dry, unpainted, wood that is not protected by shelter is ignited by a small brand or spark. This is called "piloted ignition".
9,985**	31.5	40	Wooden buildings, paper, window drapes and trees will spontaneously ignite after a few minutes exposure.

** Calculated using the relationship 1 Btu/hr ft^2 = 3.1546 Watts/square meter (W/m^2).

From several of the above examples, it can be seen that the level of thermal radiation damage may not only depend on the intensity of the heat flux, but also on the length of time that the receptor is receiving that heat flux. For example, at a heat flux

intensity of 9,985 Btu/hr ft^2, spontaneous ignition of wooden buildings occurs *after a*

few minutes. At 555 Btu/hr ft^2, the pain threshold is reached *after 60 seconds*.

Therefore, a safe separation distance will be considered to afford protection from a certain

level of heat flux for a specific time period. If that time period is exceeded, damage may

occur.

In order to estimate a safe separation distance, a level of protection is chosen, such

as protecting wooden buildings from spontaneous ignition for a few minutes. The

corresponding heat flux is found and inserted into Equation 4-7 as the appropriate

K-value. The procedure described in the next section is used to determine an appropriate

gas flow rate.

4.1.3 Determination of Gas Flow Rate

In order to determine the flow rate of gas escaping from a pipeline rupture, a variation of

Equation 2-15 will be used. The use of Equation 2-15 for determining the gas rate from

full bore ruptures is similar to the procedure used by Wilson (11), in which Equation 2-5

(for choked conditions) was used to determine the initial mass release rate from ruptures.

While choked conditions would likewise be expected with high pressure pipeline

punctures and blowdowns, the use of Equation 2-15 provides a convenient means of

estimating gas flow rate knowing only the pipeline diameter and an upstream pressure.

Recall that Equation 2-15, as presented below, is applicable for use during pipeline

punctures and blowdowns:

$$Q = D^2 P_1 \qquad\qquad (2\text{-}15)$$

As described previously, "Q" represents the volume of gas in Mcf/hr at a pressure of 14.9 psi and 60° F with a specific gravity of 0.60. In other words, Q provides the flow rate at approximately standard conditions. To use Equation 2-15, "D" (the diameter of the nipple or orifice in inches) is considered to be the nominal diameter of the pipeline for a worst-case blowdown scenario. Since "P_1" is the absolute pressure (in psi) at a point upstream from the opening, this variable will represent the pre-rupture incident operating pressure at the location of the rupture.

By examining the rate of gas lost through actual pipeline ruptures and comparing this rate with values obtained using Equation 2-15, an evaluation can be made as to whether a modifying factor must be applied to Equation 2-15. Table 4.2 presents eight pipeline accidents investigated and reported upon by the NTSB and the Canadian TSB in which the following parameters are known: pipeline diameter, incident operating pressure, rupture isolation time, and volume of gas lost.

Table 4.2
Pipeline Rupture Parameters

Accident Report Number	Reference Number	Pipeline Diameter Inches	Incident Operating Pressure psia	Isolation time hours	Total Volume of Gas Lost, scf
P90H0606	41	12.75	696.7	2.75	3.78×10^7
83-02	42	20	834.7	1.42	4.68×10^7
P91H0041	43	20	933.7	0.75	3.13×10^6
79-FP006	44	30	574.7	2.83	2.01×10^8
P90H1006	45	30	726.7	0.58	8.73×10^7
95-01	3	36	984.7	2.50	2.97×10^8
P94H0036	46	36	1014.7	0.63	1.48×10^8
P94H0003	47	42	1221.7	6.67	3.52×10^8

As described in Chapter 2, critical conditions produce the maximum gas flow rate. Therefore, it will be assumed that, using the incident operating pressure, Equation 2-15 (or Equation 2-15 with a modifying factor) will predict a maximum initial flow rate. Furthermore, this maximum flow rate will decrease as the pipeline is depressurized. The maximum flow rate will be identified as V_{CALC}.

Another flow parameter that can be calculated is the average flow rate, V_{AVG}. The average flow rate represents the total volume of gas that is lost divided by the time required to isolate the ruptured pipeline segment. Since V_{AVG} represents an average, or constant value of flow, the flow rate remains the same from initiation of rupture to isolation of the pipeline.

Table 4.3 presents the results of computations of V_{AVG}, V_{CALC}, and the ratio V_{AVG}/V_{CALC}.

Table 4.3
Flow Rate Parameters

Accident Report Number	V_{AVG} scf/hr	V_{CALC} scf/hr	V_{AVG}/V_{CALC} Ratio
P90H0606	1.37×10^7	1.13×10^8	0.12
83-02	3.30×10^7	3.34×10^8	0.10
P91H0041	4.17×10^6	3.73×10^8	0.01
79-FP006	7.10×10^7	5.17×10^8	0.14
P90H1006	1.51×10^8	6.54×10^8	0.23
95-01	1.19×10^8	1.28×10^9	0.09
P94H0036	2.35×10^8	1.32×10^9	0.18
P94H0003	5.28×10^7	2.16×10^9	0.02

For the accidents listed above, V_{AVG} is found to vary between 1% and 23% of V_{CALC}, with an average of 11%. Since during an actual pipeline rupture the initial mass flow rate will be very high, the flow rate would not be expected to have a value lower than V_{AVG}. Furthermore, if the assumption is made that the actual flow rate will not be greater than V_{CALC}, then the actual initial flow rate would be expected to lie between V_{AVG} and V_{CALC}. Therefore, assume that the initial flow rate is found at the midpoint between $0.11V_{CALC}$ (i.e., V_{AVG}) and V_{CALC}, which is equal to $0.56\ V_{CALC}$. This result is very similar to the result found by Wilson and expressed as Equation 2-11, where the initial mass release rate was found to be 50% of the value found using Equation 2-5 (12).

Inserting the maximum initial flow rate into the point source equation would not accurately reflect thermal radiation conditions, since the heat flux at a given receptor location will decrease with the decreasing gas flow. Therefore, assume that a representative gas flow rate to use in the point source equation exists between 0.56 V_{CALC} and V_{AVG} (or 0.11 V_{CALC}). The midpoint of this range is 0.34 V_{CALC}, which then leads to the following equation for determining flow rate:

$$V'=(1,000)(0.34)D^2P \qquad (4\text{-}8)$$

where

V'= Gas flow rate, scf/hr
D = Pipeline Diameter, inches
P = Incident Operating Pressure, psia

It should be noted that multiplication by 1,000 in Equation 4-8 converts Mcf/hr to scf/hr.

By inserting Equation 4-8 into Equation 4-7, the following relationship is

obtained:

$$BR = \{(11.873(1,000)(0.34)\ D^2 P/K) - (H/2)^2\}^{1/2}$$

$$= \{(4,036.82)\ D^2 P/K) - (H/2)^2\}^{1/2} \qquad (4\text{-}9)$$

The burn radius is now expressed as a function of the pipeline diameter, operating

pressure, heat flux and the flame height. In the next section of this chapter, an expression

for the flame height will be developed which can be inserted into Equation 4-9.

4.1.4 Determination of Flame Height

In a manner similar to the method for determining the expression for gas flow rate, the

information obtained from actual pipeline accidents can be used to estimate flame height.

Recalling the Hawthorne Equation that was provided in Chapter 2:

$$L/D = (5.3/C_T)\{(T_F/(\alpha_T T_N))(C_T + (1-C_T)(M_S/M_N)\}^{1/2} \qquad (2\text{-}16)$$

where, in dimensions of mass (M), length (L), time (t) and temperature (T), the various

terms are:

L = visible flame length (L)
D = nozzle diameter (L)
T_F = adiabatic flame temperature (absolute T)
T_N = temperature of nozzle fluid (absolute T)
M_S = molecular weight of surrounding fluid (unitless)
M_N = molecular weight of nozzle fluid (unitless)
C_T = mol fraction of nozzle fluid in the unreacted stoichiometric mixture (decimal)
α_T = mols of reactants/mols products for the stoichiometric mixture (decimal)

Equation 2-16 is applicable to vertical flame jets in still air. Since the assumption was made that the flame jet from a pipeline rupture will be vertical, the equation can be used in the evaluation of flame height.

Using the values of $C_T = 0.091$, $\alpha_T = 1$ and $T_F/T_N = 7.4$ for methane (20) in Equation 2-16, along with a molecular weight of 29.0 (48) for air and a molecular weight of 16.042 for methane (8), the following expression is obtained:

$$L/D = (5.3/0.091)\{(7.4/1)(0.091+(1-0.091)(29.0/16.042))\}1/2$$

$$= 208.6 \qquad\qquad (4\text{-}10)$$

Therefore, for a given gas, the flame length is directly proportional to the jet (or nozzle) diameter. This observation can be applied to the NTSB pipeline accident data, where estimation of flame heights are provided. If the assumption is made that the jet diameter is equal to the pipeline diameter for a full bore rupture, the following is obtained:

Table 4.4
Flame Height Data

Accident Report Number	Reference Number	Diameter (D) Inches	Diameter (D/12) Feet	Reported Flame Height (H), Feet	H/(D/12)
86-009	49	20	1.67	300	180
95-01	3	36	3.00	450	150
77-01	50	20	1.67	200	120
71-01	51	14	1.17	125	107
87-01	2	30	2.50	450	180

The average $H/(D/12)$ is 147, so assume that this ratio can be used to estimate

flame height. Therefore, the following relationship is obtained:

$$H=147(D/12)$$

$$=12.25(D) \tag{4-11}$$

where

D = Pipeline diameter (in)

While it is understood that the calculated L/D value (208.6) is of a similar order of

magnitude to the average H/D value (147), it is this average H/D value that will be used

in subsequent calculations. This is justified since the original work of Hawthorne (21)

used small diameter nozzles to produce the jet instead of full pipeline diameters.

By inserting equation 4-11 into Equation 4-9, the final burn radius equation is

found:

$$BR = \{(4,036.82)\ D^2P/K) - (12.25D/2)^2\}^{1/2}$$

$$= D\{(4,036.82)P/K) - 37.52\}^{1/2} \tag{4-12}$$

where

BR = Burn Radius (ft)
D = Pipeline Diameter (in)
P = Incident operating pressure (psia)
K = Heat flux (Btu/hr ft^2)

Equation 4-12 provides a means by which the burn radius (and hence the safe separation distance) can be found knowing only the pipeline diameter, incident operating pressure and the level of damage (i.e., heat flux) to be considered. Since pipeline operating pressures are typically specified as gauge pressures, Equation 4-12 can be modified for application to gauge pressures by substituting the quantity (P' + 14.7) for P, where P' is the incident operating pressure in psig.

Using Equation 4-12, charts can be developed for estimating the burn radius. The method for constructing these charts is presented in the next section.

4.1.5 Construction of Charts to Predict Safe Separation Distances

The following procedure is used to construct charts for the rapid estimation of safe separation distances. The first step involves deciding what degree of thermal radiation damage to consider. For example, the damage might be spontaneous ignition of wooden buildings after a few minutes exposure to the ignited gas. Protection for a few minutes may allow enough time for emergency responders to arrive at the scene and initiate protective measures (such as watering down the buildings). Based on the information in both Appendix A and Table 4, the heat flux corresponding to the specified level of damage is 9,985 Btu/hr ft^2. This value is inserted into Equation 4-12 for K:

$$BR = D\{(4,036.82)P/9,985) - 37.52\}^{1/2} \qquad (4\text{-}13)$$

Equation 4-13 is an expression of the burn radius as a function of only diameter and incident operating pressure. For various pipeline diameters, graphs are then constructed of the burn radius (on the y-axis) and the incident operating pressure (on the x-axis). In
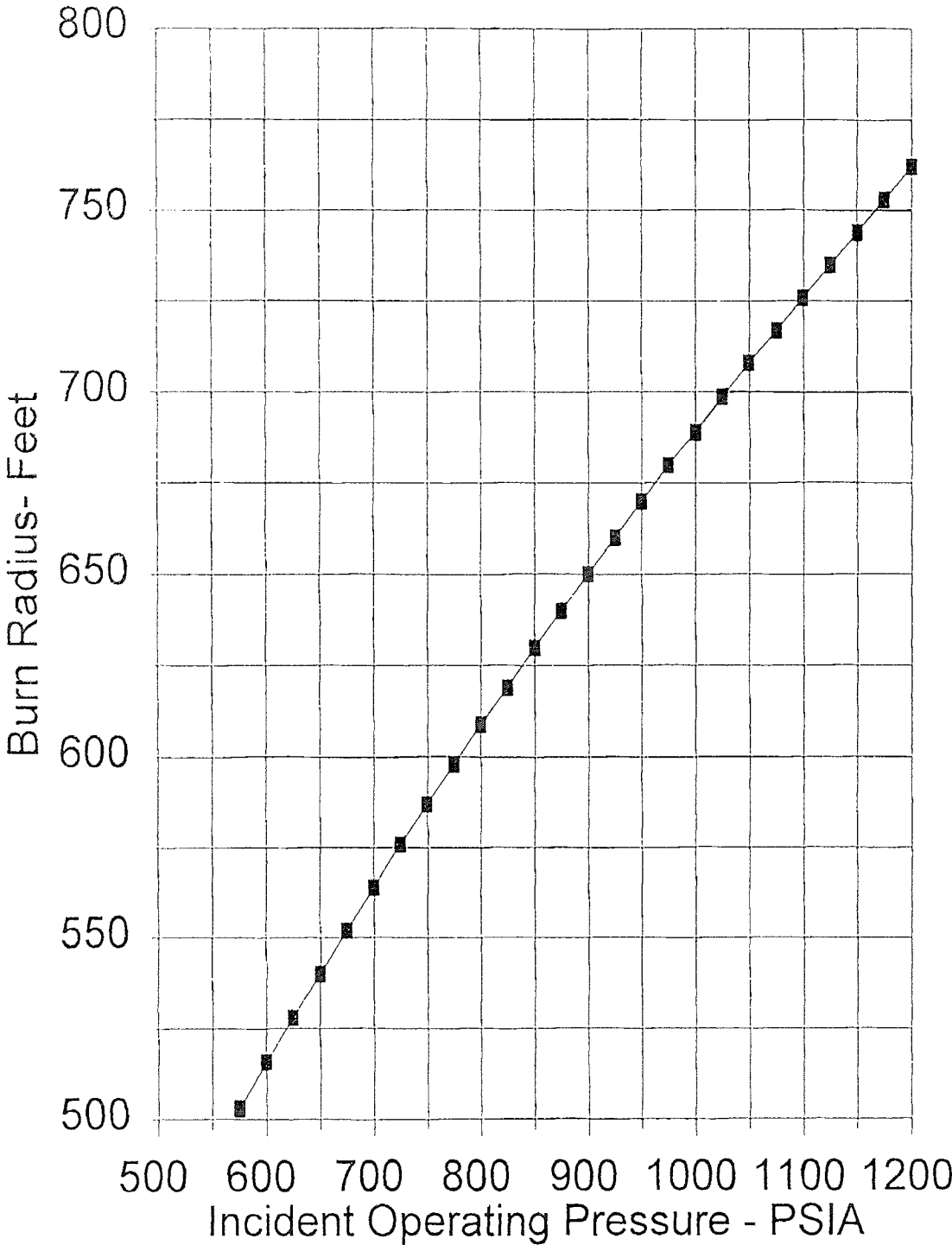
Figure 4.2 - Example of a Burn Radius Chart for a 36"
Diameter Pipeline, K = 9,985 Btu/hr sq. ft.

the example, a pipeline diameter of 36" can be used with incident operating pressures in the range of 575 psia to 1,200 psia to construct a chart similar to the one shown in Figure 4.2. Once the graph is completed, it can be used either to determine a safe separation distance given a specified incident operating pressure, or to determine the incident operating pressure required to maintain a specified safe separation distance.

Charts for estimating safe separation distances (or burn radii) are provided in Appendix B for heat fluxes (from Appendix A) of 3,962 Btu/hr ft^2 (piloted ignition of wood); 6,340 Btu/hr ft^2 (blistering of bare skin in 4 seconds and 1 % lethality in 20 seconds); 9,510 Btu/hr ft^2 (causes third degree burns in 30 seconds); and 9,985 Btu/hr ft^2 (spontaneous ignition of wooden structures after a few minutes). The charts have been developed for pipeline diameters of 14", 16", 18", 20", 24", 30" and 36", with incident operating pressures in the range of 575 psia to 1,200 psia. It should be noted that the charts do not consider that portion of the heat flux due to solar radiation. An accurate value of the solar heat flux would be dependent on factors such as the weather conditions, the time of day and the time of year. Since the solar heat flux amounts to only a few hundred Btu/hr ft^2 while the non-solar heat flux is several thousand Btu/hr ft^2, omission of this factor will not significantly affect the results.

Equation 4-12 will be used in the next chapter for comparing (for verification purposes) predicted values of burn radii using the model developed herein to information from actual pipeline accidents and to the results of prior research.

CHAPTER 5

COMPARISON OF METHOD TO PIPELINE ACCIDENT DATA
AND TO PREVIOUS RESEARCH

The previous chapter presented Equation 4-12 as a means by which a burn radius can be determined through knowledge of a pipelines's diameter, incident operating pressure and the level of thermal radiation damage. In this chapter, the utilization of Equation 4-12 will be evaluated by first comparing the results it produces to data from two highly documented pipeline accidents that occurred in the United States. These accidents (located in Edison, New Jersey and Lancaster, Kentucky) were selected for this detailed analysis since these were the only two accidents for which extensive descriptions of the thermal radiation damage could be obtained from the NTSB. Additionally, an attempt is made to compare the results from Equation 4-12 with other pipeline accidents in which less extensive information is reported.

The second part of this chapter will compare the results of Equation 4-12 to separation distance calculations that have been developed by other countries (i.e., Great Britain and the Netherlands) through the use of the principles of hazard analysis.

5.1 Comparison to Pipeline Accident Data

This section provides a comparison of burn radii obtained from actual pipeline rupture events to corresponding estimates developed through use of Equation 4-12. Since review of the pipeline accident information reveals that burn patterns are not truly symmetric (due to numerous factors including variation in wind velocity and direction during a rupture condition), the actual burn radii will be defined conservatively as the farthest horizontal distance from the rupture at which the specified level of thermal radiation damage is observed. Since the point source method assumes a circular (i.e. symmetric) burn pattern around the rupture, there may be locations around the rupture for which Equation 4-12 overestimates the extent of thermal radiation damage based upon the above noted assumption. However, comparison of the results obtained from Equation 4-12 to the maximum horizontal burn distances is an approach which provides a level of confidence that the estimated burn radii should approximate, and not be significantly less than, the actual burn radii (which would be undesirable in actual practice).

The following section evaluates the damage produced by the pipeline rupture which occurred in Edison, New Jersey, on March 23, 1994.

5.1.1 PAR 95-01

This Pipeline Accident Report (3) describes the rupture of a 36 inch natural gas transmission pipeline owned and operated by the Texas Eastern Transmission Corporation. The rupture occurred at approximately 11:55 p.m. on March 23, 1994, on the property of Quality Materials, Inc. in Edison, New Jersey. Ignition of the escaping
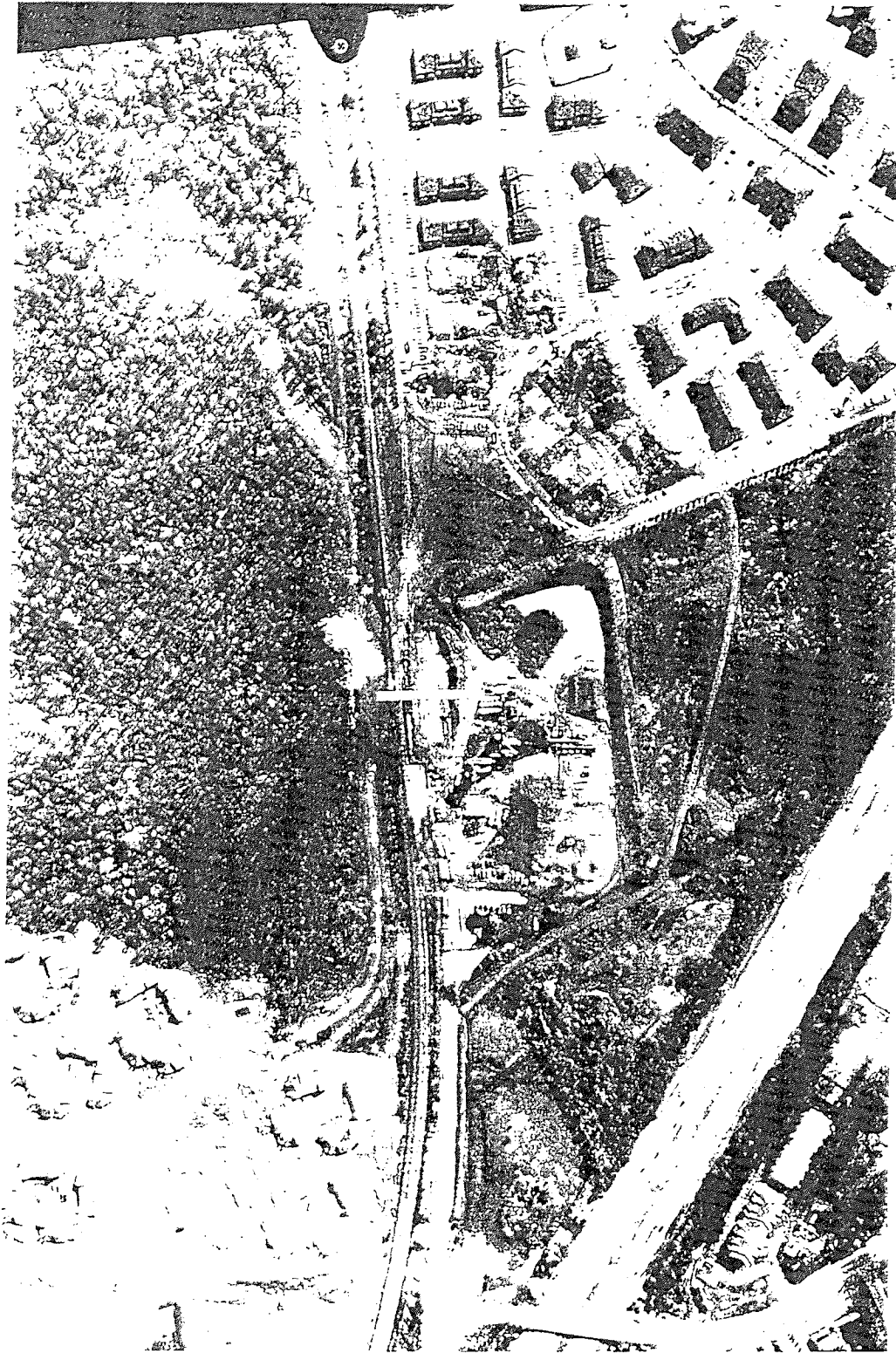
Figure 5.1 - Location of Edison, New Jersey Accident

gas occurred within 2 minutes after the rupture, producing flames 400 to 500 feet high. While no deaths were directly attributed to the accident, the rupture produced extensive damage including the destruction of several buildings of a nearby apartment complex. The total cost of the damage exceeded 25 million dollars. The NTSB determined that the probable cause of the rupture was mechanical damage to the exterior pipeline surface. The damage reduced the pipeline wall thickness and probably resulted in a crack that grew to a critical size.

The accident location is shown in a copy of the aerial photograph presented as Figure 5.1. This photograph (without the "+" symbol) was obtained from the NTSB (C. Batten: personal communication, February 1996), and was taken on March 30, 1994. In the photograph, north is approximately located to the upper right, and the location of the rupture is identified with the "+" symbol. The Durham Woods Apartments (i.e., the apartment complex which received significant damage) are located in the lower right of the photograph. An enlarged portion of this photograph depicts the rupture location (without the "+" symbol) and the Durham Woods Apartments, and is presented in Appendix C as Figure C.1. Another figure is provided (see Figure C.2) which is based on a sketch obtained from the NTSB (C. Batten: personal communication, February 1996) identifying the various buildings in the apartment complex.

As indicated previously. the rupture occurred at approximately 11:55 p.m., with ignition of the gas less than two minutes later. According to the PAR, the Edison Township Fire Department arrived at the accident scene at approximately 12:02 a.m. At that time, building number 12 was "fully involved" in fire, and the three buildings adjacent to it were quickly becoming involved. These are buildings numbered 9, 10 and 11 as shown on Figure C.2. Based on a discussion with Edison Township (personal communication, February 1996), buildings numbered 11, 12 and 24 were involved in fire upon arrival of the Fire Department, and buildings numbered 7, 8, 16, 19, 23 and 25 would have burned if these structures were not wetted down (it should be noted that buildings numbered 20, 21 and 22 were also destroyed by the accident).

If the buildings were set back from the rupture at a distance beyond the location of buildings 9, 10, 11, 12 and 24 (i.e., those buildings which were apparently involved in fire after a few minutes exposure to thermal radiation), then this distance would have provided protection for a few minutes from spontaneous ignition. This distance can be estimated using Equation 4-12, and verified by comparing the calculated burn radius to the actual location of the damage. However, since an appropriate scale could not be obtained for Figure C.1 (since a scale was not provided with Figure 5.1), a scale for this figure must first be developed.

Figure C.3 is an illustration of a portion of the accident location, and is based on a diagram that was likewise obtained from the NTSB (C. Batten: personal communication, February 1996). Using the existing scale on this figure, a landmark is selected which is clearly defined in both Figure C.3 and Figure C.1 and which can be used for scale comparison. The landmark chosen is the north-south length of buildings numbered 21, 22 and 23 (which have similar lengths). Using the scale on Figure C.3, the length of these buildings is approximately 158 feet. The length of the image of building number 23 on the author's original Figure C.1 is 0.625 inches. Therefore, the scale for Figure C.1 is 158 feet per 0.625 inches, or 253 feet per inch. The white bar at the bottom of Figure C.1 represents a length of 253 feet.

In order to use Equation 4-12, an appropriate heat flux must first be selected. Since the concern is protecting structures from spontaneous ignition for several minutes, a heat flux of 9,985 Btu/hr ft^2 from Appendix A will be selected. Inserting this value for heat flux into Equation 4-12, as well as the pipeline diameter of 36 inches and the incident operating pressure of 984.7 psia, the burn radius becomes:

$$BR = 36\{[(4{,}036.82)(984.7)/(9{,}985)] - 37.52\}^{1/2}$$

$$= 684 \text{ feet}$$

On Figure C.1, the distance from the rupture (taken as the midpoint of the open space between the two exposed ends of pipeline, or the center of the "+" symbol on Figure 5.1) and the approximate midpoint of the footprint for building number 9 (i.e., the building farthest from the rupture that was becoming involved in fire when the Fire Department arrived) is 772 feet. The estimated burn radius differs from the actual burn radius by less

than 12 percent. It can therefore be seen that the predicted burn radius does in fact

approximate the distance to those buildings which were involved in fire a few minutes

after the rupture.

A burn radius can likewise be estimated for determining the distance beyond

which buildings will not ignite at all. For the Edison accident, this distance would extend

beyond the location of those buildings which were wetted down. In order to predict the

distance with Equation 4-12, a heat flux of 3,962 Btu/hr ft^2 is selected From Appendix A.

This is the heat flux at which piloted ignition of wood occurs, so below this heat flux

wood is not expected to ignite. From Equation 4-12, the burn radius becomes:

$$BR = 36\{[(4,036.82)(984.7)/(3,962)] - 37.52\}^{1/2}$$

$$= 1,119 \text{ feet}$$

Using the same scale as before, the distance from the rupture point to the midpoint

of building number 25 (i.e., the building farthest from the rupture that was wetted down)

is 1,101 feet. The predicted burn radius is therefore very similar to the actual distance

determined from Figure C.1, with a difference of less than 2 percent.

The above analysis has shown that Equation 4-12 provides a good estimation of

burn radii for the Edison, New Jersey accident. The next section presents an analysis of

the damage associated with an accident that occurred near Lancaster, Kentucky.
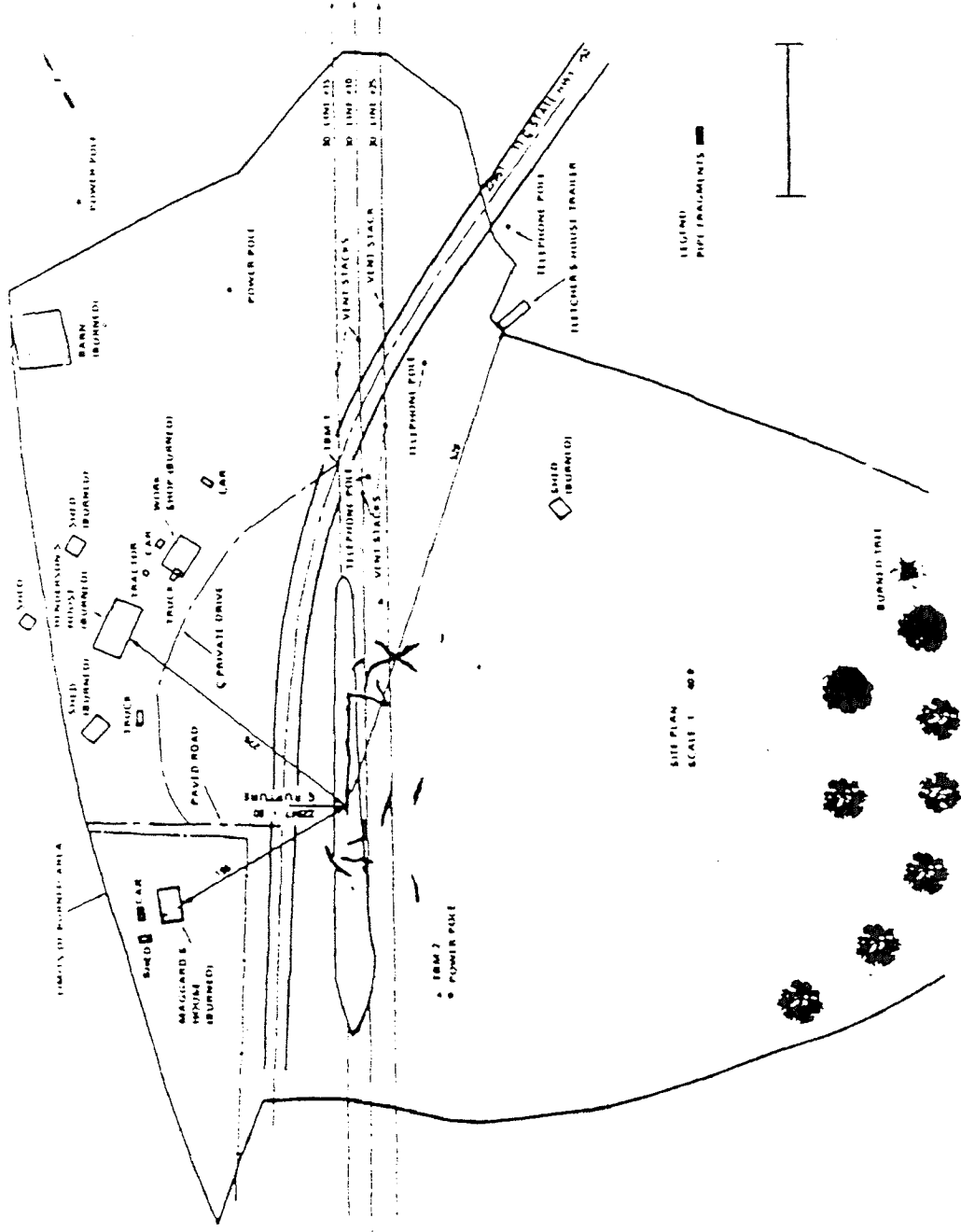
Figure 5.2 – Location of Lancaster, Kentucky Accident

5.1.2 PAR 87-01

The accident described in this PAR (2) involves the rupture of a 30-inch diameter

pipeline owned by the Texas Eastern Gas Pipeline Company. The rupture and fire, which

occurred near Lancaster, Kentucky, injured eight persons and resulted in $500,000

damage to property adjacent to the pipeline. A depiction of the accident scene

(reproduced from the PAR) is presented in Figure 5.2. The NTSB identified the probable

cause of the accident as being the failure of the Texas Eastern Gas Pipeline Company to

perform a comprehensive investigation of detected corrosion damage and to repair this

damage.

The PAR indicates that the rupture occurred at 2:05 a.m. Based on the transcript

of a hearing conducted by the NTSB (52), emergency responders arrived at the scene at

2:07 a.m and found that the area beginning at the Fletcher's trailer and extending to the

structures behind the Henderson's home was involved in fire (see Figure 5.2).

Specifically, during the aforementioned hearing, Mr. Mike Murphy of the Garrod County

Disaster and Emergency Services states that upon arrival at the accident scene:

> "The area from approximately the Fletcher's House Trailer back through this area,
>
> around the cross - - we could see quite easily that the Maggard Home was
>
> involved, that the Henderson Home was involved, the barns back in this area. So,
>
> basically, a large ball of fire in the area that was mentioned, however, there was a
>
> tremendous amount of exposure type fire from the other buildings that we have
>
> talked about - - the barn. There was a significant amount of grass in the area on
>
> fire."

In a manner similar to that used for the Edison, New Jersey accident, a burn radius

can be estimated using a heat flux of 9,985 Btu/hr ft^2, since structures were ignited a few

minutes after the rupture. Inserting this value once again into Equation 4-12, with the

pipeline diameter of 30 inches and the incident operating pressure of 1001.7 psia, the

burn radius becomes:

$$BR = 30\{[(4,036.82)(1,001.7)/(9,985)] - 37.52\}^{1/2}$$

$$= 575 \text{ feet}$$

Although Figure 5.2 does not have a scale, a scale can be determined using the

276 foot distance identified on the figure which corresponds to the distance from the

rupture to the Henderson's house. On the original figure in the PAR, the 276 foot

distance corresponds to 1.675 inches. Therefore, the appropriate scale is 276 feet per

1.675 inches, or 165 feet per inch. The black line in the lower right of Figure 5.2

represents this 165 foot length. Using this scale, the distance from the rupture to the

midpoint of the footprint of the burned barn (i.e., the structure farthest from the rupture

which was presumably burning a few minutes after the rupture) is 585 feet. The

difference in the calculated versus the actual burn radius is less than 2 percent. As with

the New Jersey accident, the predicted burn radius corresponds closely to the actual

damage that was observed.

The information obtained for this accident is also sufficient for comparing burn

radii estimated with Equation 4-12 to distances resulting in injuries to people. Based on

the information provided in the hearing transcript (52), Mr. and Mrs. Henderson

experienced second and third degree burns while their 12 year old daughter suffered

second degree burns. The Hendersons escaped from the scene of the rupture by leaving their house through the back door, running through a field and "over a bank at the river cliff" where the heat flux was low enough to allow them to rest.

Predicting the burn radii corresponding to a specific level of injury is more complex than predicting the distance for structural damage. Unlike structures, people can escape from the scene of a rupture and consequently experience heat fluxes which decrease with time and distance. Furthermore, escape velocities (i.e., the speed at which people run from the rupture) can vary as well as the level of clothing which the affected people are wearing (32). Although the exact path that the Henderson's took to escape is unknown, and the level of clothing they wore was not available in the information that was reviewed, it is known that they experienced a specific level of injury (i.e. second and third degree burns).

Using the specifications of the ruptured pipeline, one can show that Equation 4-12 predicts the occurrence of second and third degree burns to persons fleeing directly away from the rupture. First, a representative escape velocity must be determined. Hockey and Rew (32) provide escape velocities of 1 m/s (3.28 ft/s), 2.5 m/s (8.2 ft/s), 4 m/s (13.1 ft/s) and 6 m/s (19.69 ft/s). A representative escape velocity is considered to be 2.5 m/s (8.2 ft/s), which would reasonably be expected since people are fleeing the fire in the early morning hours after being asleep. Furthermore, it is assumed that the house provides shelter from the thermal radiation for the time in which the residents react to the accident (i.e., several seconds). From Figure 5.2, if a person exits from the rear of the Henderson's house (and, from Figure 5.2, knowing that the house is approximately 29 feet wide), that

person will be approximately 276 + 29 = 305 feet from the rupture when first exposed to

thermal radiation outside the house. After the first second, the person will be

305 + 8.2 = 313.2 feet from the rupture; after two seconds the separation distance

increases to 305 + 2(8.2) = 321.4 feet, and so on. Equation 4-12 can be rewritten as

follows in order to express heat flux as a function of separation distance, pipeline

diameter and incident operating pressure:

$$K = 4036.82(P)/[(BR^2/D^2) + 37.52]$$ (5-1)

Through use of Equation 5-1, the relationship of incident heat flux to exposure

time can be examined for this accident. Furthermore, the following equation from

Appendix A can be used for determining the average heat flux which will result in severe

blistering:

$$q_2 = 50/t_c^{0.71}$$ (5-2)

where:

q_2 = Average heat flux (kW/m^2)
t_c = Duration of exposure (seconds)

Table 5.1 provides the incident heat flux experienced over the first thirty seconds

by a person fleeing the Lancaster, Kentucky rupture.

Table 5.1
Heat Flux Experienced at Lancaster, Kentucky Accident

Time Seconds	Distance from Rupture, feet	Heat Flux - Btu/hr ft^2	
		Equation 5-1	Equation 5-2*
0	305	28,703	-------
2	321.4	26,552	9,689
4	337.8	24,610	5,923
6	354.2	22,856	4,442
8	370.6	21,269	3,621
10	387.0	19,829	3,090
12	403.4	18,521	2,715
14	419.8	17,330	2,434
16	436.2	16,244	2,214
18	452.6	15,252	2,036
20	469.0	14,343	1,889
22	485.4	13,510	1,766
24	501.9	12,740	1,660
26	518.3	12,035	1,568
28	534.7	11,385	1,488
30	551.1	10,784	1,417

* Values converted from kW/m^2 using the relationship 1 Btu/hr ft^2 = 3.1546 kW/m^2

In Figure C.4 the information from Table 5.1 is plotted on the chart of heat flux versus exposure time. It can be seen that at all times considered, the estimated heat flux (calculated from Equation 5-1) is greater than the average heat flux necessary to cause severe blistering. Therefore, Equation 5-1 correctly predicts that persons fleeing the rupture will suffer at least second degree burns. Furthermore, it was previously mentioned that a heat flux of 9,510 Btu/hr ft^2 will cause third degree burns in 30 seconds. Equation 5-1 predicts that, at an escape velocity of 8.2 ft/s, third degree burns should occur since the estimated heat flux is larger than 9,510 Btu/hr ft^2. As documented by the NTSB, Mr. and Mrs. Henderson suffered both second and third degree burns.

While the available damage information from other pipeline accidents is not as extensive as for the two pipeline accidents that have been considered, the following section compares the available burn radii information to the estimates produced by Equation 4-12.

5.1.3 Other Data

While the information that was reviewed for the following accidents is not as detailed as the information obtained for the two accidents described above, burn radii estimated with Equation 4-12 are compared to the approximate burn radii that are based on the available damage information from other accidents documented by the NTSB. It should be noted that the following specific accidents were selected for comparison since a sufficient amount information is available to approximate burn radii and the incident operating pressures and pipeline diameters are within the ranges of Equation 4-12 (i.e., 575 to 1,200 psia and 14 inches to 36 inches in diameter).

1.   **PAR 71-01 (51) - Houston, Texas - September 9, 1969:** This accident involved the rupture of a 14 inch pipeline at a pressure of approximately 789 psig (803.7 psia). Figure 2 in the PAR indicates that the roof of a house 300 feet from the rupture was scorched. In a manner similar to the analysis performed for the Edison, New Jersey accident, a heat flux of 3,962 Btu/hr ft^2 can be used to estimate the distance beyond which structures will not ignite. Using Equation 4-12, the burn radius becomes:

$$BR = 14\{[(4,036.82)(803.7)/(3,962)] - 37.52\}^{1/2}$$

$$= 391 \text{ feet}$$

The estimated burn radius represents a difference of 30 percent from the actual value.

2. **PAR 75-02 (53) - Bealeton, Virginia - June 9, 1974:** The accident, which involved the rupture of a 30 inch pipeline operating at 718 psig (732.7 psia), produced a burn area 700 feet long and 400 feet wide. Figure 4 of the PAR indicates that the burn area was not symmetrical, but rather downstream of the rupture. Therefore, the actual burn radius will be considered to be 700 feet. The estimated burn radius is found as follows, using Equation 4-12 with a heat flux of 3,962 Btu/hr ft^2 (i.e. the heat flux for piloted ignition of wood, which is assumed to be the heat flux associated with the extent of a burn area):

$$BR = 30\{[(4,036.82)(732.7)/(3,962)] - 37.52\}^{1/2}$$

$$= 799 \text{ feet}$$

This value represents a difference of 14 percent from the actual value.

3. **PAR 77-01 (50) - Cartwright, Louisianna - August 9, 1976:** The rupture of a 20-inch pipe operating at 770 psig (784.7 psia) resulted in a burn area of approximately 12 acres. It is unclear from the information that was reviewed whether or not the burn area was symmetric. Figure 2 of the PAR indicates damage surrounding the pipeline. Complicating matters is the fact that horizontal flames vented from the rupture for a distance of 100 to 150 feet. If a symmetric burn area is considered, then a burn radius can be found by first calculating the

total burn area in square feet . Since one acre represents 43,560 square feet, the

total burn area is 12(43,560) = 522,720 ft^2. From the equation for the area of a

circle (i.e., area = π[radius]^2) , the actual burn radius becomes:

$$BR = (522,720/\pi)^{1/2} = 408 \text{ feet}$$

By comparison, use of Equation 4-12 with a heat flux of 3962 Btu/hr ft^2 produces

the following:

$$BR = 20\{[(4,036.82)(784.7)/(3,962)] - 37.52\}^{1/2}$$

$$= 552 \text{ feet}$$

For this accident, the estimated burn radius differs from the actual value by 35

percent.

4.   **DCA-85-FP-003 (54) - Jacksonville, Louisianna - November 25, 1984:** The

pipeline involved in this accident had a diameter of 30 inches and was operating at

1,016 psig (1,030.7 psia). A non-symmetrical damage area was produced, with

the rupture incinerating an area 900 feet north, 500 feet south and 180 feet to the

east and west of the rupture. If the burn radius is considered to be the maximum

linear distance from the rupture to the edge of the incinerated area, the radius is

then 900 feet. Again, using Equation 4-12 and a heat flux of 3,962 Btu/hr ft^2, the

estimated burn radius becomes:

$$BR = 30\{[(4,036.82)(1030.7)/(3,962)] - 37.52\}^{1/2}$$

$$= 955 \text{ feet}$$

The estimated burn radius differs from the actual burn radius by only 6 percent.

5.   **DCA-86-FP-009 (49) - Cale, Arkansas - February 24, 1986:** The information

available for this accident indicates that a 20 inch pipeline operating at 750 psig

(764.7 psia) ruptured and resulted in a burn area of 15 acres. Since 1 acre is

equivalent to 43,560 ft^2, the burn area (in square feet) is 15(43,560) = 653,400 ft^2.

Since details of the actual burn shape were not available, a circular burn patten is

considered, and the actual burn radius becomes (using the equation for the area of

a circle):

$$BR = (653,400/\pi)^{1/2} = 456 \text{ feet}$$

Using a heat flux of 3,962 Btu/hr ft^2, Equation 4-12 estimates the burn radius to

be:

$$BR = 20\{[(4,036.82)(764.7)/(3,962)] - 37.52\}^{1/2}$$

$$= 545 \text{ feet}$$

The difference in actual versus estimated values is approximately 20 percent.

6.   **PAR 87-01 (2) - Beaumont, Kentucky - April 27, 1985:** This accident

(described in the same report as the Lancaster, Kentucky accident) involved the

rupture of a 30 inch diameter pipeline operating at 990 psig (1,004.7 psia). The

accident incinerated an area 700 feet long and 500 feet wide. From Figure 3 in

the PAR, the burn area is not truly symmetric; rather, the longest dimension from

the rupture is approximately 500 feet. If this dimension is considered the actual

burn radius, then the estimated burn radius is:

$$BR = 30\{[(4{,}036.82)(1{,}004.7)/(3{,}962)] - 37.52\}^{1/2}$$

$$= 942 \text{ feet.}$$

This estimation represents the largest difference observed between predicted and actual burn radii, with a value of 88 percent.

5.2 Comparison to Separation Distances Developed through Hazard Analysis

5.2.1 Separation Distances Imposed in the Dutch Regulations

Earlier chapters discussed the Dutch regulations and the two types of separation distances that have been developed. The following discussion is based on personal communications from Hans van Poelje of N.V. Nederlandse Gasunie dated November 30, 1995; June 21, 1996; and September 30, 1996. The first type of separation distance is called a proximity, or building distance. This is the distance between a pipeline and residential buildings (or special structures) and corresponds to a 10^{-6} individual risk. The second type of distance is called a survey, or effect distance. This distance is determined for the purpose of identifying the location classification and corresponds to a 10^{-8} individual risk.

Based upon the available information, the building distances imposed in the Dutch regulations can be compared to distances that are estimated through use of Equation 4-12. However, since Equation 4-12 was not developed using risk assessment

techniques, a basis for comparison must first be selected. For comparison to building

distances, Equation 4-12 will use as a basis a heat flux of 9,985 Btu/hr ft^2. As was shown

earlier in this chapter, this level of thermal radiation results in the destruction of buildings

after a few minutes exposure.

The Dutch regulations specify three ranges of operating pressures (20 to 50 bar;

50 to 80 bar; and 80 to 110 bar) and pipeline diameters from 2 inches to 48 inches. In

order to provide a meaningful comparison, the range of pipeline diameters and pressures

used in the development of Equation 4-12 will be evaluated (i.e., diameters from 14 to 36

inches and pressures from 575 to 1,200 psia). By converting the Dutch pressure ranges

from bar to psia (by using the relationship 1.01325 bar equals 14.696 psia, and converting

gauge to absolute pressure), the pressure ranges become: 304.8 to 739.9 psia; 739.9 to

1,175.0 psia; and 1,175.0 to 1,610.1 psia. Although the midpoints of these ranges are

approximately 522.3 psia, 957.4 psia, and 1,392.6 psia, the three pressures which will be

used in Equation 4-12 are 522.3 psia; 957.4 psia and 1,200.0 psia. The pressure of

1,200.0 psia is used in lieu of 1,392.6 psia since 1,200.0 psia represents the upper limit of

pressure used to develop Equation 4-12, yet still lies within the third range.

The comparisons are presented in Table C.1 of Appendix C. It can be seen that

Equation 4-12 estimates significantly larger separation distances than the building

distances determined by the Dutch. However, as shown through the analyses of the

Edison, New Jersey and Lancaster, Kentucky accidents, the building distances developed by the Dutch will not be protective of structures. For a 36-inch diameter pipeline, the maximum building distance is 148 feet. This distance would clearly not have been protective of structures for the two aforementioned accidents.

Although the building distances and burn radii do not correspond, the trends in both at conditions of constant pressure (with varying diameter) and constant diameter (with varying pressure) do correspond closely. If pressure is held constant, then the following ratio is produced when using Equation 4-12:

$$BR_1/BR_2 = [D_1\{(4,036.82)P/K) - 37.52\}^{1/2}]/[D_2\{(4,036.82)P/K) - 37.52\}^{1/2}]$$

$$= D_1/D_2 \qquad\qquad (5-3)$$

If diameters are held constant, then Equation 4-12 produces the following ratios:

$$BR_1/BR_2 = [D\{(4,036.82)P_1/K) - 37.52\}^{1/2}]/[D\{(4,036.82)P_2/K) - 37.52\}^{1/2}]$$

$$= [\{((4,036.82)P_1/K) - 37.52\}/\{((4,036.82)P_2/K) - 37.52\}]^{1/2} \qquad (5-4)$$

Tables C.2 and C.3 of Appendix C present the comparison of building distances for constant pressure and diameter. It can be seen that both the Dutch approach and Equation 4-12 produce very similar trends (i.e. similar ratios) whether conditions of constant pressure or constant diameter are evaluated.

5.2.2 Separation Distances Determined by the British Health and Safety Executive

Hill and Catmur performed a study for the British Health and Safety Executive (31) to

evaluate how risks from various hazardous pipelines compared. As part of the above

study, distances from a vertical flame jet to a heat flux level of 10 kW/m^2

(3,170 Btu/hr ft^2) are provided for the pipelines under consideration. The authors

simulated the flame jet as an inclined line source with a receptor 1.5 meters (4.92 feet)

high at ground level. Furthermore, the authors indicate that the model which was used

provides the maximum view factor between the source and receptor, with the thermal

radiation being a function of the flame's emissivity, the transmissivity of the air, the view

factor and the radiant energy of the burning compound.

A comparison can be made between those distances and the distances estimated

using Equation 4-12. This comparison is presented in Table 5.2, for pipelines with

diameters within the range of 14 inches to 36 inches, and operating pressures within the

range from 500 psia to 1,200 psia:

Table 5.2
Comparison of Health and Safety Executive Results with Equation 4-12

Pipeline Diameter Inches	Pressure Barg	Psia	Separation Distances-Feet British*	Equation 4-12	Percent Difference
24	70	1030.0	820	857	4.5
16	70	1030.0	564	571	1.2

* Converted from meters using the relationship 1 meter equals 3.2808 feet.

The separation distances found from Equation 4-12 agree very closely with those
predicted by Hill and Catmur. If the ranges of diameters and pressures is extended to
include all of the natural gas pipelines in the study, the comparison in Table 5.3 is
obtained:

Table 5.3
Comparison of all Natural Gas Pipelines

Pipeline Diameter Inches	Pressure Barg	Psia	Separation Distances-Feet British*	Equation 4-12	Percent Difference
42	70	1030.0	1,385	1,499	8.2
24	70	1030.0	820	857	4.5
16	70	1030.0	564	571	1.2
6	70	1030.0	226	214	5.3
24	16	246.8	443	399	9.9
24	7	116.2	351	252	28.2
6	16	246.8	138	100	27.5
6	7	116.2	95	63	33.7

* Converted from meters using the relationship 1 meter equals 3.2808 feet.

It can be seen that even outside the range of diameters and pressures for which
Equation 4-12 was developed that this relationship still produces results which
approximate those of the British. The higher percent differences reflected in the last three
entries of Table 5.3 are probably due to the use of low operating pressures, either singly
or in combination with small diameters, which are outside the range for which Equation
4-12 was developed.

In summary, the analyses performed in this chapter have shown that the methodology developed in this thesis can be used to provide estimations of burn radii which are consistent with the burn radii determined for those accidents reported upon by the NTSB where there is ample documentation to conduct an analysis using the approach developed herein. Additionally, this methodology produces results consistent with the work published by the British Health and Safety Executive. While the burn radii estimated with Equation 4-12 are not similar to the building distances developed by the Dutch, it is clear from analyses performed in this chapter that the distances developed by the Dutch would not be protective of buildings. However, the trends in both the building distances and the distances estimated with Equation 4-12 (i.e., the variation of distance with both pressure and diameter) are found to be very consistent.

The next chapter provides additional evaluation of the methodology developed in this thesis. Specifically, an analysis will be performed in which the sensitivity of the burn radius is evaluated based on variations of the assumptions stated in Chapter 4.

CHAPTER 6

RESULTS AND DISCUSSION

The previous chapters have described the work that was performed for this thesis. This work included the development and testing of a relationship for the estimation of burn radii based on a pipeline's diameter and incident operating pressure. Consequently, the primary result of this thesis is Equation 4-12:

$$BR = D\{(4,036.82)P/K) - 37.52\}^{1/2} \qquad (4-12)$$

where

BR = Burn Radius (ft)
D = Pipeline Diameter (in)
P = Incident operating pressure (psia)
K = Heat flux (Btu/hr ft^2)

Through the use of Equation 4-12, charts have been developed which can be used to estimate burn radii. These charts are provided in Appendix B for heat flux values (listed in Appendix A) of 3,962 Btu/hr ft^2 (piloted ignition of wood); 6,340 Btu/hr ft^2 (blistering of bare skin in 4 seconds and 1 % lethality in 20 seconds); 9,510 Btu/hr ft^2 (causes third degree burns in 30 seconds); and 9,985 Btu/hr ft^2 (spontaneous ignition of wooden structures after a few minutes). Equation 4-12 and the charts in Appendix B are applicable to natural gas pipelines with diameters ranging from 14 inches to 36 inches and incident operating pressures in the range of 575 psia to 1,200 psia. The above ranges of diameters and pressures are applicable to most major natural gas transmission pipelines operating in the United States.

In Chapter 5, the sensitivity of Equation 4-12 to changes in pressure (at constant diameter) and to changes in diameter (at constant pressure) was discussed in relation to the work performed by the Dutch. In this chapter, an analysis will be performed to evaluate the sensitivity of Equation 4-12 to variations in heat flux. Furthermore, this analysis will be expanded to include the effects of variations in atmospheric transmissivity, wind direction and wind speed on the estimation of the burn radius.

6.1 Effect of Variation in Heat Flux on Burn Radius

Selection of an appropriate heat flux for use in Equation 4-12 is critical in the estimation of an appropriate burn radius. It is therefore worthwhile to evaluate the effect that a variation in heat flux can have on the burn radius. Equation 4-12 was developed for use with natural gas pipelines having diameters from 14 inches to 36 inches and incident operating pressures from 575 psia to 1,200 psia; therefore, the following conditions (which span the range of diameters and pressures) will be used in the analysis:

Table 6.1
Pipeline Conditions

Pipeline Diameter	Incident Operating Pressure
14 Inches	575 psia
14 Inches	1,200 psia
36 Inches	575 psia
36 Inches	1,200 psia

In addition, since heat flux values from 3,962 Btu/hr ft^2 to 9,985 Btu/hr ft^2 were shown

in Chapter 5 to provide results (i.e., burn radii estimates) similar to those observed during

actual pipeline ruptures, the analysis will be limited to values within this range.

Through use of Equation 4-12, burn radii are estimated for each of the pipeline

conditions specified in Table 6.1, at the following heat flux levels: 3,962 Btu/hr ft^2; 6,340

Btu/hr ft^2; 9,510 Btu/hr ft^2; and 9,985 Btu/hr ft^2. Table 6.2 provides a tabular

representation of this information.

Table 6.2
Burn Radii at Various Heat Fluxes

Heat Flux Btu/hr ft^2	Pipeline Conditions - Diameter/Incident Operating Pressure			
	14"/575psia	14"/1,200 psia	36"/575 psia	36"/1,200 psia
3,962	328	482	843	1,239
6,340	254	377	653	970
9,510	201	304	517	782
9,985	195	296	503	762

From the above results, it can be seen that the burn radius varies from a minimum

of 195 feet to a maximum of 1,239 feet. The variation of burn radius with heat flux is

evident from the columns of Table 6.2, which illustrate the decrease in burn radius with

increasing heat flux for each of the four pipeline conditions. The use of Equation 4-12

necessitates the selection of a single value of heat flux, which is presumed to be

associated with a specific level of thermal radiation damage. However, from the heat flux

information presented in Appendix A, it can be seen that a range of heat flux values could

be associated with a particular level of damage. Therefore, it is appropriate to examine

the effect that a variation in heat flux has on the estimated burn radius. Table 6.3

provides the results of burn radius calculations for each of the four heat flux values of

Table 6.2, in which each of the heat flux values is varied (i.e., increased and decreased)

by 25 percent. This amount of variation is consistent with the variation of heat flux

values in Appendix A, for a specified level of thermal radiation damage.

Table 6.3
Variation of Heat Flux Values

Heat Flux Btu/hr ft^2	Burn Radius and Percent Difference* for Pipeline Conditions - Diameter/Incident Operating Pressure			
	14"/575psia	14"/1,200 psia	36"/575 psia	36"/1,200 psia
2,972	381(16)	559(16)	982(16)	1,437(16)
3,962	328	482	843	1,239
4,953	291(-11)	429(-11)	747(-11)	1,104(-11)
4,755	297(17)	439(16)	764(17)	1,128(16)
6,340	254	377	653	970
7,925	224(-12)	335(-11)	575(-12)	862(-11)
7,133	238(18)	355(17)	611(18)	912(17)
9,510	201	304	517	782
11,888	176(-12)	269(-12)	452(-13)	692(-12)
7,489	231(18)	346(17)	594(18)	889(17)
9,985	195	296	503	762
12,481	171(-12)	262(-11)	439(-13)	674(-12)

*Burn radius is the first value specified in the table; percent difference is parenthesized.

From Table 6.3, it can be seen that over and under estimating the heat flux by 25

percent can result in maximum variations in the burn radius of -13 percent and 18

percent, respectively. These variations are considered reasonable in light of the large

numerical variation in the heat flux values (i.e., variations of at least 990 Btu/hr ft^2).

In Chapter 4, it was explained that Equation 4-12 does not account for the heat flux due to solar radiation. Appendix A indicates that this heat flux varies from 250 to 380 Btu/hr ft^2. If a representative value for solar heat flux is selected to be 315 Btu/hr ft^2 (i.e., the midpoint of the solar heat flux range), then a comparison of the burn radii with and without solar radiation can be made. This comparison is shown in Table 6.4, in which the burn radii for the four pipeline conditions are calculated with and without the contribution of the solar heat flux.

Table 6.4

Variation of Heat Flux Values (Contribution of Solar Heat Flux)

Heat Flux Btu/hr ft^2	Burn Radius and Percent Difference* for Pipeline Conditions - Diameter/Incident Operating Pressure			
	14"/575psia	14"/1,200 psia	36"/575 psia	36"/1,200 psia
3,962	328	482	843	1,239
4,277	315(-4)	463(-4)	809(-4)	1,191(-4)
6,340	254	377	653	970
6,655	247(-3)	368(-2)	635(-3)	946(-3)
9,510	201	304	517	782
9,825	197(-2)	299(-2)	507(-2)	768(-2)
9,985	195	296	503	762
10,300	192(-2)	291(-2)	493(-2)	749(-2)

*Burn radius is the first value specified in the table; percent difference is parenthesized.

The results in Table 6.4 indicate that a variation in heat flux of several hundred Btu's/hr ft^2 will not have a significant impact on the burn radius. Therefore, the assumption to exclude solar radiation during the development of Equation 4-12 is appropriate.

6.2 Effect of Variation in Atmospheric Transmissivity on Burn Radius

During development of Equation 4-12, the following relationship was used to provide an estimate of atmospheric transmissivity:

$$\tau = 0.79(100/r)^{1/16}(100/D)^{1/16} \tag{4-4}$$

where

r = relative humidity, %
D = distance to flame, feet

As explained in Chapter 4, the authors of this equation (36) caution that Equation 4-4 is "strictly applicable" when the flame is radiating at a temperature of 2240° F, relative humidity is greater than 10%, dry bulb temperature is 80° F and the distance from the flame is greater than 100 feet but less than 500 feet. However, the authors also indicate that an "order of magnitude" estimate can be made under a wider range of conditions. For purposes of simplifying Equation 4-12, a value for atmospheric transmissivity was determined assuming a distance from the flame of 500 feet and a relative humidity of 50 percent. Using Equation 4-4, this value was calculated to be 0.746.

The sensitivity of the burn radius to changes in atmospheric transmissivity can be evaluated at the four conditions identified in Section 6.1 by varying both the relative humidity and the distance used in Equation 4-4. Table 6.5 provides the atmospheric transmissivities that are obtained from Equation 4-4 when relative humidities range from 10 percent to 100 percent and distances vary from 100 to 500 feet:

Table 6.5
Atmospheric Transmissivities

Humidity, Percent	Distance from Flame - Feet				
	100	200	300	400	500
10	0.912	0.874	0.852	0.837	0.825
20	0.874	0.837	0.816	0.801	0.790
30	0.852	0.816	0.795	0.781	0.770
40	0.837	0.801	0.781	0.767	0.757
50	0.825	0.790	0.770	0.757	0.746
60	0.816	0.781	0.762	0.748	0.738
70	0.808	0.774	0.754	0.741	0.731
80	0.801	0.767	0.748	0.735	0.724
90	0.795	0.762	0.742	0.729	0.719
100	0.790	0.757	0.738	0.724	0.714

Table 6.5 indicates that for relative humidities from 10 to 100% and distances from 100 to 500 feet, the transmissivity varies from 0.912 to 0.714. It can be seen that the atmospheric transmissivity decreases with increasing relative humidity and distance, since for these conditions a larger amount of thermal radiation is absorbed by the atmosphere.

It was previously mentioned that the burn radius produced by Equation 4-12 varies from 195 feet to 1,239 feet. The range of possible atmospheric transmissivities associated with Equation 4-12 can be found by determining the transmissivities at the smallest burn radius (and lowest applicable relative humidity) and at the highest burn radius (and highest applicable relative humidity). The smallest burn radius and applicable relative humidity is respectively considered to be 195 feet and 10 percent. Using Equation 4-4, the atmospheric transmissivity is:

$$\tau = 0.79(100/10)^{1/16}(100/195)^{1/16}$$

$$= 0.875$$

Since the maximum burn radius of 1,239 feet is outside the range for which Equation 4-4 is strictly applicable, (i.e., 100 to 500 feet), the value of atmospheric transmissivity at this distance is estimated using a general plot of transmissivity versus path length (20). As indicated in (20), this plot is for a source temperature of 1400 K, which is the general flame temperature for the burning of hydrocarbon fuels. From the plot, the value of τ for a path length of 1,239 feet (or 378 meters) using the dashed line representing 100 percent relative humidity (which will result in a minimum value of τ) is approximately 0.470. Therefore, the atmospheric transmissivity can vary from a maximum of 0.875 to a minimum of 0.470. Equation 4-12 can be rewritten to make τ a variable by dividing the (4,036.82)P/K term by 0.746 (the previously assumed value of τ); the equation then becomes:

$$BR = D\{(4{,}036.82/0.746)P/K) - 37.52\}^{1/2}$$

$$= D\{(5{,}411.29\tau)P/K) - 37.52\}^{1/2} \qquad (6\text{-}1)$$

The burn radius can now be computed at the four pipeline conditions using the maximum, minimum and previously assumed values of τ. The results of these calculations are provided in Table D.1 of Appendix D. In addition, Table D.2 of Appendix D provides the percent difference between the burn radii that are calculated using the assumed value of τ (0.746) and the burn radii that are calculated using the maximum and minimum values of τ (0.875 and 0.470, respectively). From Tables D.1 and D.2, it can be seen that Equation 4-12 can under predict and over predict the burn radius by 9 percent and 34 percent, respectively. While an overestimation of the burn radius by approximately a third may initially appear to be significant, it must be remembered that this percentage corresponds to extreme conditions (i.e., relative humidity of 100 percent and a distance of 1,239 feet from the flame). Furthermore, since these percentages correspond to a range, the actual percent difference in any situation would be expected to lie within this range and be less than the extreme values.

The combined effects of variations in heat flux and atmospheric transmissivity can be shown through calculation of burn radii at the four pipeline conditions and heat flux values identified in Table 6.3, using atmospheric transmissivities which vary from 0.470 to 0.875. Table D.3 in Appendix D provides the calculated burn radii at all of the aforementioned conditions, while Table D.4 lists the percentage differences of these variations from burn radii calculated at the previously described conditions (i.e., pipeline diameters of 14 inches and 36 inches; incident operating pressures of 575 psia and 1,200

psia; heat flux values of 3,962 Btu/hr ft^2; 6,340 Btu/hr ft^2; 9,510 Btu/hr ft^2; and 9,985

Btu/hr ft^2; and a value of 0.746 for atmospheric transmissivity). The largest variations

are seen for the combination of low τ and high K (i.e., "low" and "high" in relation to the

pipeline condition being considered); this combination results in underprediction of the

burn radius by an average of 33 percent. However, a combination of high τ and high K

result in an underprediction which averages only 3 percent. Conversely, a combination of

high τ and low K produces overpredictions of burn radii averaging 27 percent, while

combining a low τ with a low K results in an average underprediction of 9 percent. It

must again be noted that these percentages correspond to extreme conditions, and that

the actual percent difference in any situation would lie within ranges bounded by these

values.

6.3 Effect of Variation in Wind Speed and Direction on Burn Radius

As described previously, Equation 4-12 is developed assuming a vertical flame (i.e., no

wind) and, consequently, a symmetrical burn area. Graphical information has been

obtained from the Canadian TSB (L. Gales: personal communication, September 10,

1996) which relates heat flux to distance at wind speeds of 10 kilometers per hour (6.2

miles per hour) and 20 kilometers per hour (12.4 miles per hour) at upwind, downwind

and crosswind locations. The wind speeds cited herein are appropriate for this

discussion, since they span a range which is representative of many cities in the United

States. As an example, Table 6.6 provides the mean yearly wind speeds for several major

cities (55).

Table 6.6
Wind Speeds for Several U.S. Cities

City	Mean Yearly Wind Speed, miles per hour
Atlantic City, NJ	10.1
Newark, NJ	10.2
Philadelphia, PA	9.5
Charleston, SC	8.6
Madison, WI	9.8
Nashville, TN	8.0
Columbus, OH	8.5
Helena, MT	7.7
Shreveport, LA	8.4
Orlando, FL	8.5

The graphs were prepared for pipeline diameters of 24, 36 and 42 inches at a pressure of 1,000 psig (1014.7 psia) and, with the exception of graphs for the 42 inch diameter pipeline (which is outside the diameter range of Equation 4-12), have been provided in Appendix E. It should be noted that the graphs show the progression of heat flux with time, with the curve for time zero at the top. It is this curve which produces the maximum heat flux at a specified distance.

Burn radii at heat flux values of 9,510 Btu/hr ft^2; 7,925 Btu/hr ft^2; 6,340 Btu/hr ft^2 and 4,755 Btu/hr ft^2 were obtained from the time zero curves in Appendix E and compared to distances determined using Equation 4-12. These heat flux values were selected since they lie within the previously identified range of 3,962 Btu/hr ft^2 to 9,985 Btu/hr ft^2 for which Equation 4-12 is applicable. Furthermore, these heat flux values facilitate reading distances from the figures in Appendix E.

The comparison of distances and the calculation of percentage differences is respectively provided in Tables D.5 and D.6 (for the 24 inch diameter pipeline) and Tables D.7 and D.8 (for the 36 inch diameter pipeline). The distances listed in Tables D.5 and D.7 show that the burn radius is not symmetrical when there is wind, and that the radius is greater in the downwind direction than in the upwind direction. From Tables D.6 and D.8, it can be seen that the largest percentage difference between the Canadian distances and the distances estimated with Equation 4-12 occurs for the upwind condition (56 percent for the 36 inch diameter pipeline and 32 percent for the 24 inch diameter pipeline), and that for upwind conditions the percentages decrease with decreasing wind speed. However, an assumption was previously made that Equation 4-12 will predict the longest dimension of a burn area, which would be the distance associated with the downwind condition. The maximum percent difference between the Canadian distances and the distances estimated using Equation 4-12 is less if the downwind condition is considered: 27 percent for the 36 inch pipeline and -16 percent for the 24 inch pipeline. Furthermore, for all locations and wind speeds the percent difference decreases with decreasing heat flux (so that overestimations are associated with a heat flux of 9,510 Btu/hr ft^2 and underestimations can appear when considering lower values of heat flux). However, given the variability in weather conditions which may be present during an actual pipeline rupture, the differences in burn radius cited herein are considered to be reasonable.

In summary, the analyses performed in this chapter serve to illustrate that the assumptions made during the development of Equation 4-12 are appropriate. Equation 4-12 and the charts of Appendix B can be used to provide estimations of burn radii for various pipeline diameters and incident operating pressures. However, it must be stressed that safe separation distances determined through the use of Equation 4-12 or the Appendix B charts are *estimations*. There are numerous variables, several of which have been considered in this chapter, which will influence the burn radius associated with a pipeline rupture. The advantage to using the method described in this thesis is that the method is straightforward and provides reasonable estimates of actual burn radii.

The next chapter provides a summary of this thesis through several concluding remarks. Recommendations are also made for additional work, which can be used to refine the procedure for estimating safe separation distances.

CHAPTER 7

CONCLUSIONS AND RECOMMENDATIONS

The work described in this thesis has led to the development of a method for estimating safe separation distances from natural gas transmission pipelines. This method was verified based on information from actual pipeline accidents, and provides a means to determine the safe separation distance, as a measurement of the burn radius, through knowledge of the pipeline's diameter and incident operating pressure. The method can be used by regulators to determine the distances at which future development might be placed from existing pipelines or, perhaps more realistically, the method can be used to evaluate appropriate incident operating pressures for pipelines which traverse densely populated areas.

The procedure described in this thesis is easy to apply and does not require extensive computational efforts. The basis for estimation is Equation 4-12, which describes the burn radius as a function of a pipelines's diameter and incident operating pressure. As illustrated in the charts found in Appendix B of this thesis, Equation 4-12 is readily represented in graphical form. The method is applicable to pipelines with diameters ranging from 14 inches to 36 inches and incident operating pressures from 575 psia to 1,200 psia, which constitute the mass majority of natural gas transmission pipelines in service in the United States. For levels of thermal radiation damage corresponding to heat flux values from 3,962 Btu/hr ft^2 to 9,985 Btu/hr ft^2, the method will predict safe separation distances ranging from 195 feet to 1,200 feet. The range of heat flux values noted above are applicable to the major consequences to life, limb and property that should be of interest to most analysts.

Several recommendations can be made for future research endeavors that can refine the work that has been performed herein. As advances are made in the areas of fire protection and hazard assessment, new information may be developed concerning the relationship between heat flux levels and corresponding levels of thermal radiation damage. This new information can then be used to prepare burn radius charts for which the heat flux level corresponding to a specified level of damage is more accurately known. Another recommended area for future work includes the refinement of the procedure to predict atmospheric transmissivity, as the current method only provides order of magnitude estimates at distances beyond 500 feet.

A recommendation can also be made with regard to the reporting of pipeline accident data, since the reports produced by the NTSB and the Canadian TSB vary in the type and amount of accident-related information. Consistent reporting of data such as the volume of gas released, the duration of release and flame characteristics would be beneficial, in that the model developed in this thesis can be tested more accurately. Furthermore, this additional information may also be used to expand the diameter and pressure ranges for which Equation 4-12 is applicable

Although there are areas amenable to refinement, the methodology proposed herein will provide reasonable estimates of safe separation distances for the ranges of diameters, incident operating pressures and values of heat flux that have been previously identified.

APPENDIX A - HEAT FLUX LEVELS

Table A.1
Summary of Heat Flux Levels

Heat Flux Btu/hr ft^2	kW/m^2	Reference Number	Consequence
222**	0.7	37	Exposed skin reddens and burns on prolonged exposure.
250-380**	0.79-1.2	32, 35	Heat flux of solar radiation.
300	0.95**	***	115 seconds to severe pain; 663 seconds to second degree burn.
317**	1	34, 39	Level which is just tolerable by a clothed person. Also, this is the heat flux of solar radiation on a clear, hot summer day.
380**	1.2	56	Solar heat flux at noontime during the summer.
500*	1.57*	39	Flux limit from a flare if personnel are required to work in the area.
500*	1.58*	35	Value of heat flux for a flare where personnel are continuously exposed.
500	1.58**	36	Level at which personnel should not be exposed to for more than 2 hours.
500	1.6	39	Level to produce minor discomfort.
507**	1.6	32, 34, 56	Minimum heat flux to be painful. Also, no discomfort felt for long exposures to the thermal radiation.
550-555**	1.74-1.75	35, 37	Pain threshold occurs after 60 second exposure.
600	1.89**	***	45 seconds to severe pain; 187 seconds to second degree burn.
634**	2.0	37	Causes damage to PVC insulated cables.

Table A.1
Summary of Heat Flux Levels
(Continued)

Heat Flux Btu/hr ft^2	kW/m^2	Reference Number	Consequence
666**	2.1	56	Minimum heat flux necessary to cause pain after 1 minute.
740	2.33	35	Pain threshold reached at 40 seconds.
920	2.90	35	Pain threshold reached at 30 seconds.
1,000*	3.15*	39	Heat flux from flare at which personnel can quickly leave the immediate vicinity without being harmed.
1,000	3.15**	***, 36	Level at which personnel should not be exposed to for more than 10 minutes. Also, 27 seconds to severe pain and 92 seconds to second degree burn.
1,268**	4.0	32, 34	0% fatality at this heat flux level. However, heat flux is sufficient to cause pain to personnel if they cannot reach shelter in 20 seconds. Also, blistering of the skin (second degree burns) is likely.
1,300	4.1**	***	18 seconds to severe pain and 57 seconds to second degree burn.
1,490**	4.7	56	Heat flux level which causes pain in 15-20 seconds and injury after 30 seconds. Also, this is the recommended flux level for residential areas at a frequency of 50×10^{-6}/yr.

94

Table A.1
Summary of Heat Flux Levels
(Continued)

Heat Flux Btu/hr ft^2	kW/m^2	Reference Number	Consequence
1500	4.73	35, 40, 57	Pain threshold for a 15-16 second exposure. After this time period, blistering and permanent skin damage can occur. Also, this is the heat flux in areas where emergency actions occuring for several minutes may be performed by personnel without shielding but with appropriate clothing. This is also the level which can be tolerated for an indefinite period of time by an active worker wearing a hard hat, long sleeve shirt and gloves.
1,500	4.73**	36	Level at which personnel should not be exposed to for more than 2 minutes.
1,585**	5.0	37	Pain threshold reached after a 15 second exposure.
1,600	5.05**	***	13 seconds to severe pain and 40 seconds to second degree burn
1,650	5.2**	57	Heat flux which can be tolerated up to 5 minutes by a person wearing a hard hat, long sleeve shirt and gloves.
1,900	5.99**	***	11 seconds to severe pain and 30 seconds to second degree burn.
1,902**	6	58	Bare skin blisters if this heat flux is experienced for 20 seconds.
2,000	6.31**	36	Level at which personnel should not be exposed to for more than 20 seconds.

95

Table A.1
Summary of Heat Flux Levels
(Continued)

Heat Flux Btu/hr ft^2	kW/m^2	Reference Number	Consequence
2,000-2,029**	6.3-6.4	35, 37, 38	Pain threshold reached in 8 seconds and blistering occurs in 20 seconds. This is the maximum tolerable heat flux for short term human exposure. This is also the heat intensity in areas where emergency actions lasting up to 1 minute may be required by personnel without shielding but with appropriate clothing.
2,200	6.94	35	9 second exposure results in the pain threshold.
2,500	7.89**	***	7 seconds to severe pain and 20 seconds to second degree burn.
2,536**	8	39	Death occurs within minutes unless appropriate shelter is found.
3,000	9.46	35, 57	Pain threshold reached in 6 seconds. This is also the value of heat flux (if solar radiation is included) for a flare at any location to which people have access (such as at grade underneath the flare or a service platform of a nearby tower). In this instance exposure should be limited to a few seconds since the heat flux level is adequate for escape only. Furthermore, limited over-exposure of a person wearing hard hat, long sleeve shirt and gloves results in a skin reaction similar to a mild sunburn.
3,011**	9.5	32, 34, 37	Pain threshold occurs in 6-8 seconds, and second degree burns occur after 20 sec.
3,200	10.09	***	5 seconds to severe pain and 14 seconds to second degree burn.

Table A.1
Summary of Heat Flux Levels
(Continued)

Heat Flux Btu/hr ft^2	kW/m^2	Reference Number	Consequence
3,700	11.67	35	Pain threshold reached at 4 seconds.
3,709**	11.7	56	Mechanical integrity of thin, partially insulated steel can be lost.
3,800	11.99**	***	4 seconds to severe pain and 11 seconds to second degree burn.
3,962**	12.5	32, 34, 37	Piloted ignition of wood exposed to this heat flux for a prolonged period. Also, plastic tubing melts.
3,994**	12.6	32, 34, 39, 56	Exposed, dry, unpainted wood can be ignited at this heat flux. Piloted ignition of cotton can also occur. This is the recommended flux level for residential areas at a frequency of 10×10^{-6}/yr. Flammable materials in buildings may be damaged after 1,000 seconds.
4,000	12.5	39	Suitable heat flux level for control rooms or workshops.
4,755**	15.0	37	This is the heat flux limit of Class 2 building materials.
5,000*	15.77	35	Heat intensity on plant structures and in locations where operators are not likely to be working and where shelter from radiant heat is available.
5,072**	16.0	37, 39	Severe burns occur after 5 seconds, and wood ignites spontaneously.
6,300	19.87	35	Pain threshold reached in 2 seconds.

Table A.1
Summary of Heat Flux Levels
(Continued)

Heat Flux Btu/hr ft^2	kW/m^2	Reference Number	Consequence
6,340**	20	58	A four second exposure causes blistering of bare skin. This is also the heat flux level at which 1% lethality occurs for a twenty second exposure.
7,291**	23.0	56	Mechanical integrity of thin, uninsulated steel can be lost. This is also the recommended flux level for potentially hazardous adjacent installations at a frequency of 50×10^{-6}.
7,500	23.7	35	White rats experience burns on their bare skin in approximately 6 seconds.
7,925**	25.0	37	Prolonged exposure at this heat flux ignites wood.
9,510**	30.0	37	Heat flux limit for Class 1 building materials.
9,985**	31.5	40	After a few minutes exposure to this heat flux, wooden buildings, paper, window drapes and trees ignite spontaneously.
10,778**	34	58	Piloted ignition of cellulosic material for a twenty second exposure.
11,095**	35	58	50% lethality occurs for a twenty second exposure to this heat flux.
11,887**	37.5	32, 34	Process equipment becomes damaged. This is also the minimum energy required to ignite wood at indefinitely long exposures.

Table A.1
Summary of Heat Flux Levels
(Continued)

Heat Flux		Reference	
Btu/hr ft^2	kW/m^2	Number	Consequence
11,983**	37.8	34	Flammable materials in process installations can be damaged after an exposure of 1,000 seconds.
12,046**	38	56	Heat flux (for a 20 second exposure) corresponding to 50% mortality.
20,922**	66	58	Piloted ignition of cellulosic material in four seconds. Also, 1% lethality for a four second exposure.
37,089	117	58	Heat flux resulting in 50% lethality for a four second exposure.
Various Flux Levels and Exposure Times		39	$(I-25,400)t^{4/5} = 6,730$ for spontaneous ignition of wood; I in units of W/m^2.
		39	$(I-13,400)t^{2/3} = 8,050$ for piloted ignition of wood; I in units of W/m^2.
		39	First degree burns assumed if (t)I$^{1.15}$ > 550,000; t in seconds and I expressed as W/m^2.
		34	Graph of tolerance times to burn-injury levels for various incident heat fluxes.

Table A.1
Summary of Heat Flux Levels
(Continued)

Heat Flux Btu/hr ft^2	kW/m^2	Reference Number	Consequence
		34	Average heat flux which will cause severe blistering based on duration: $q_2 = 50/t_c^{0.71}$, q_2 in kW/square meter and t_c in seconds.

NOTES

*   Includes solar radiation

**   Calculated using the relationship: $1 Btu/hr\ ft^2 = 3.1546\ W/m^2$

***   Provided in material obtained from the TSB of Canada (personal communication, February 28, 1997).

APPENDIX B - BURN RADIUS CHARTS
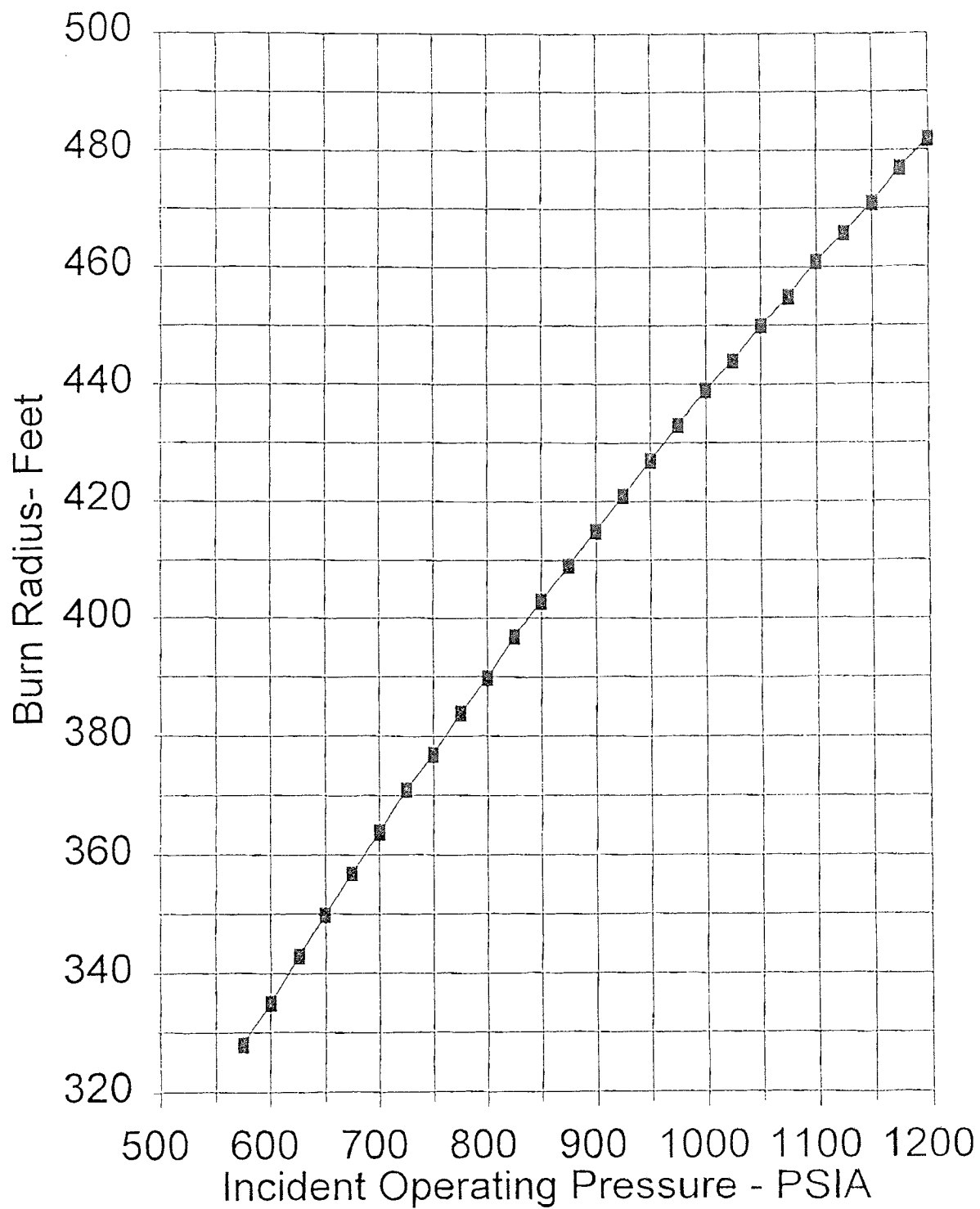
Figure B.1 - Burn Radius for 14" Diameter Pipeline
K = 3,962 Btu/hr sq. ft.
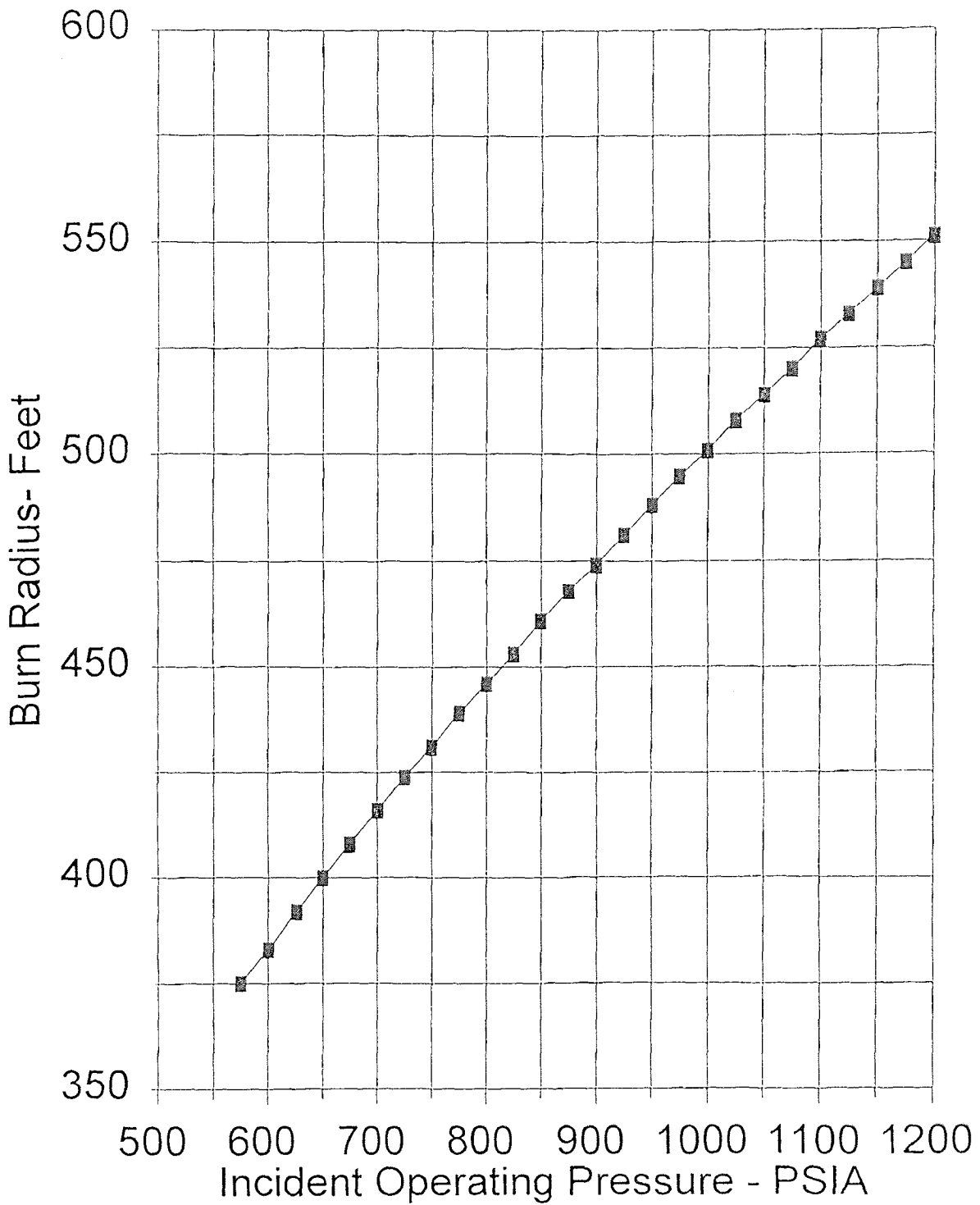
Figure B.2 - Burn Radius for 16" Diameter Pipeline
K = 3,962 Btu/hr sq. ft.
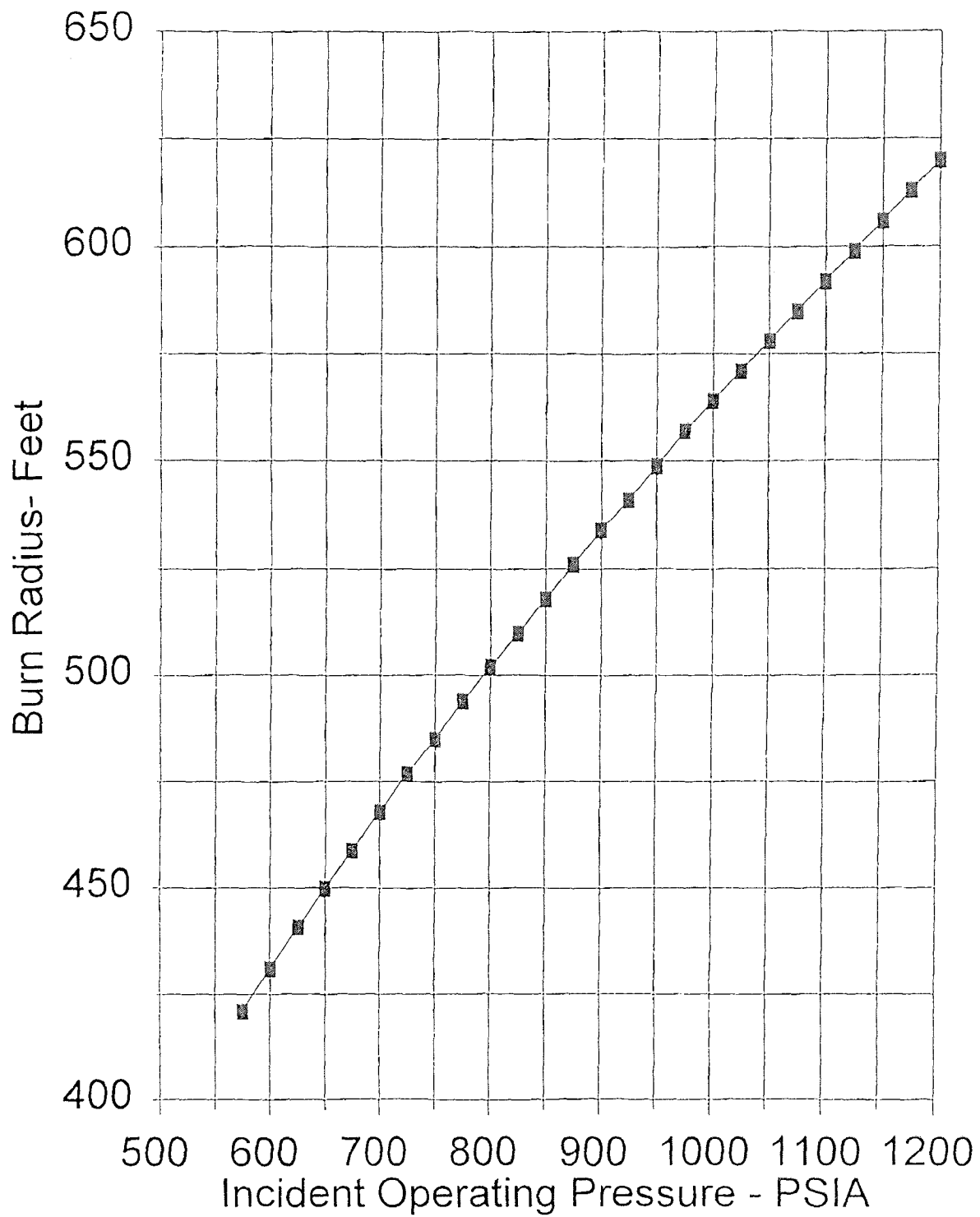
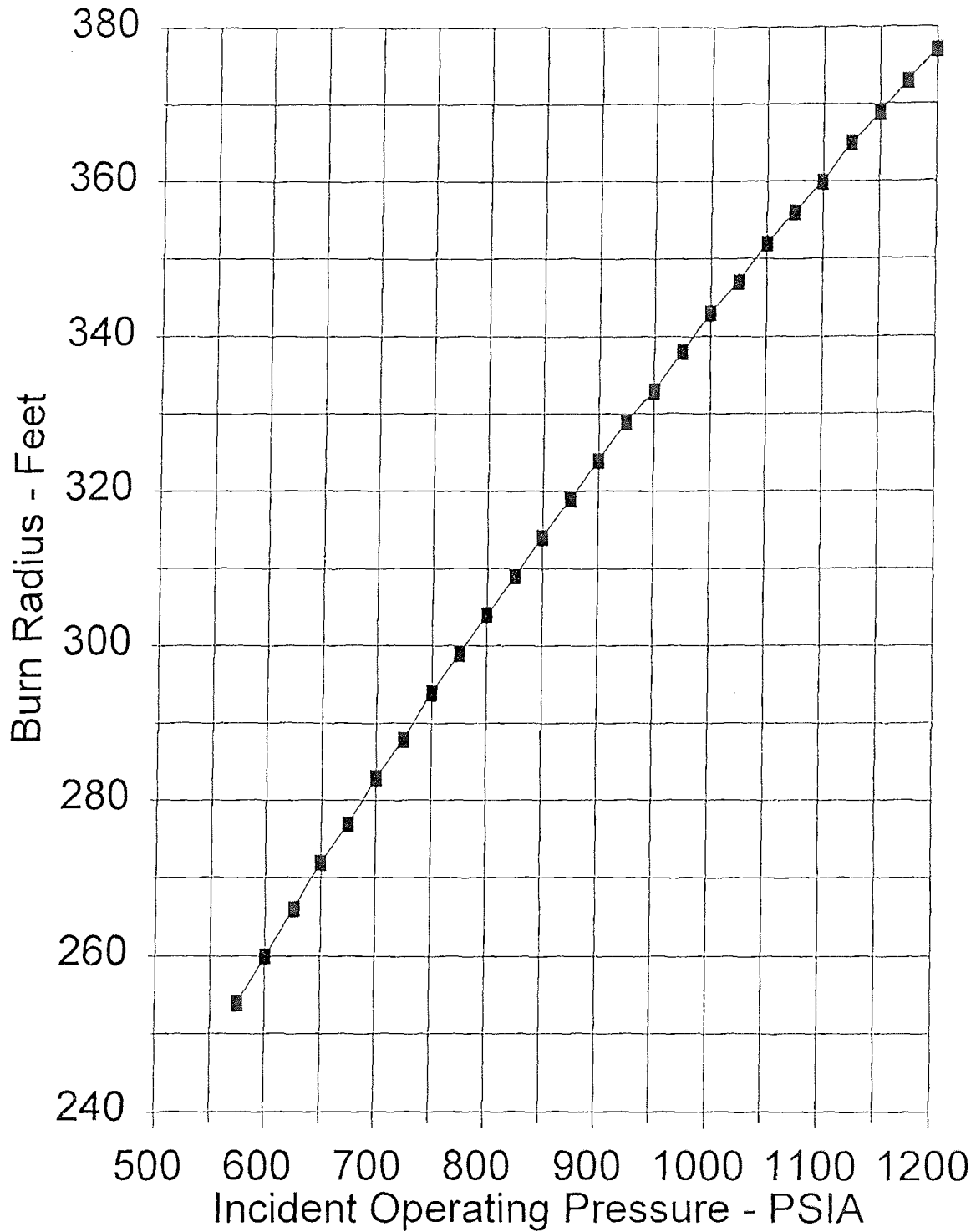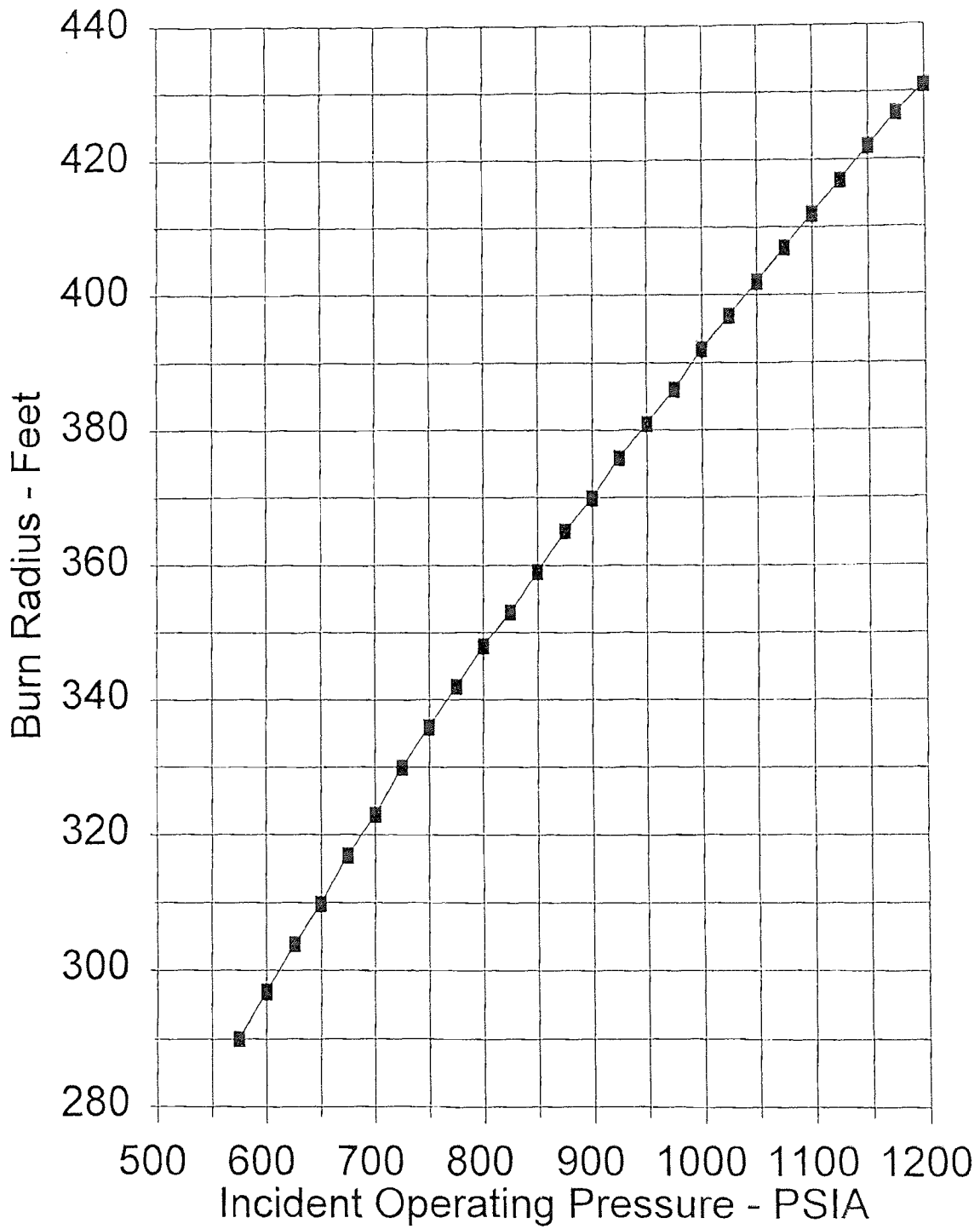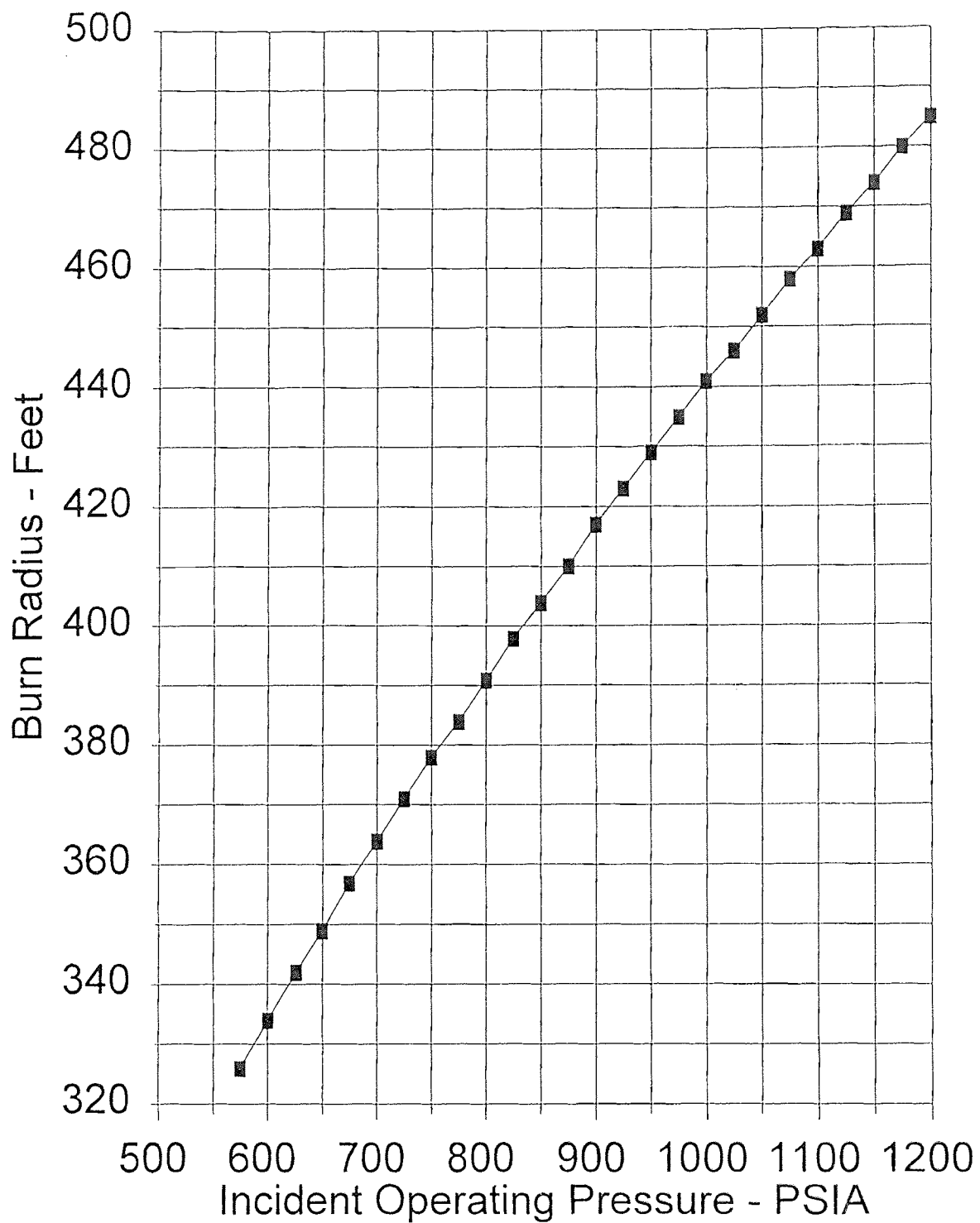Figure B.3 - Burn Radius for 18" Diameter Pipeline
K = 3,962 Btu/hr sq. ft.
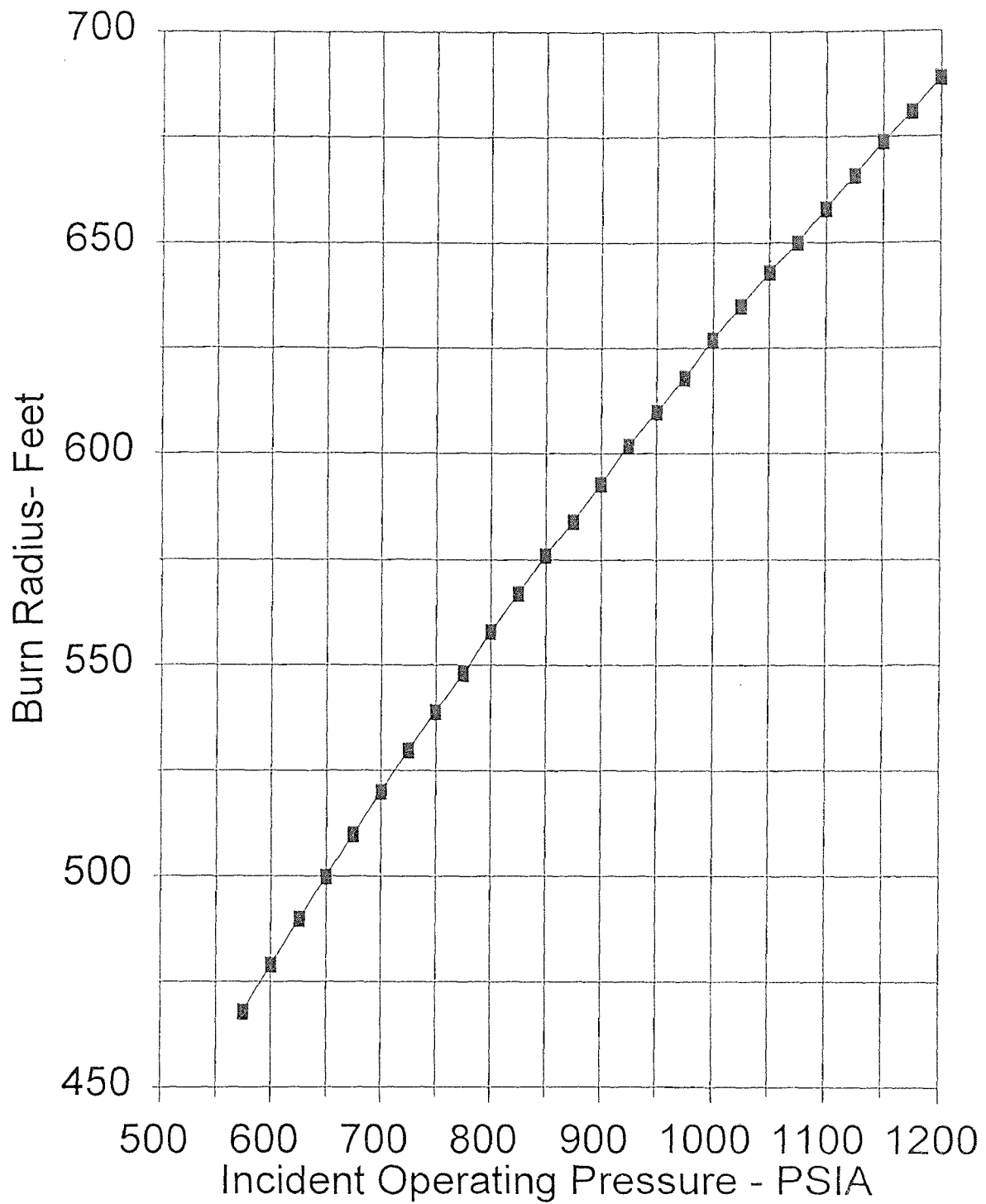
Figure B.4 - Burn Radius for 20" Diameter Pipeline
K = 3,962 Btu/hr sq. ft.
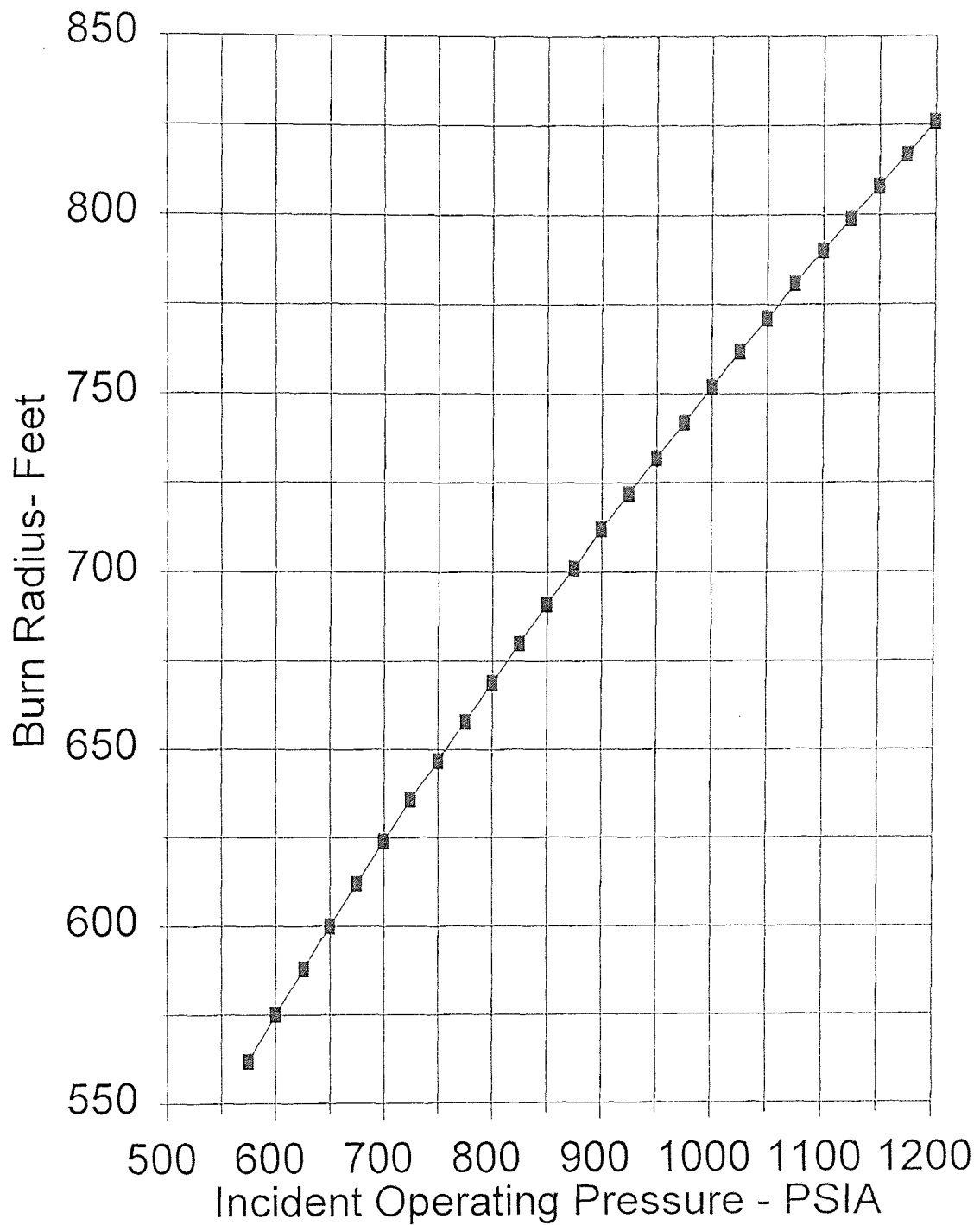
Figure B.5 - Burn Radius for 24" Diameter Pipeline
K = 3,962 Btu/hr sq. ft.
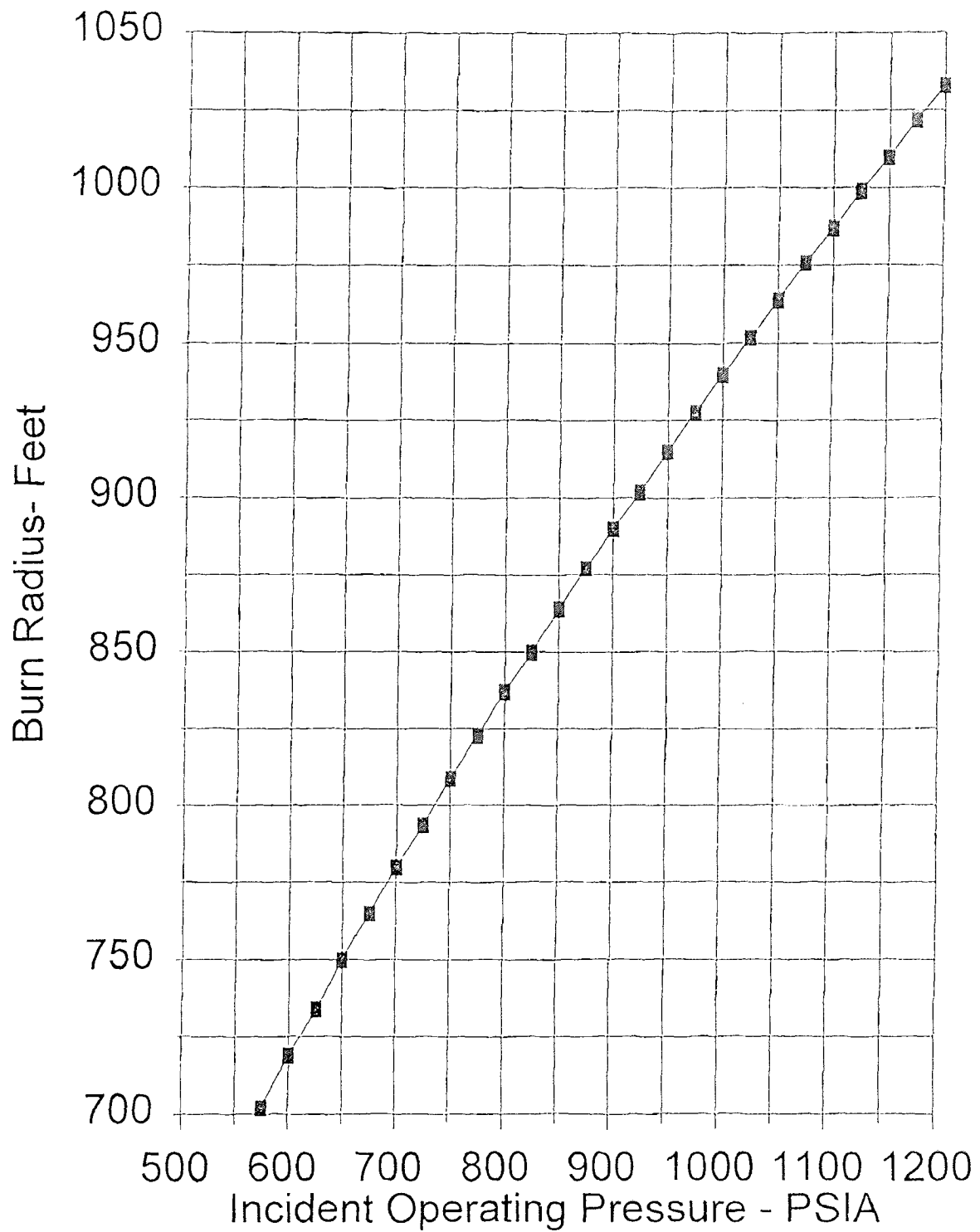
Figure B.6 - Burn Radius for 30" Diameter Pipeline
K = 3,962 Btu/hr sq. ft.
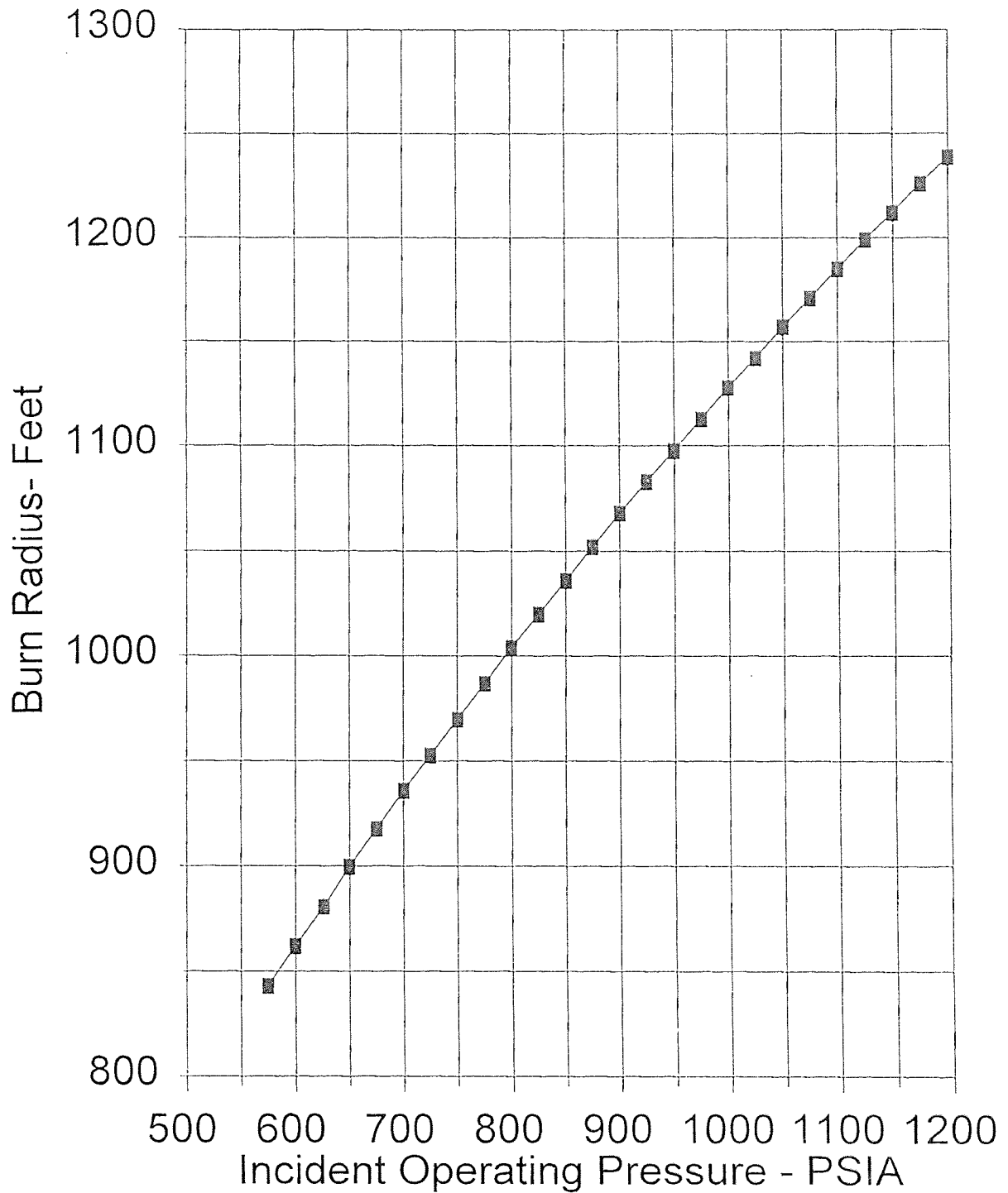
Figure B.7 - Burn Radius for 36" Diameter Pipeline
K = 3,962 Btu/hr sq. ft.

Figure B.8 - Burn Radius for 14" Diameter Pipeline
K = 6,340 Btu/hr sq. ft.

Figure B.9 - Burn Radius for 16" Diameter Pipeline
K = 6,340 Btu/hr sq. ft.

Figure B.10 - Burn Radius for 18" Diameter Pipeline
K = 6,340 Btu/hr sq. ft.

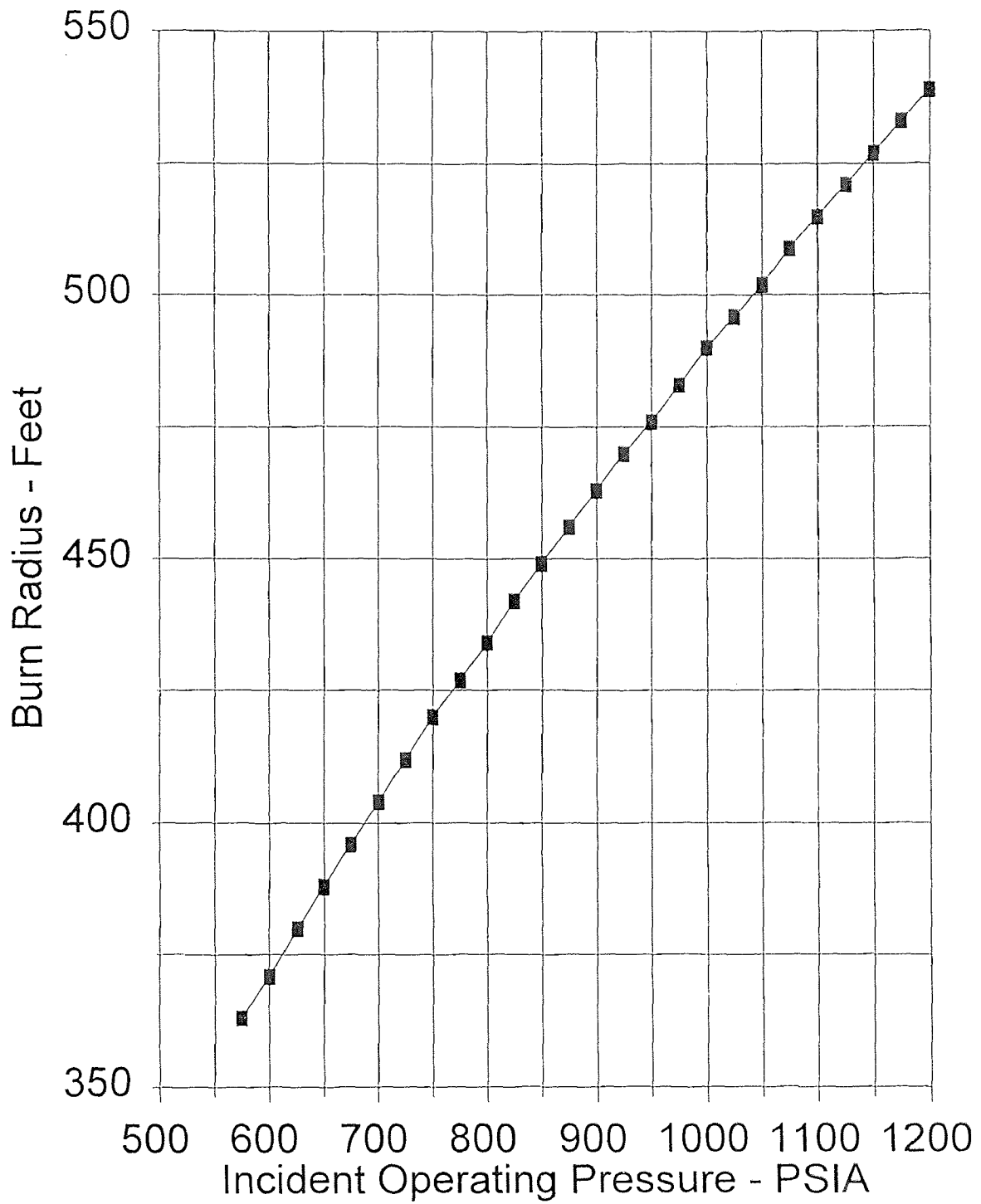Figure B.11 - Burn Radius for 20" Diameter Pipeline
K = 6,340 Btu/hr sq. ft.

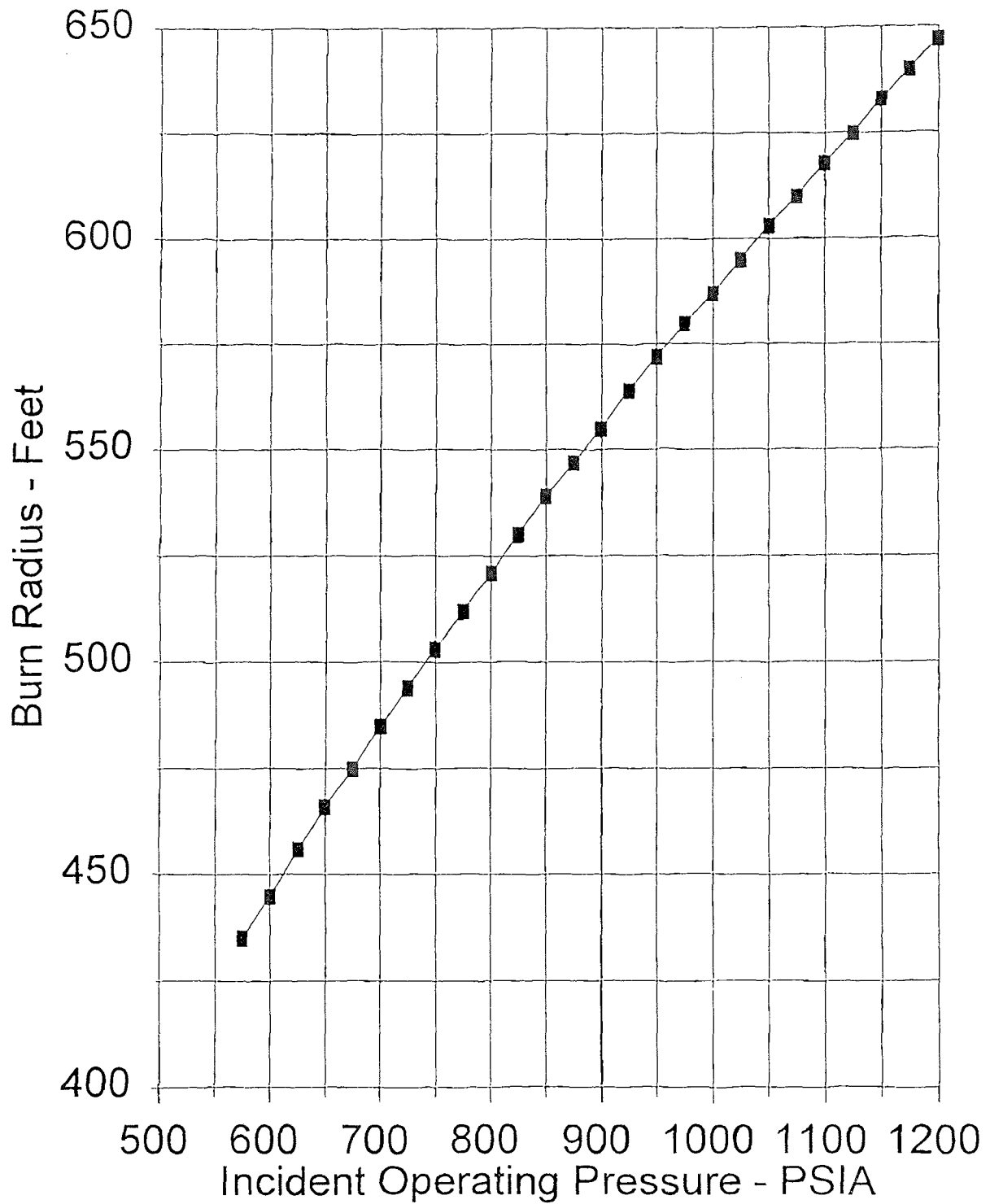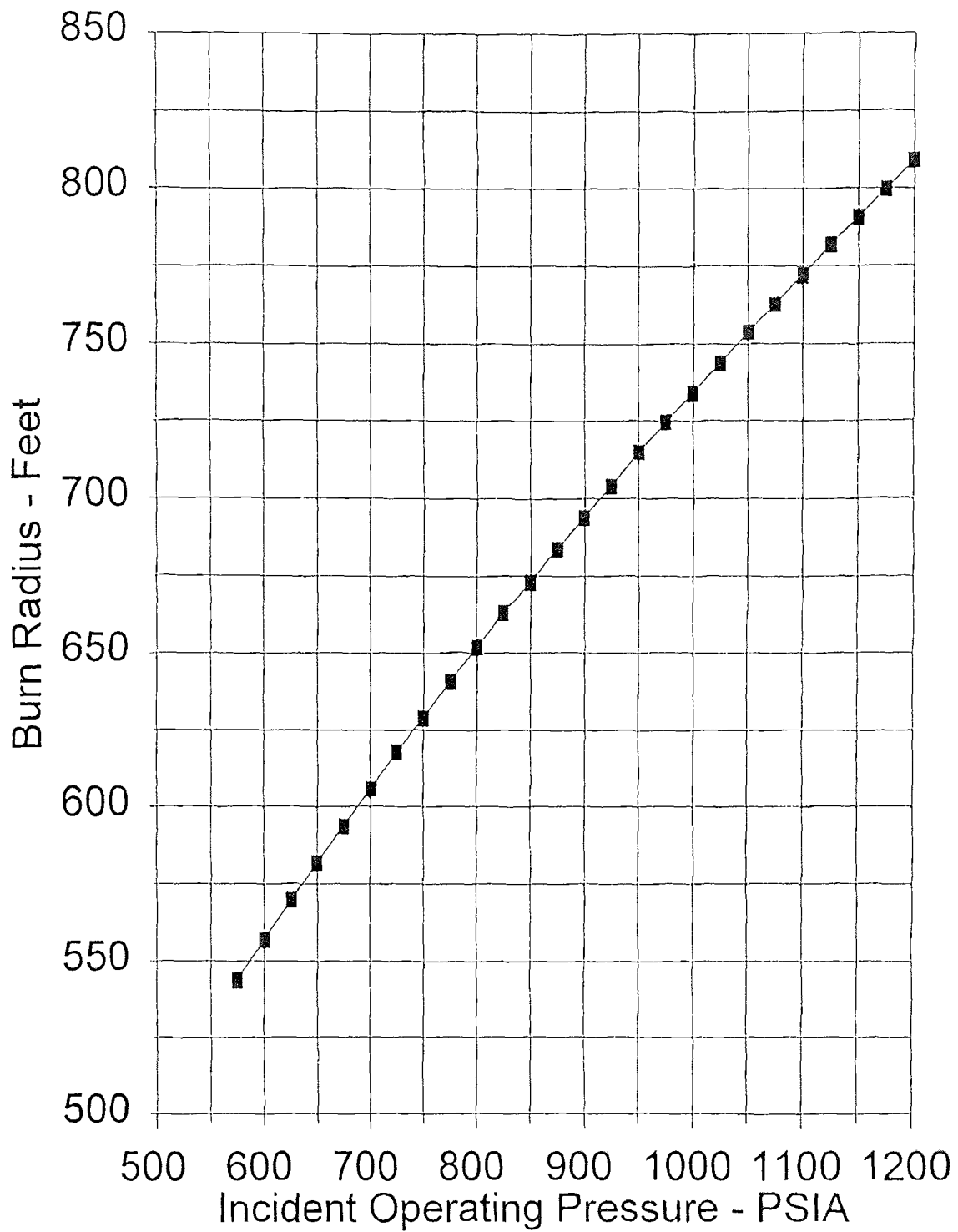Figure B.12 - Burn Radius for 24" Diameter Pipeline
K = 6,340 Btu/hr sq. ft.

Figure B.13 - Burn Radius for 30" Diameter Pipeline
K = 6,340 Btu/hr sq. ft.

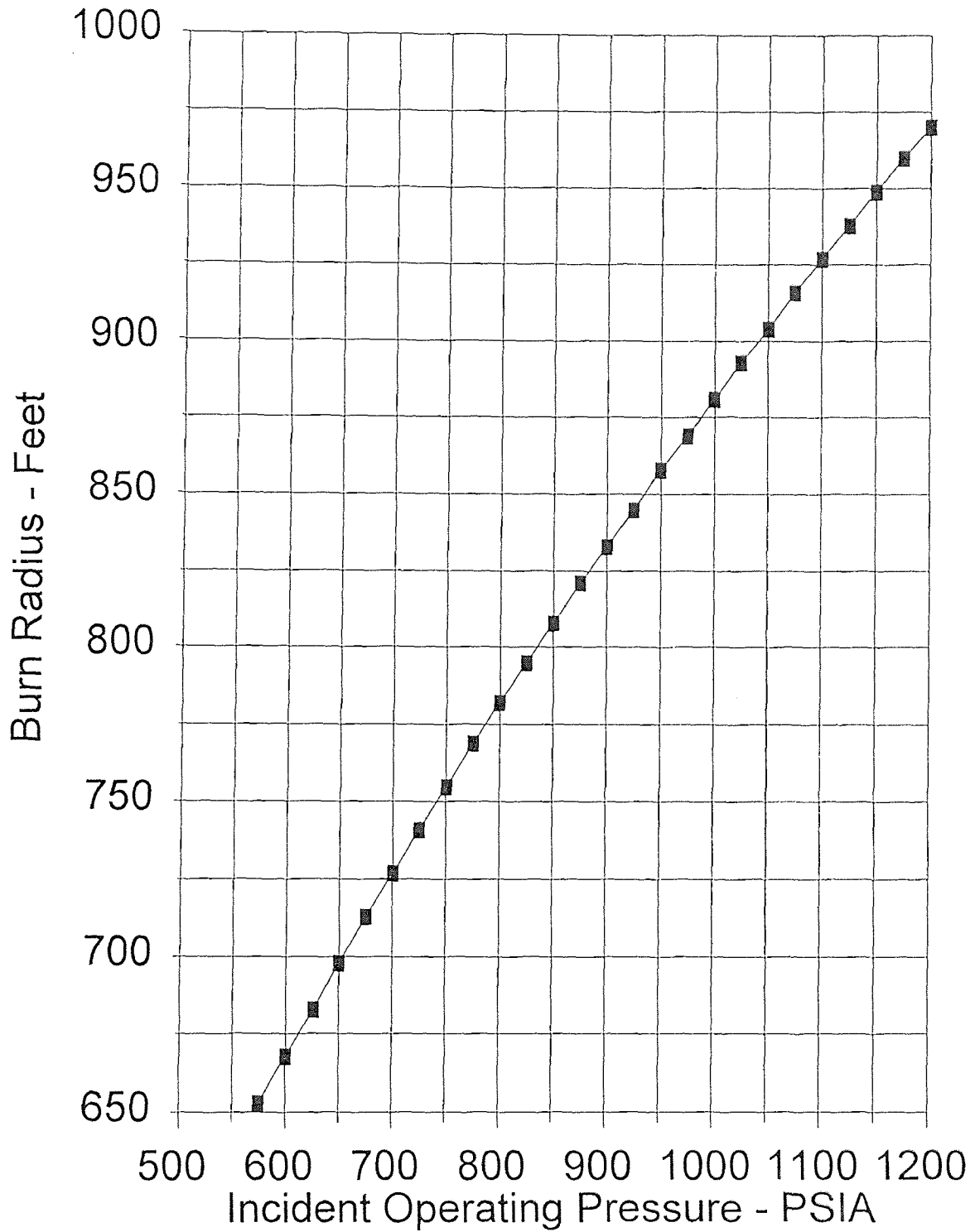Figure B.14 - Burn Radius for 36" Diameter Pipeline
K = 6,340 Btu/hr sq. ft.

Figure B.15 - Burn Radius for 14" Diameter Pipeline
K = 9,510 Btu/hr sq. ft.

Figure B.16 - Burn Radius for 16" Diameter Pipeline
K = 9,510 Btu/hr sq. ft.
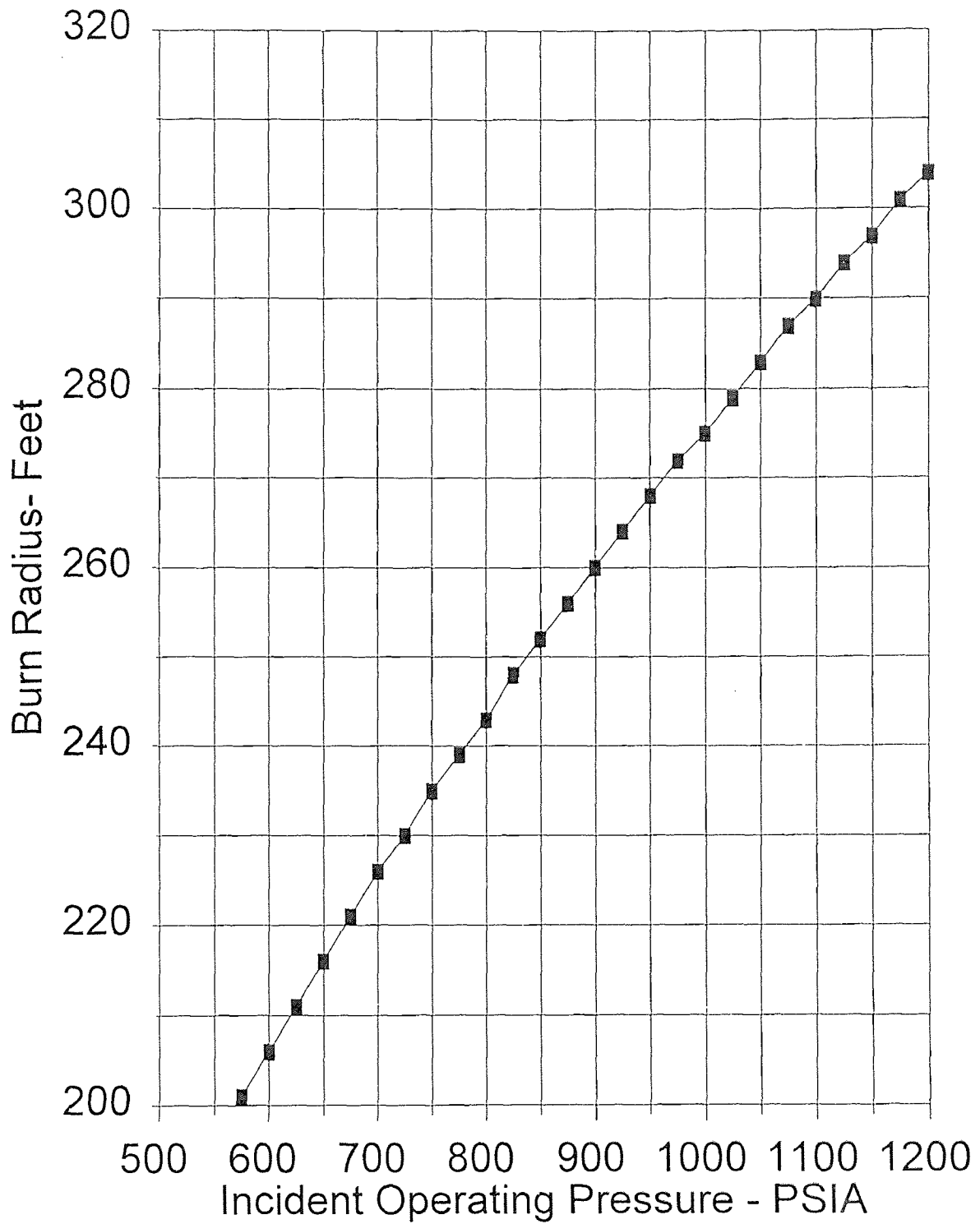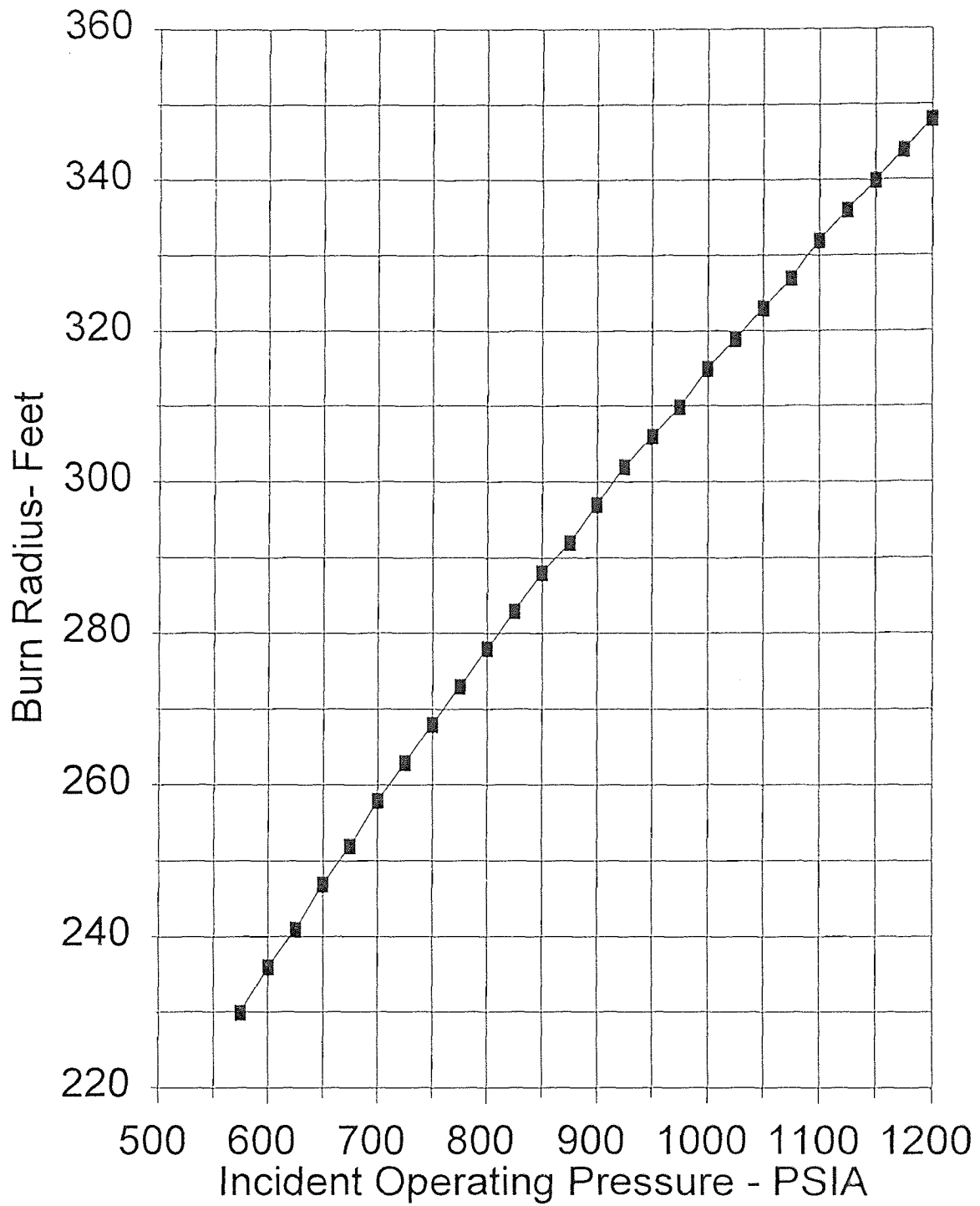
Figure B.17 - Burn Radius for 18" Diameter Pipeline
K = 9,510 Btu/hr sq. ft.

Figure B.18 - Burn Radius for 20" Diameter Pipeline
K = 9,510 Btu/hr sq. ft.

Figure B.19 - Burn Radius for 24" Diameter Pipeline
K = 9,510 Btu/hr sq. ft.
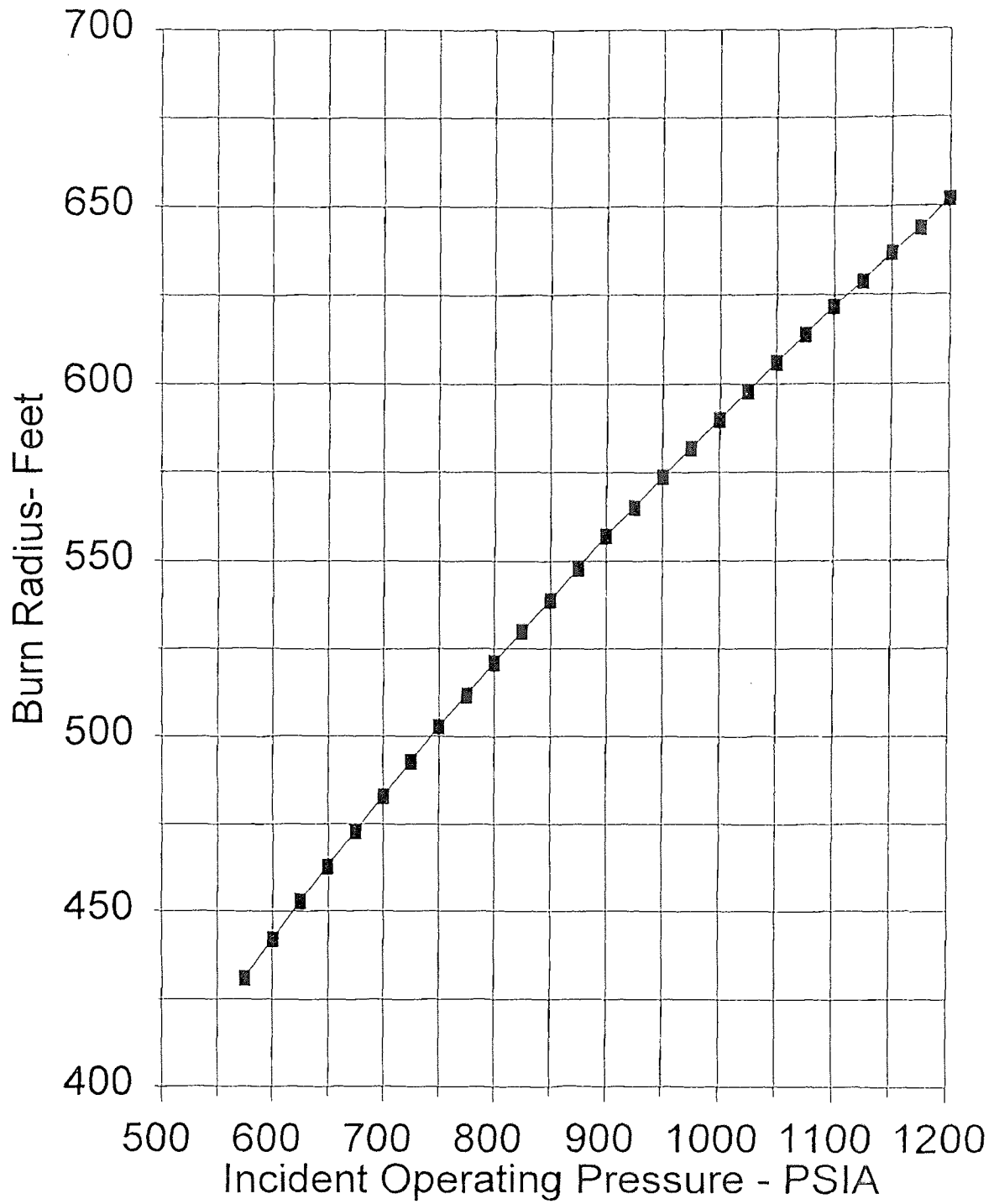
Figure B.20 - Burn Radius for 30" Diameter Pipeline
K = 9,510 Btu/hr sq. ft.
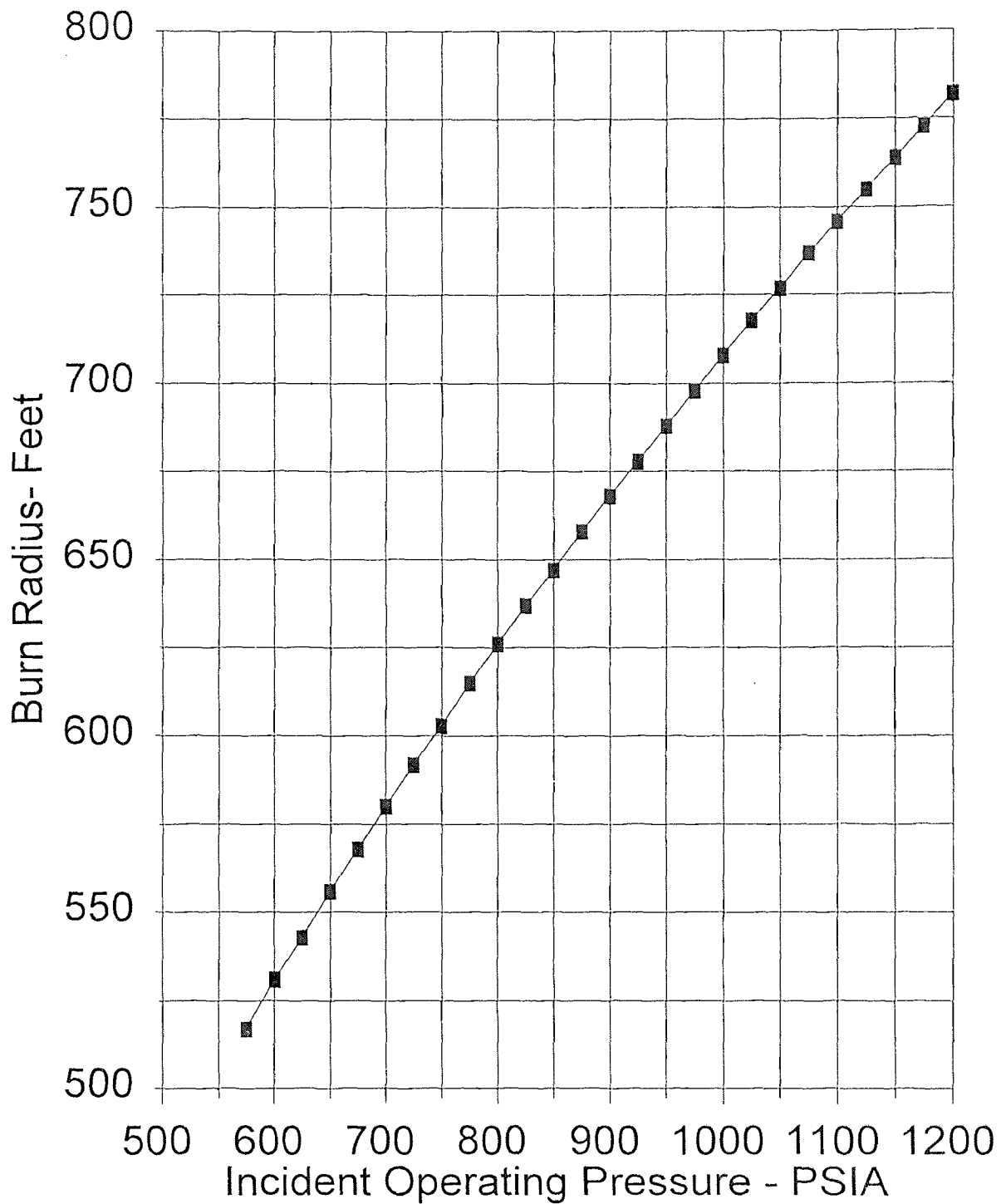
Figure B.21 - Burn Radius for 36" Diameter Pipeline
K = 9,510 Btu/hr sq. ft.
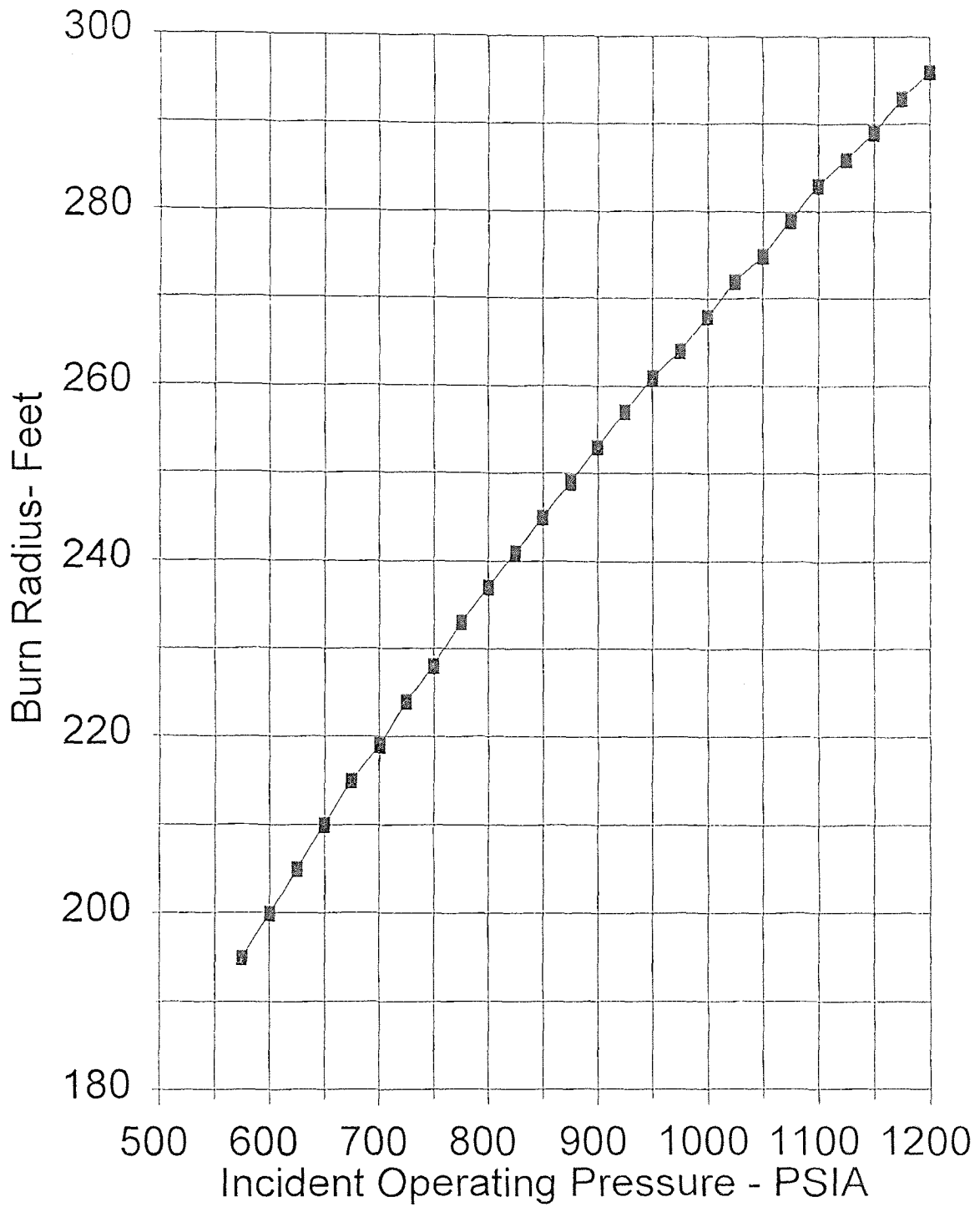
Figure B.22 - Burn Radius for 14" Diameter Pipeline
K = 9,985 Btu/hr sq. ft.
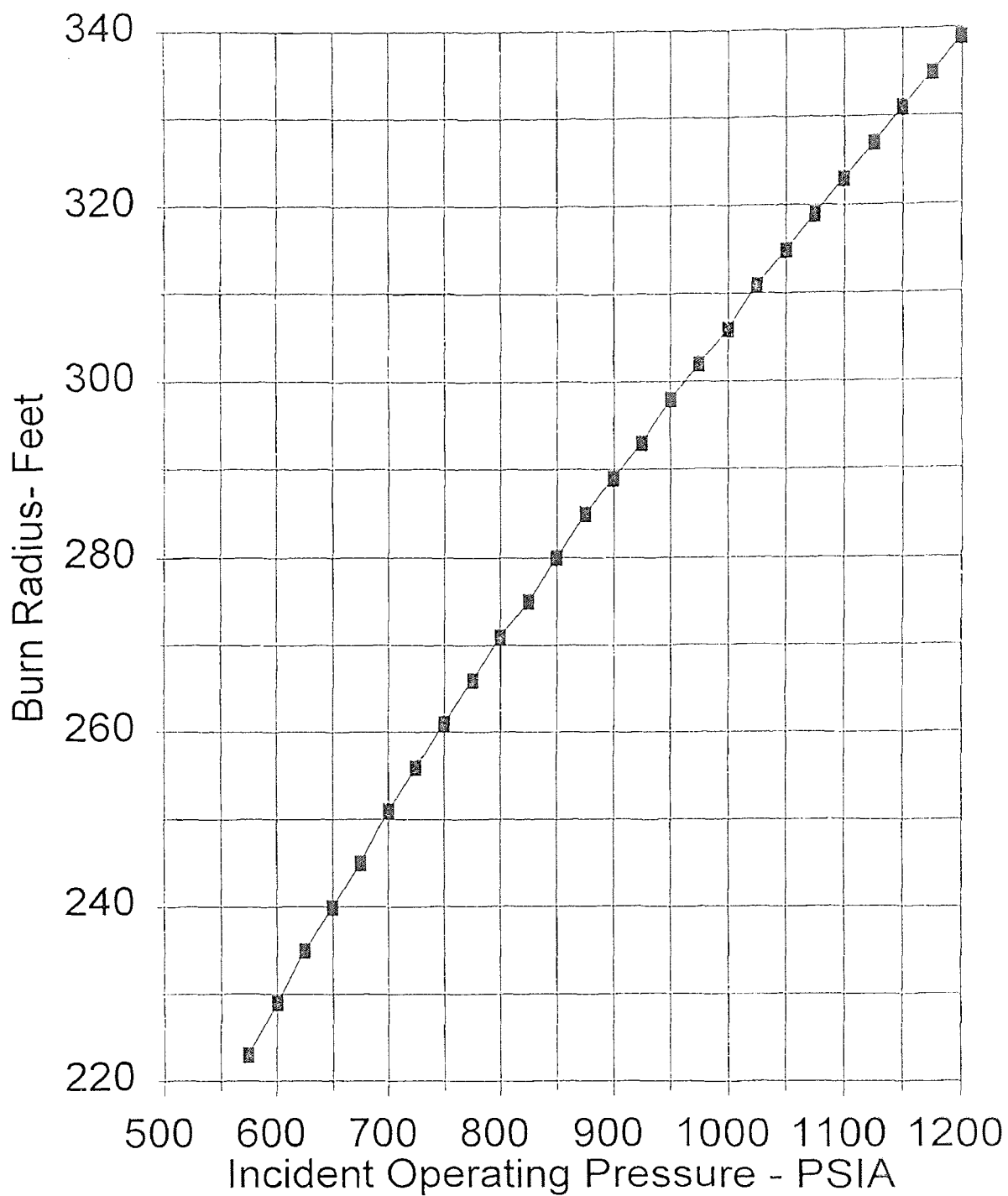
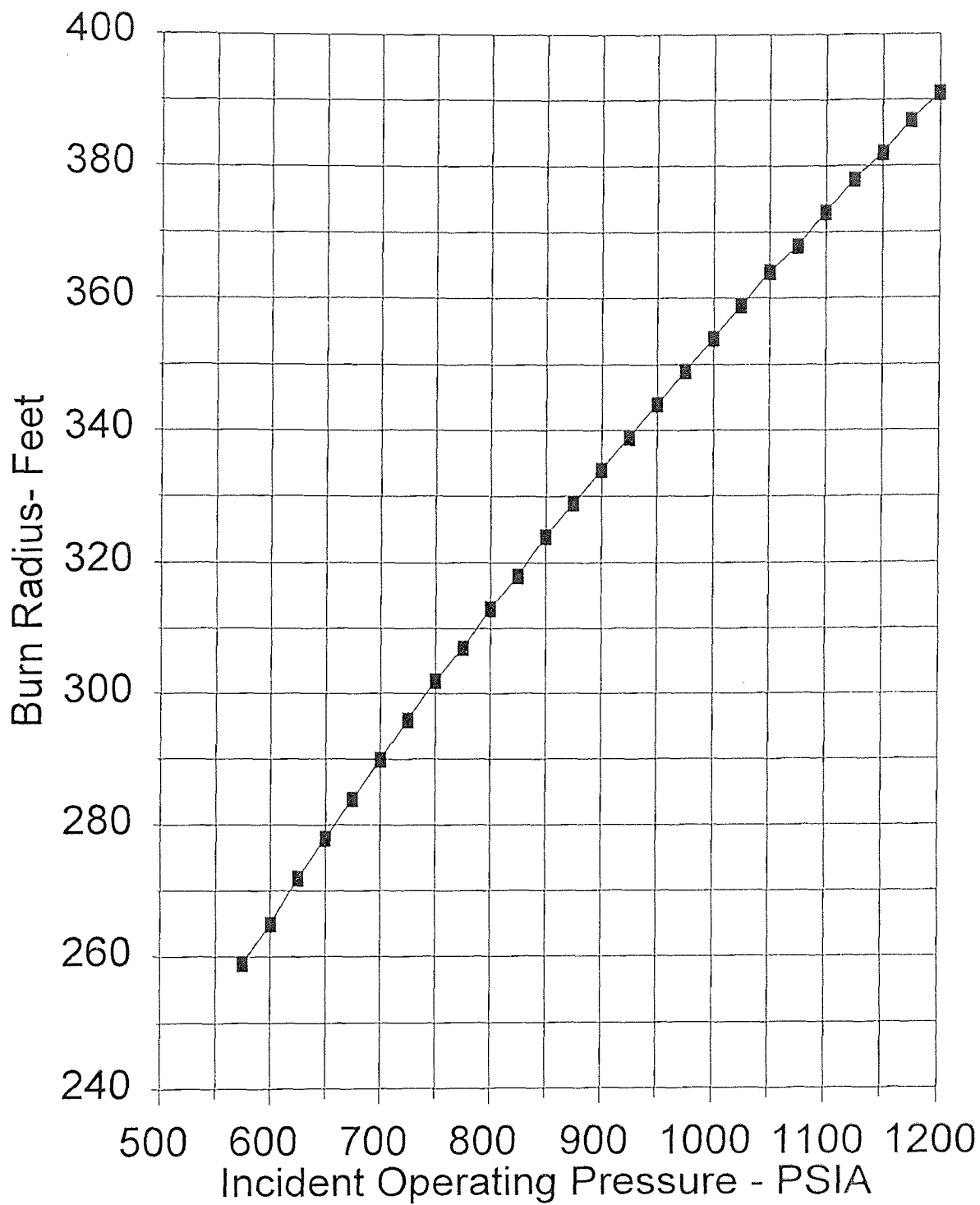Figure B.23 - Burn Radius for 16" Diameter Pipeline
K = 9,985 Btu/hr sq. ft.
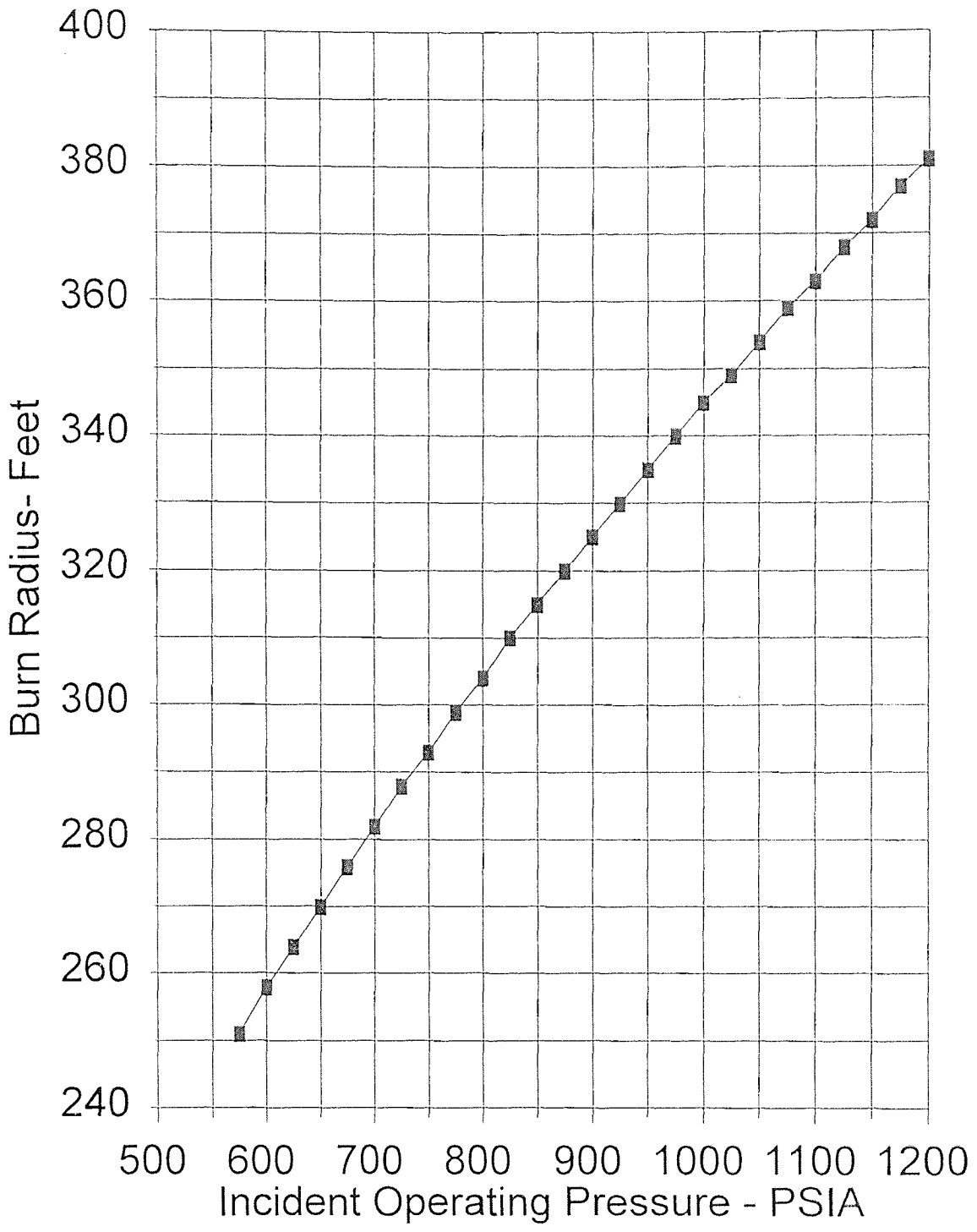
Figure B.24 - Burn Radius for 18" Diameter Pipeline
K = 9,985 Btu/hr sq. ft.
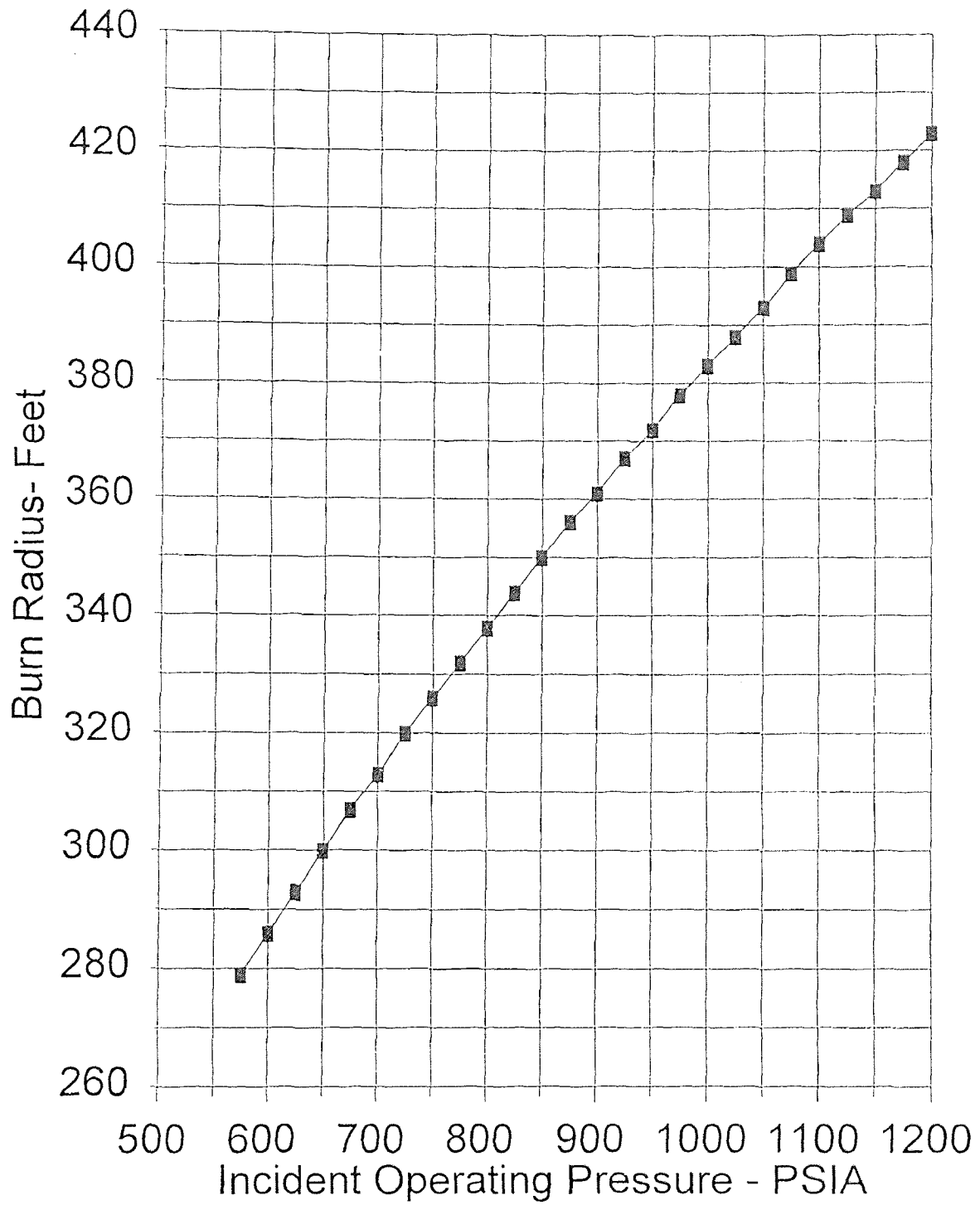
Figure B.25 - Burn Radius for 20" Diameter Pipeline
K = 9,985 Btu/hr sq. ft.
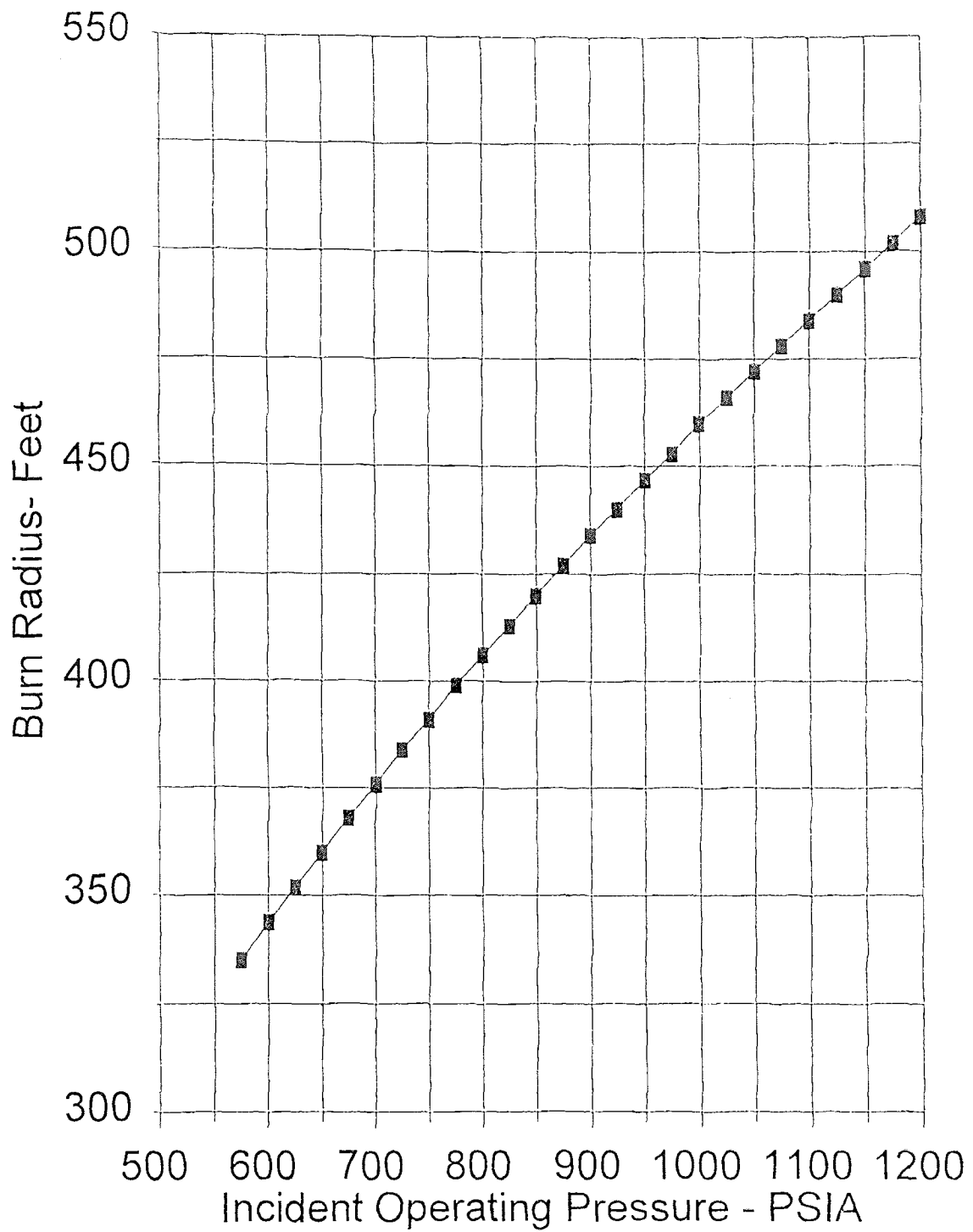
Figure B.26 - Burn Radius for 24" Diameter Pipeline
K = 9,985 Btu/hr sq. ft.

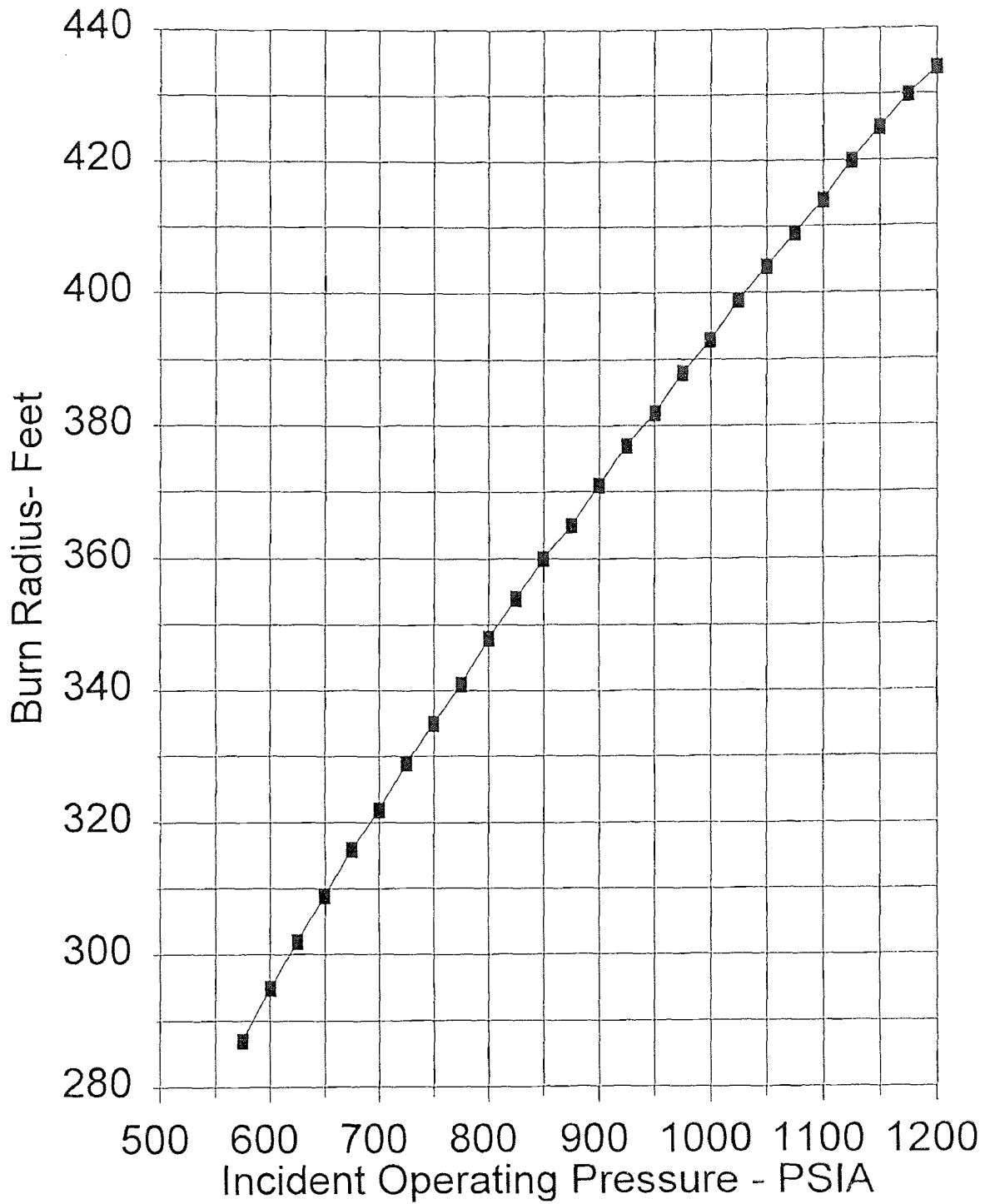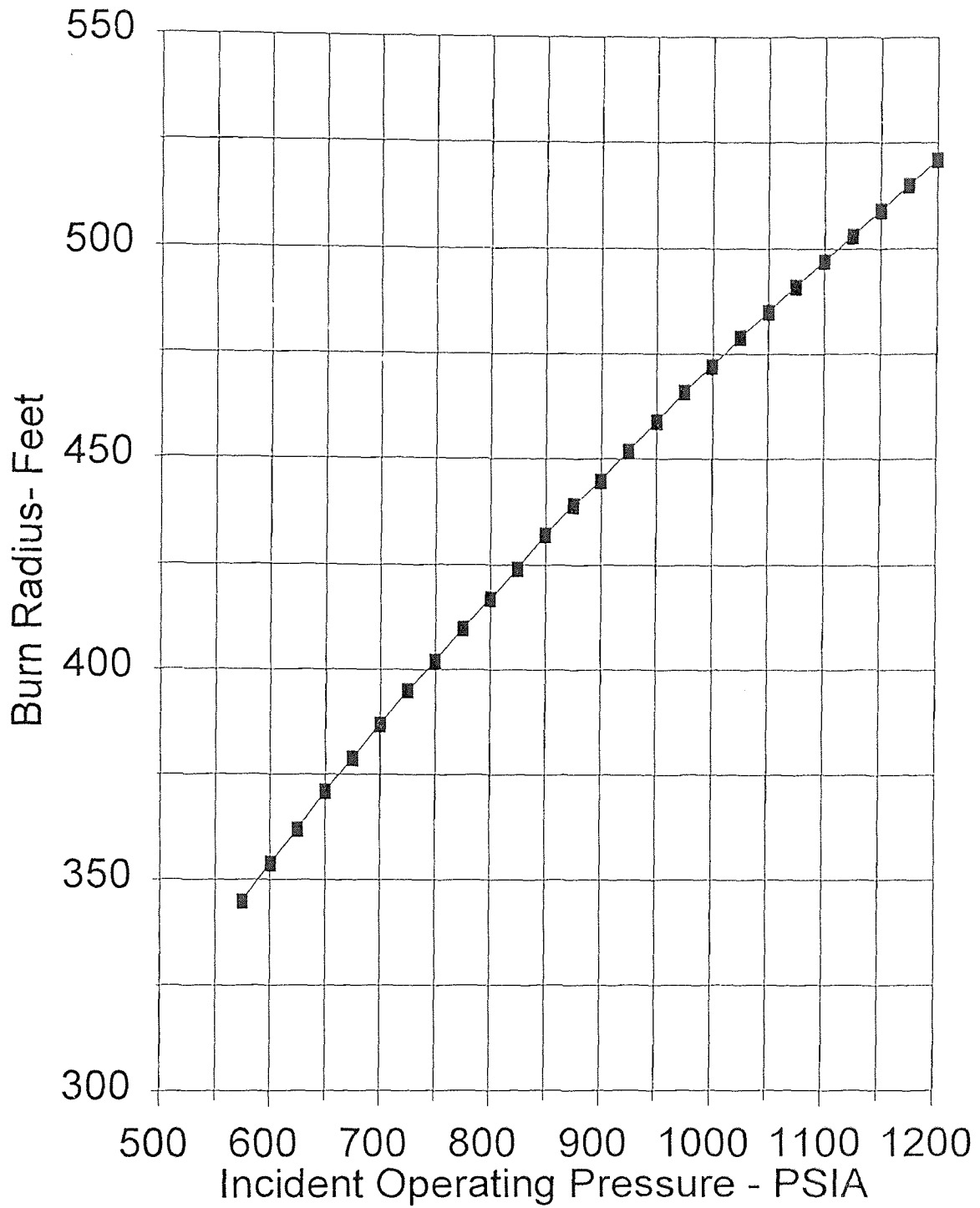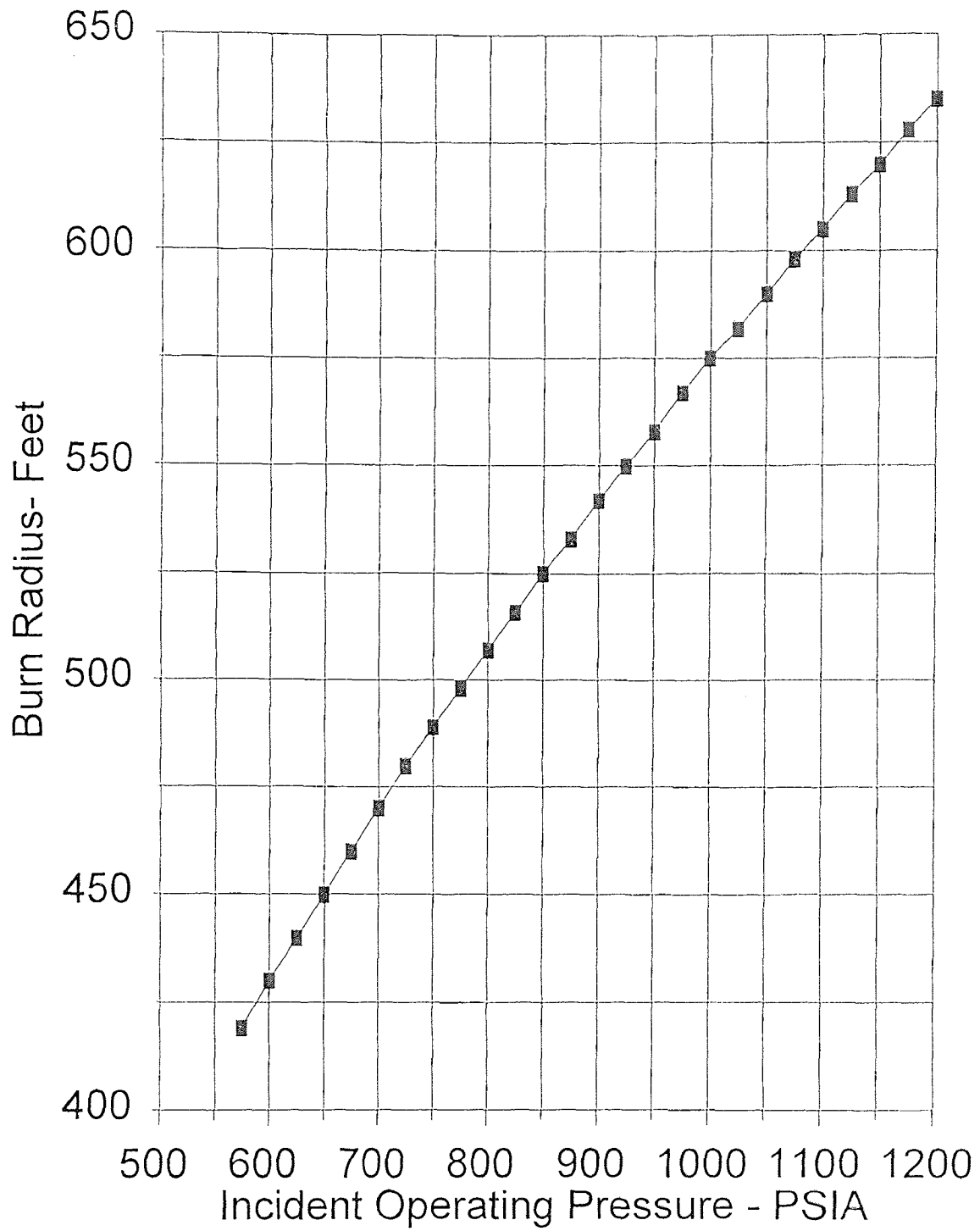Figure B.27 - Burn Radius for 30" Diameter Pipeline
K = 9,985 Btu/hr sq. ft.
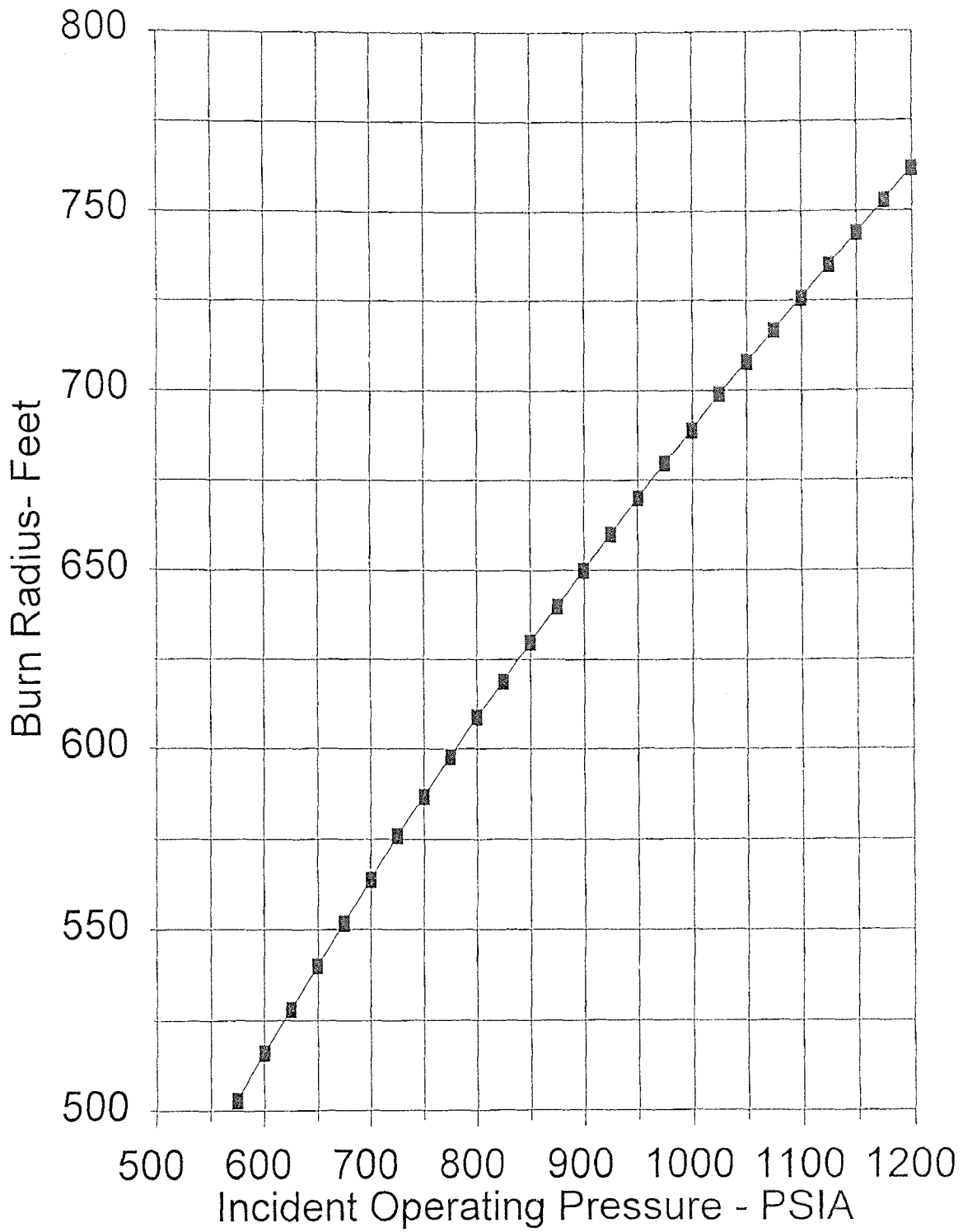
Figure B.28 - Burn Radius for 36" Diameter Pipeline
K = 9,985 Btu/hr sq. ft.

APPENDIX C - FIGURES AND TABLES FOR CHAPTER 5

130

Figure C.1 – Detailed View of Edison Accident

DURHAM WOODS
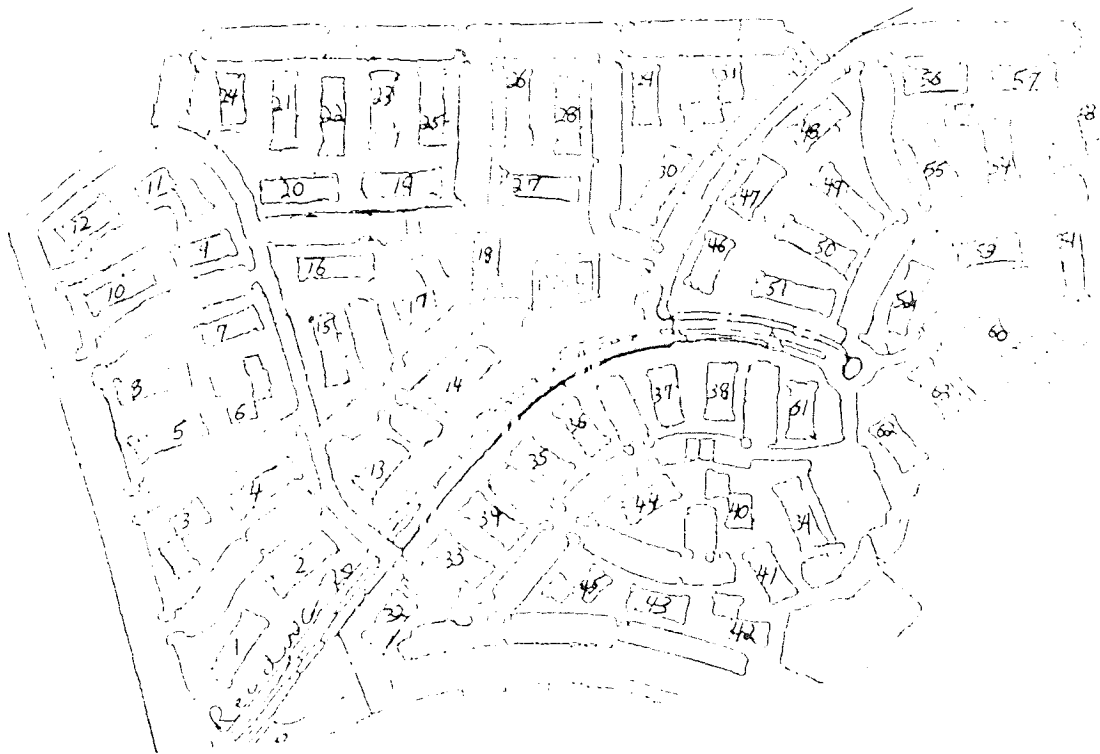
Figure C.2 - Identification of Apartment Buildings
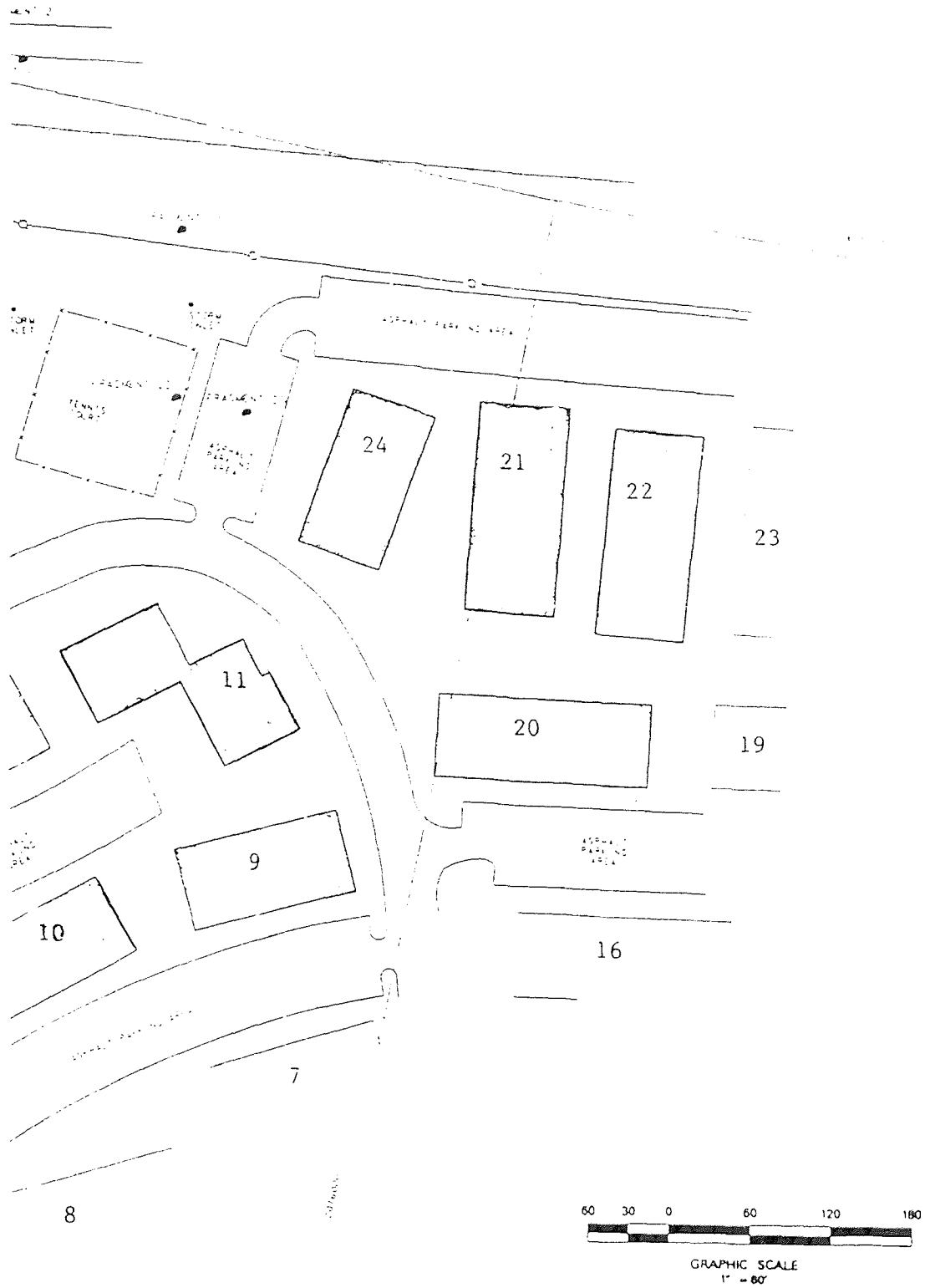
**Figure C.3 - Illustration of Apartments Used for Development
of an Appropriate Scale**
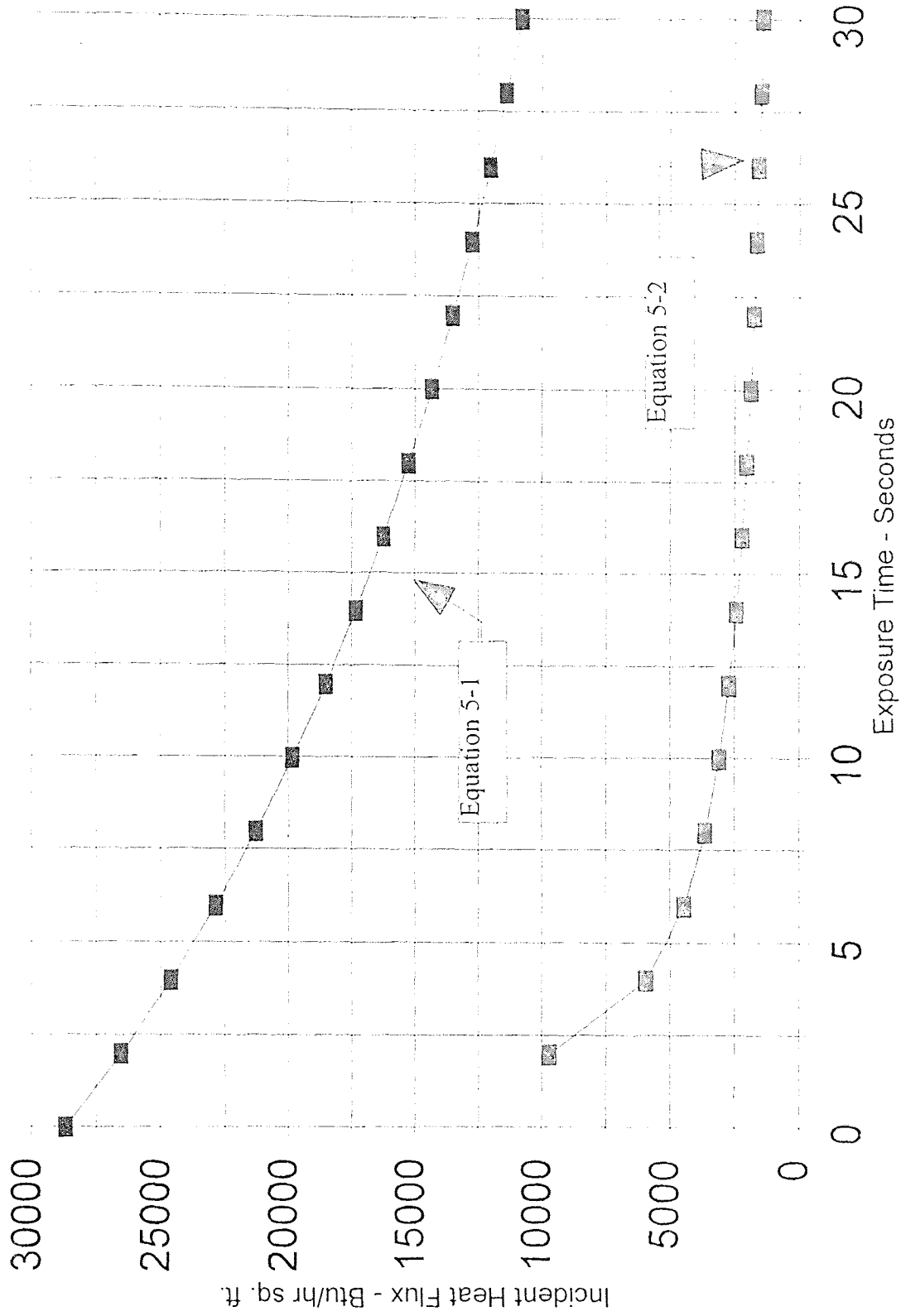
Figure C.4 - Comparison of Flux Levels Experienced Versus Levels for Blistering

Table C.1

Comparison of Building Distances to Safe Separation Ditances

Diameter Inch	Distance from Pipeline - Feet* From Dutch Regulations			Safe Separation Distance - Feet Using Equation 4-12		
	35 Bar 522.3 psia	65 Bar 957.4 psia	95 Bar 1392.6 psia	35 Bar 522.3 psia	65 Bar 957.4 psia	95 Bar 1200.0 psia
14	56	66	82	184	262	296
16	66	66	82	211	299	339
18	**	66	82	237	337	381
24	**	82	82	316	449	508
30	**	98	115	395	561	635
36	**	115	148	474	673	762

Notes: *Distances converted from meters to feet using the reationship 1 meter equals 3.2808 feet.
**Distances determined on a case by case basis.

Table C.2
Ratios of Building and Separation Distances at Various Diameters (Constant Pressure)

Diameter Ratio Selected	Ratios of Building Distances (Using Dutch Regulations)			Ratios of Separation Distances (Using Equation 4-12)		
	35 Bar 522.3 psia	65 Bar 957.4 psia	95 Bar 1392.6 psia	35 Bar 522.3 psia	65 Bar 957.4 psia	95 Bar 1200.0 psia
16"/14"	1.18	1.00	1.00	1.14	1.14	1.14
18"/14"	----	1.00	1.00	1.29	1.29	1.29
24"/14"	----	1.24	1.00	1.71	1.71	1.71
30"/14"	----	1.48	1.40	2.14	2.14	2.14
36"/14"	----	1.74	1.80	2.57	2.57	2.57
18"/16"	----	1.00	1.00	1.13	1.13	1.13
24"/16"	----	1.24	1.00	1.50	1.50	1.50
30"/16"	----	1.48	1.40	1.88	1.88	1.88
36"/16"	----	1.74	1.80	2.25	2.25	2.25
24"/18"	----	1.24	1.00	1.33	1.33	1.33
30"/18"	----	1.48	1.40	1.67	1.67	1.67
36"/18"	----	1.74	1.80	2.00	2.00	2.00
30"/24"	----	1.20	1.40	1.25	1.25	1.25
36"/24"	----	1.40	1.80	1.50	1.50	1.50
36"/30"	----	1.17	1.29	1.20	1.20	1.20

Table C.3

Ratios of Building and Separation Distances at Various Pressures (Constant Diameter)

Diameter	Ratios of Building Distances (Using Dutch Regulations)			Ratios of Separation Distances (Using Equation 4-12)		
	957.4/522.3 psia	1,392.6/522.3 psia	1,392.6/957.4 psia	957.4/522.3 psia	1,200.0/522.3 psia	1,200.0/957.4 psia
14"	1.18	1.46	1.24	1.42	1.61	1.13
16"	1.00	1.24	1.24	1.42	1.61	1.13
18"	----	----	1.24	1.42	1.61	1.13
24"	----	----	1.00	1.42	1.61	1.13
30"	----	----	1.17	1.42	1.61	1.13
36"	----	----	1.29	1.42	1.61	1.13

APPENDIX D - VARIATION OF BURN RADIUS INFORMATION

The following pages provide tables, referenced in Chapter 6, which serve to demonstrate the influence of the following factors on the burn radius:

- Atmospheric transmissivity;

- Heat flux and atmospheric transmissivity (combined); and

- Wind direction and speed.

It should be remembered that the various burn radii are calculated using Equation 4-12.

139

Table D.1

Variation of Burn Radius with Atmospheric Transmissivity

Pipeline Conditions - Diameter/Incident Operating Pressure

Heat Flux Btu/hr ft²	14"/575 psia Value of τ			14"/1,200 psia Value of τ			36"/575 psia Value of τ			36"/1,200 psia Value of τ		
	0.875	0.746	0.470	0.875	0.746	0.470	0.875	0.746	0.470	0.875	0.746	0.470
3,962	357	328	255	523	482	379	918	843	656	1,345	1,239	975
6,340	277	254	195	410	377	295	713	653	500	1,055	970	758
9,510	221	201	151	331	304	236	568	517	388	852	782	606
9,985	215	195	146	323	296	229	552	503	376	830	762	589

Table D.2

Percent Difference Between Burn Radii Obtained Using Assumed Vaue of τ and Burn Radii Determined Using Maximum and Minimum Values of τ

Pipeline Conditions - Diameter/Incident Operating Pressure

Heat Flux Btu/hr ft²	14"/575 psia Value of τ			14"/1,200 psia Value of τ			36"/575 psia Value of τ			36"/1,200 psia Value of τ		
	0.875	0.746	0.470	0.875	0.746	0.470	0.875	0.746	0.470	0.875	0.746	0.470
3,962	-8	-----	29	-8	-----	27	-8	-----	29	-8	-----	27
6,340	-8	-----	30	-8	-----	28	-8	-----	31	-8	-----	28
9,510	-9	-----	33	-8	-----	29	-9	-----	33	-8	-----	29
9,985	-9	-----	34	-8	-----	29	-9	-----	34	-8	-----	29

Note: Since τ = 0.746 is the assumed value for atmospheric transmissivity, there are no entries in those columns.

Table D.3

Variation of Burn Radii

For Combined Variations in Heat Flux and Atmospheric Transmissivity

Pipeline Conditions - Diameter/Incident Operating Pressure

Heat Flux Btu/hr ft²	14"/575psia			14"/1,200 psia			36"/575 psia			36"/1,200 psia		
	Value of τ			Value of τ			Value of τ			Value of τ		
	0.875	0.746	0.470	0.875	0.746	0.470	0.875	0.746	0.470	0.875	0.746	0.470
2,972	415	381	298	606	559	440	1,067	982	768	1,559	1,437	1,132
3,962	357	328	255	523	482	379	918	843	656	1,345	1,239	975
4,953	317	291	225	466	429	337	815	747	578	1,199	1,104	866
4,755	324	297	230	476	439	344	833	764	592	1,225	1,128	885
6,340	277	254	195	410	377	295	713	653	500	1,055	970	758
7,925	245	224	170	365	335	261	630	575	436	938	862	671
7,133	260	238	181	386	355	277	668	611	466	992	912	711
9,510	221	201	151	331	304	236	568	517	388	852	782	606
11,888	194	176	129	294	269	207	498	452	333	756	692	533
7,489	253	231	176	376	346	269	650	594	452	967	889	692
9,985	215	195	146	323	296	229	552	503	376	830	762	589
12,481	188	171	125	286	262	201	484	439	321	736	674	518

Note: Center value of each 3x3 subtable is considered to be the reference value, around which conditions are varied.

Table D.4
Percent Difference in Burn Radii
For Combined Variations in Heat Flux and Atmospheric Transmissivity

Pipeline Conditions - Diameter/Incident Operating Pressure

Heat Flux Btu/hr ft²	14"/575psia			14"/1,200 psia			36"/575 psia			36"/1,200 psia		
	Value of τ			Value of τ			Value of τ			Value of τ		
	0.875	0.746	0.470	0.875	0.746	0.470	0.875	0.746	0.470	0.875	0.746	0.470
2,972	27	16	-9	26	16	-9	27	16	-9	26	16	-9
3,962	9	--	-22	9	--	-21	9	--	-22	9	--	-21
4,953	-3	-11	-31	-3	-11	-30	-3	-11	-31	-3	-11	-30
4,755	28	17	-9	26	16	-9	28	17	-9	26	16	-9
6,340	9	--	-23	9	--	-22	9	--	-23	9	--	-22
7,925	-4	-12	-33	-3	-11	-31	-4	-12	-33	-3	-11	-31
7,133	29	18	-10	27	17	-9	29	18	-10	27	17	-9
9,510	10	--	-25	9	--	-22	10	--	-25	9	--	-23
11,888	-3	-12	-36	-3	-12	-32	-4	-13	-36	-3	-12	-32
7,489	30	18	-10	27	17	-9	29	18	-10	27	17	-9
9,985	10	--	-25	9	--	-23	10	--	-25	9	--	-23
12,481	-4	-12	-36	-3	-11	-32	-4	-13	-36	-3	-12	-32

Note: Entries designated by "--" indicate conditions at which the burn radius is considered to be the reference value.

Table D.5

Variation of Burn Radius with Wind Direction and Speed

24" Diameter Pipeline, P = 1,000 psig

Distance to Specified Heat Flux - Feet

Heat Flux		Wind Speed 12.4 miles/hr			Wind Speed 6.2 miles/hr			
kW/m^2	Btu/hr ft^2	U.W.	D.W.	C.W.	U.W.	D.W.	C.W.	Equation 4-12
30	9,510	361	472	427	394	443	420	476
25	7,925	413	548	469	443	489	466	525
20	6,340	466	686	545	495	600	535	592
15	4,755	607	823	732	682	778	732	689

Note: U.W. = Upwind
D.W. = Downwind
C.W. = Crosswind

Table D.6

Percent Difference between Equation 4-12 and the Canadian Values

24" Diameter Pipeline, P = 1,000 psig

Heat Flux		Wind Speed 12.4 miles/hr			Wind Speed 6.2 miles/hr		
kW/m^2	Btu/hr ft^2	U.W.	D.W.	C.W.	U.W.	D.W.	C.W.
30	9,510	32	1	11	21	7	13
25	7,925	27	-4	12	19	7	13
20	6,340	27	-14	9	20	-1	11
15	4,755	14	-16	-6	1	-11	-6

Note: U.W. = Upwind
D.W. = Downwind
C.W. = Crosswind

Table D.7

Variation of Burn Radius with Wind Direction and Speed

36" Diameter Pipeline, P = 1,000 psig

Distance to Specified Heat Flux - Feet

Heat Flux		Wind Speed 12.4 miles/hr			Wind Speed 6.2 miles/hr			Equation 4-12
kW/m²	Btu/hr ft²	U.W.	D.W.	C.W.	U.W.	D.W.	C.W.	
30	9,510	459	656	492	492	564	499	714
25	7,925	538	764	656	597	702	646	788
20	6,340	686	922	791	751	823	794	888
15	4,755	899	1,177	1,047	984	1,112	1,030	1,033

Note: U.W. = Upwind
D.W. = Downwind
C.W. = Crosswind

Table D.8

Percent Difference between Equation 4-12 and the Canadian Values

36" Diameter Pipeline, P = 1,000 psig

Heat Flux		Wind Speed 12.4 miles/hr			Wind Speed 6.2 miles/hr		
kW/m^2	$Btu/hr\ ft^2$	U.W.	D.W.	C.W.	U.W.	D.W.	C.W.
30	9,510	56	9	45	45	27	43
25	7,925	46	3	20	32	12	22
20	6,340	29	-4	12	18	8	12
15	4,755	15	-12	-1	5	-7	0.3

Note: U.W. = Upwind
      D.W. = Downwind
      C.W. = Crosswind

APPENDIX E - CANADIAN HEAT FLUX INFORMATION

Exhibit No._____

Undertaking given by Mr. Rothwell to Mr. Abes at Transcript

Volume 4, Page 468

Q. To provide a revised Response to NEB IR. No. 23 re Thermal Radiation Curves.

A. The attached families of curves show the variation of thermal radiation flux with distance for NPS 24, 36 and 42 pipe at an operating pressure of 1000 psig and with wind speeds of 10 and 20 km/h. Other conditions are the same as those for Figures 23.2 to 23.9 of the original response. For each case, plots for upwind, downwind and crosswind directions are given.

Since Board Staff's request concerned the predictions immediately after ignition, we have elected not to incur the delay which would have been associated with the production of colour copies of the plots. However, to follow the evolution with time of the thermal radiation flux on the monochrome copies, it is sufficient to recall that the curves are sequential with time from top to bottom, i.e. the curve for time 0 is at the top and the curve for time 900 is at the bottom.

As was discussed qualitatively at Transcription Page 465, the distances to specified levels of thermal radiation increase somewhat in the downwind direction and decrease in the upwind direction. It is normal in detailed risk assessments to take into account the statistical variation of wind direction.
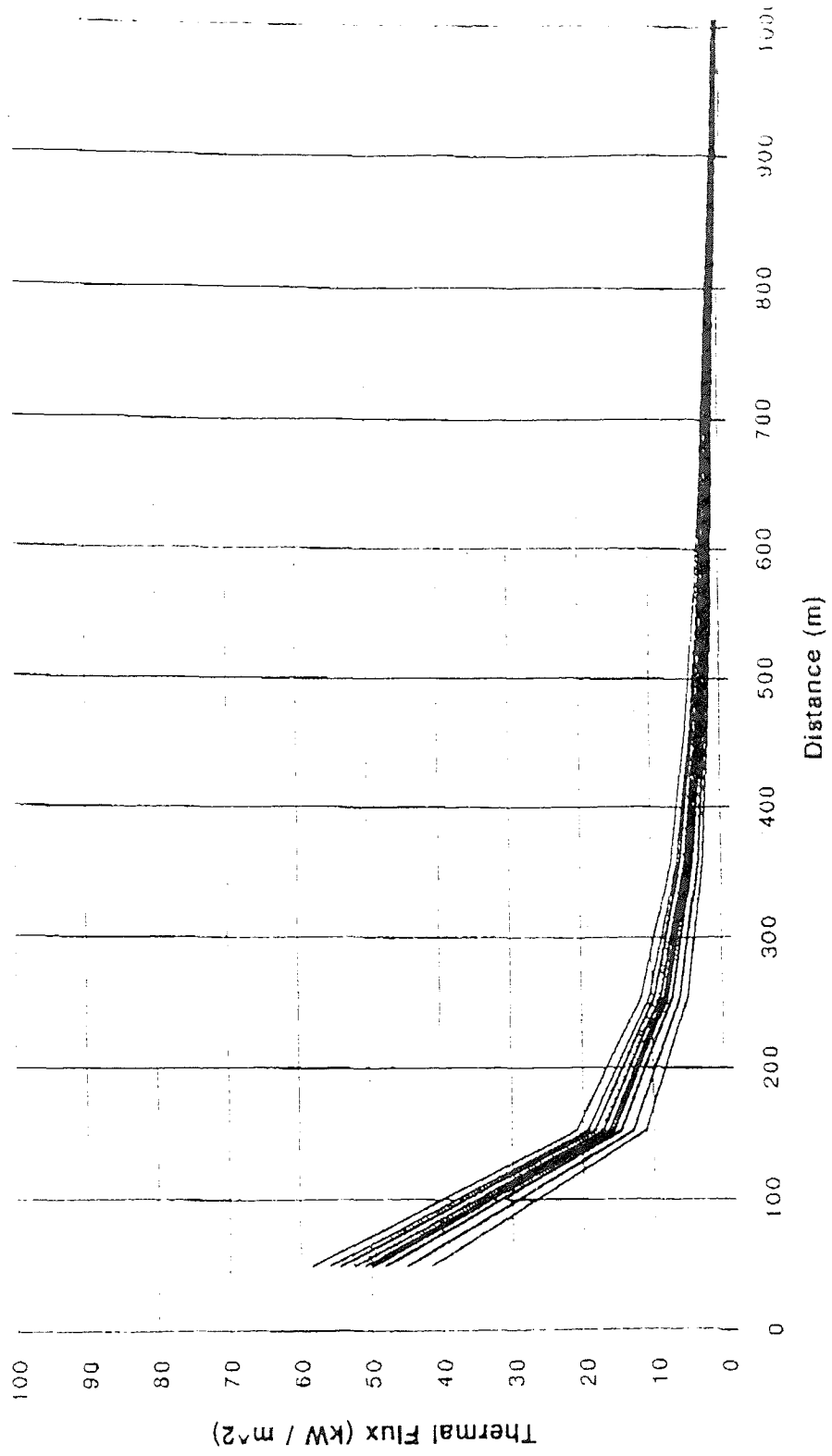
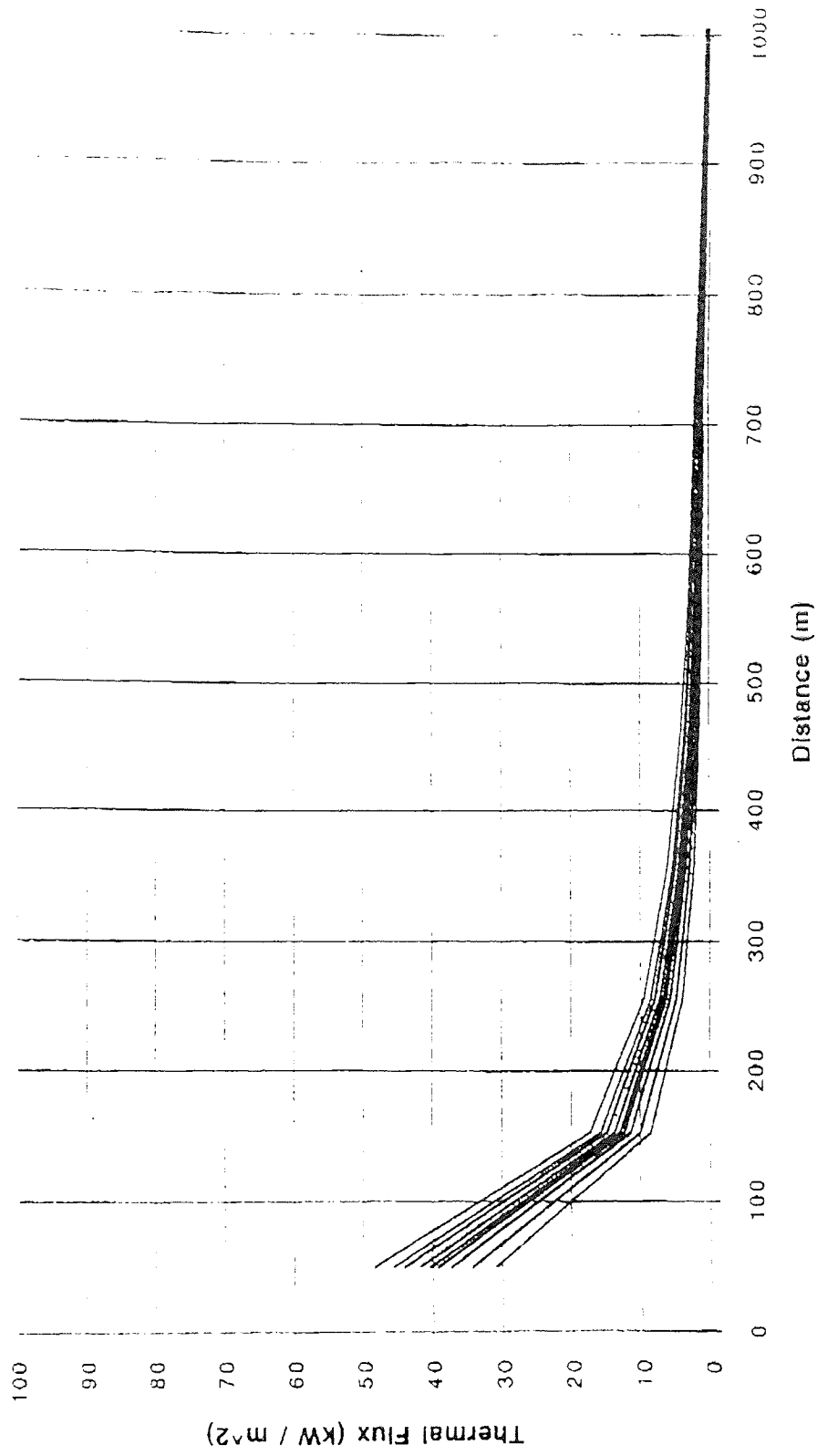NPS 24, 1000 psi, Wind Speed=10kph, Upwind Direction
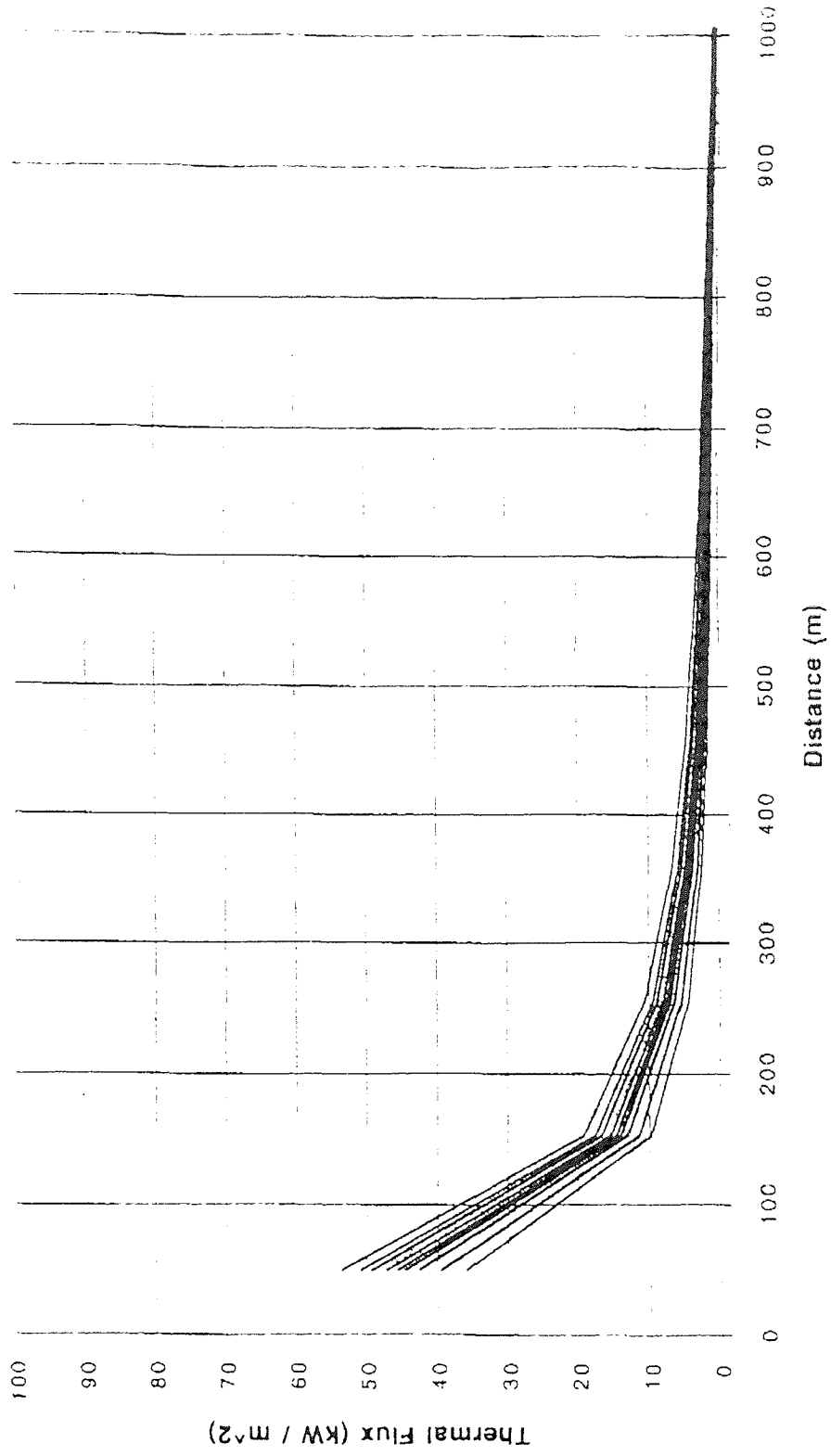
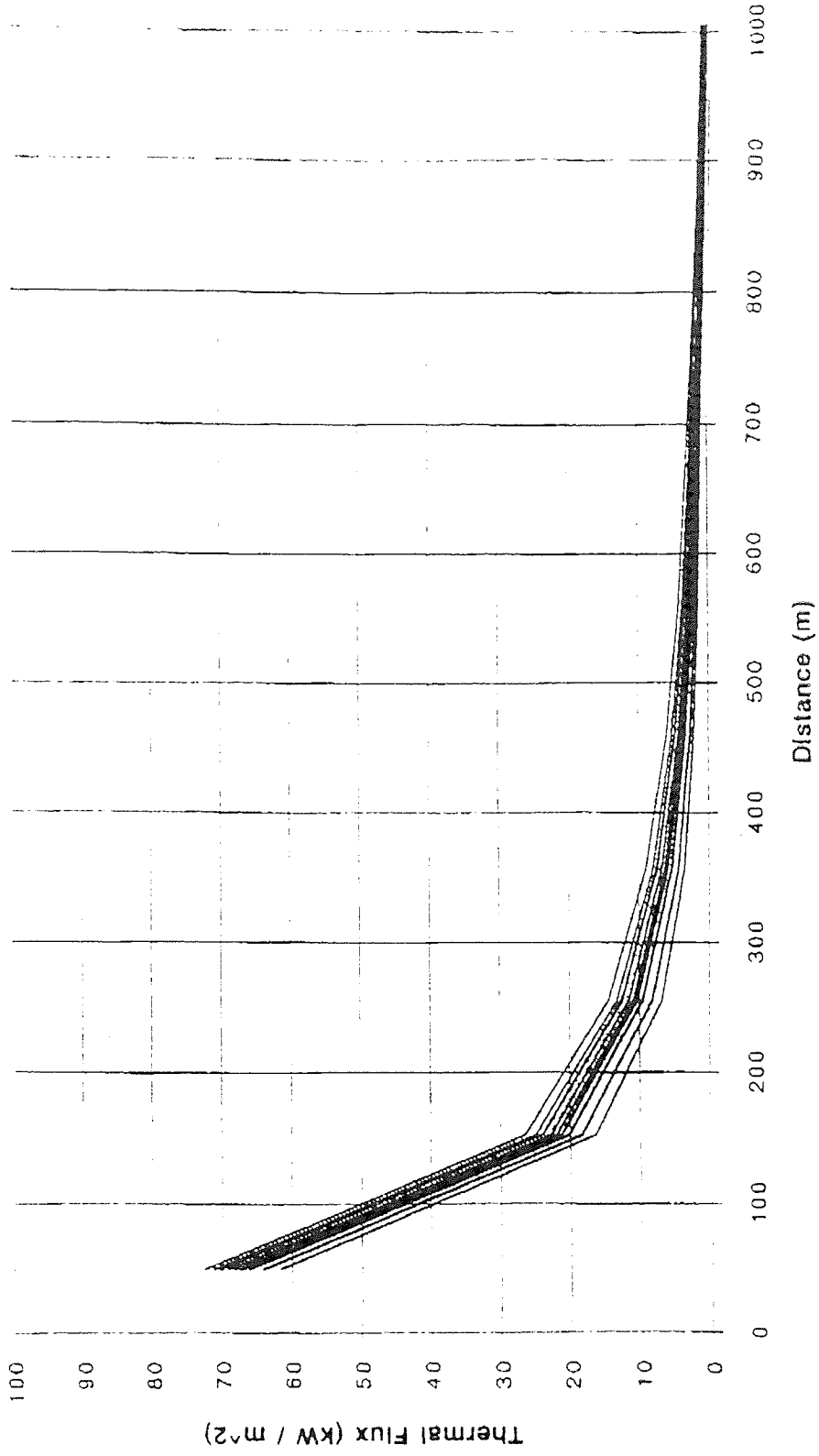NPS 24, 1000 psi, Wind Speed=10kph, Downwind Direction

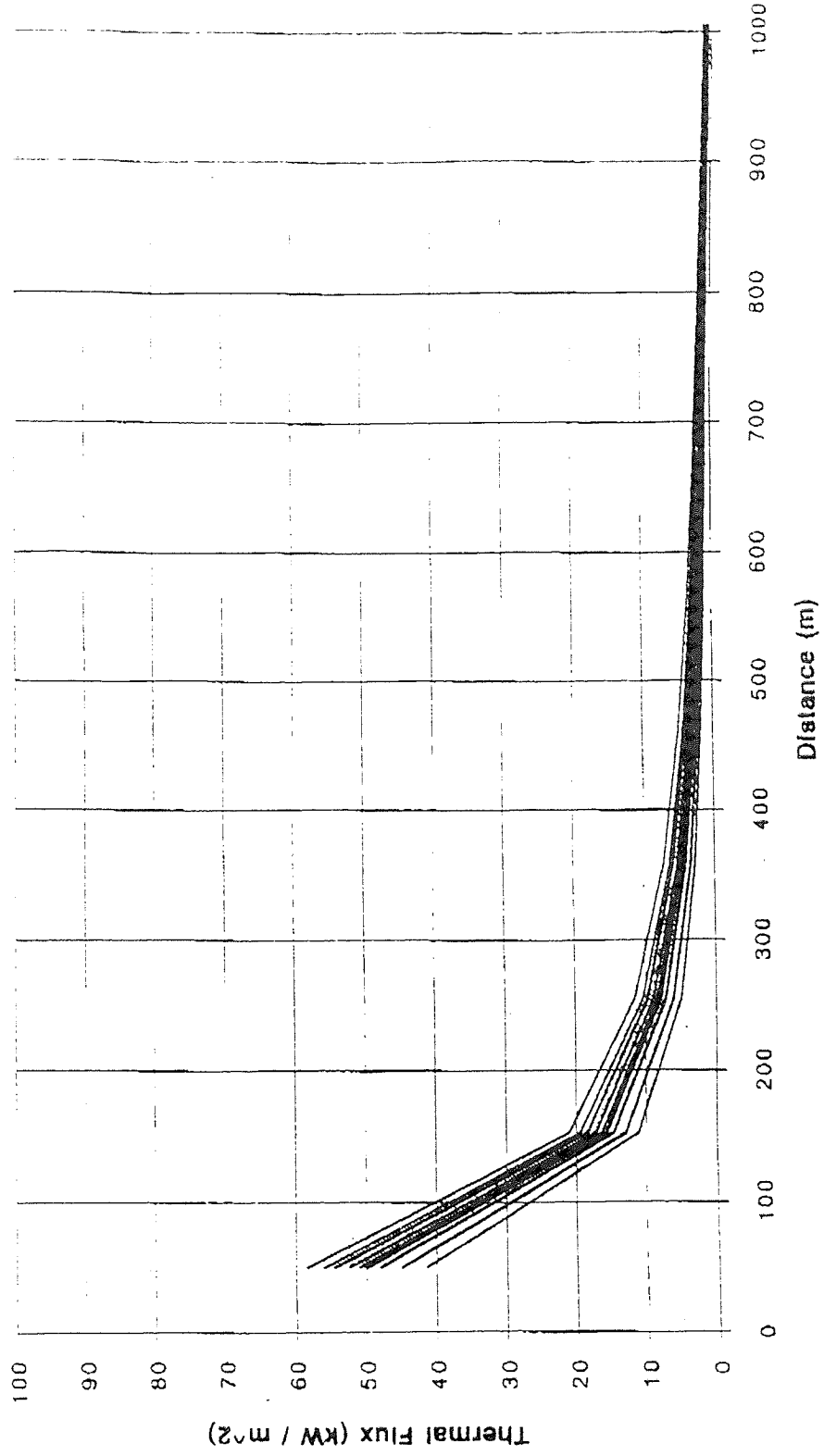NPS 24, 1000 psi, Wind Speed=10kph, Crosswind Direction
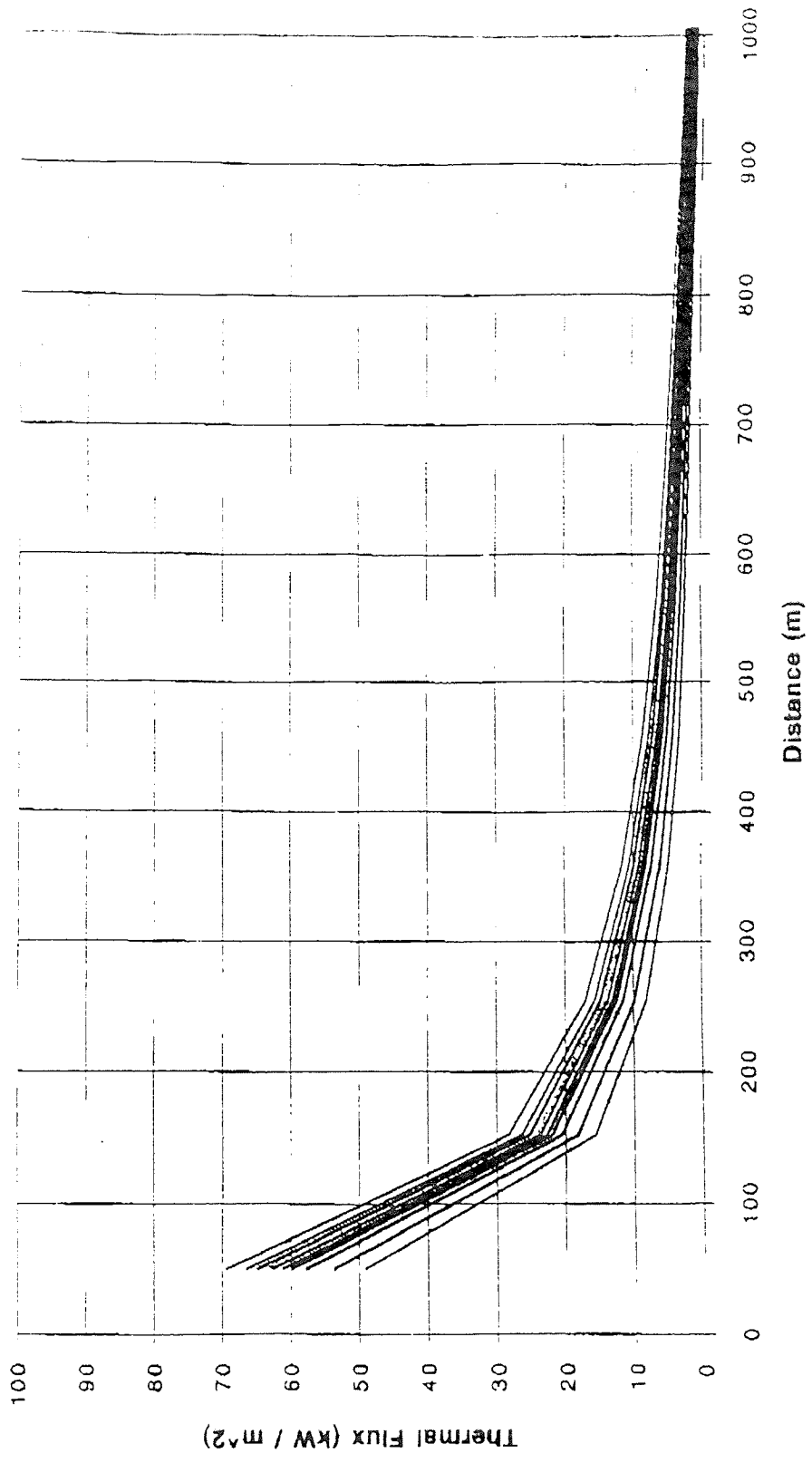
NPS 24, 1000 psi, Wind Speed=20kph, Upwind Direction

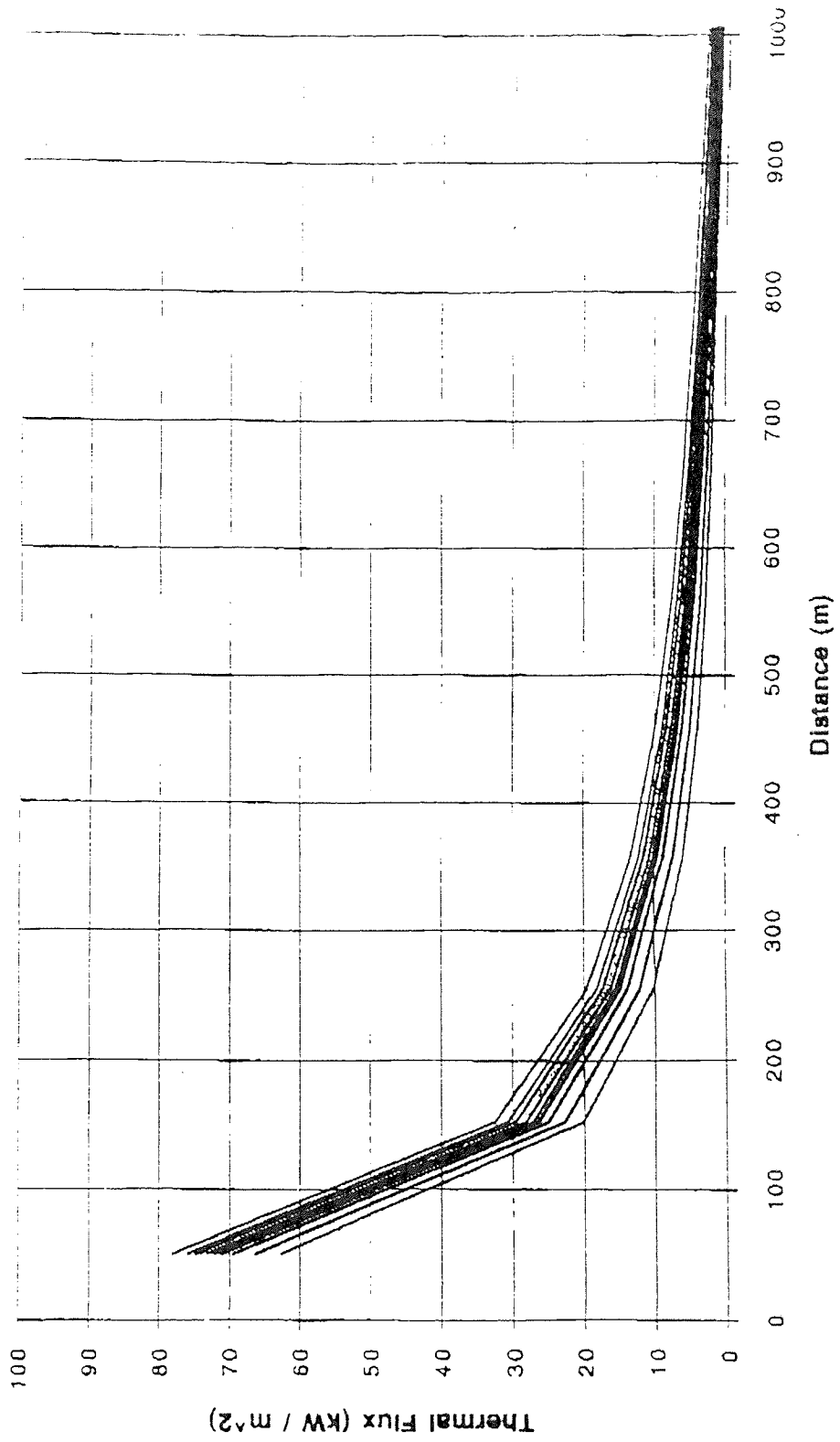NPS 24, 1000 psi, Wind Speed=20kph, Downwind Direction

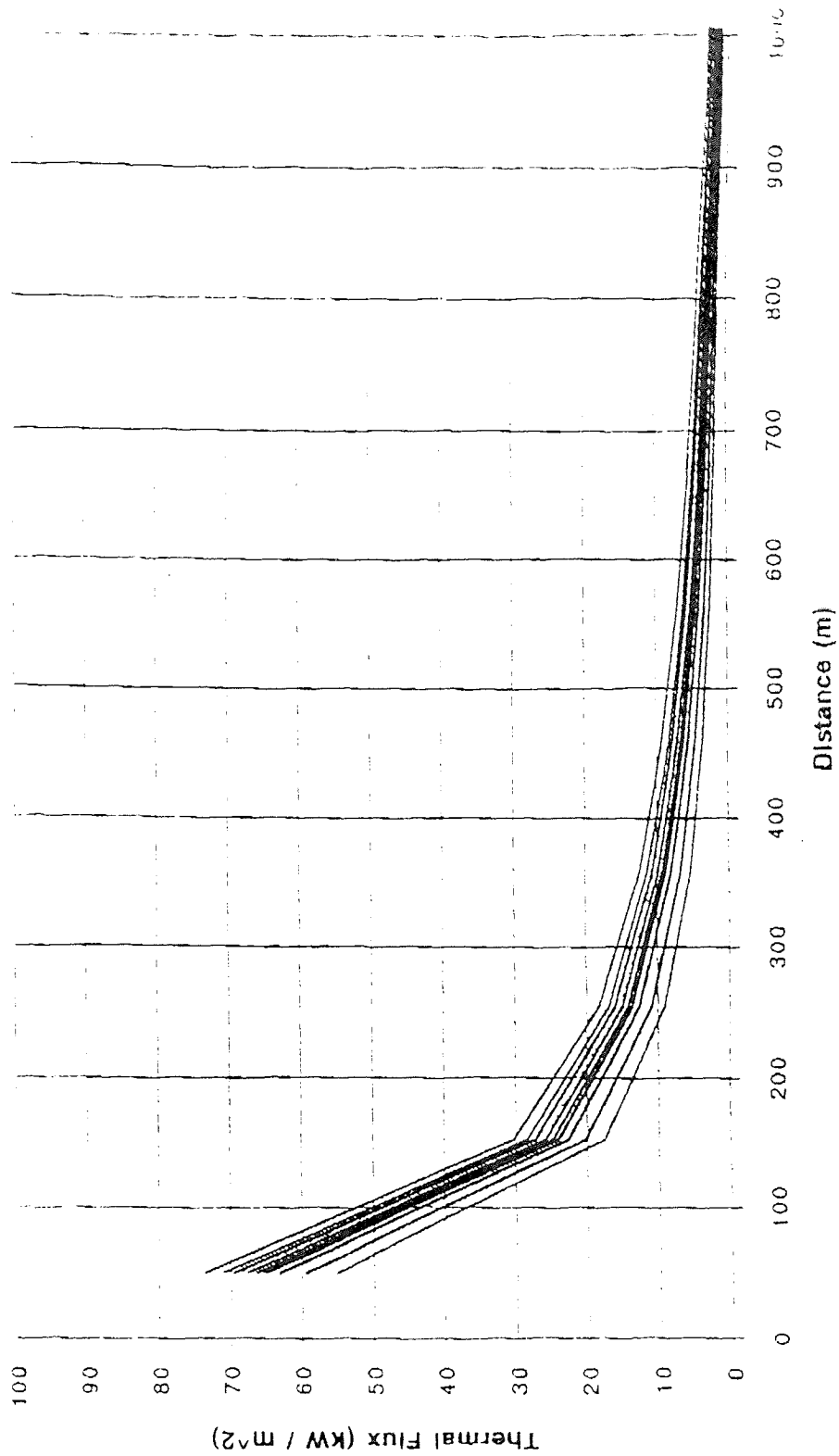NPS 24, 1000 psi, Wind Speed=20kph, Crosswind Direction

155

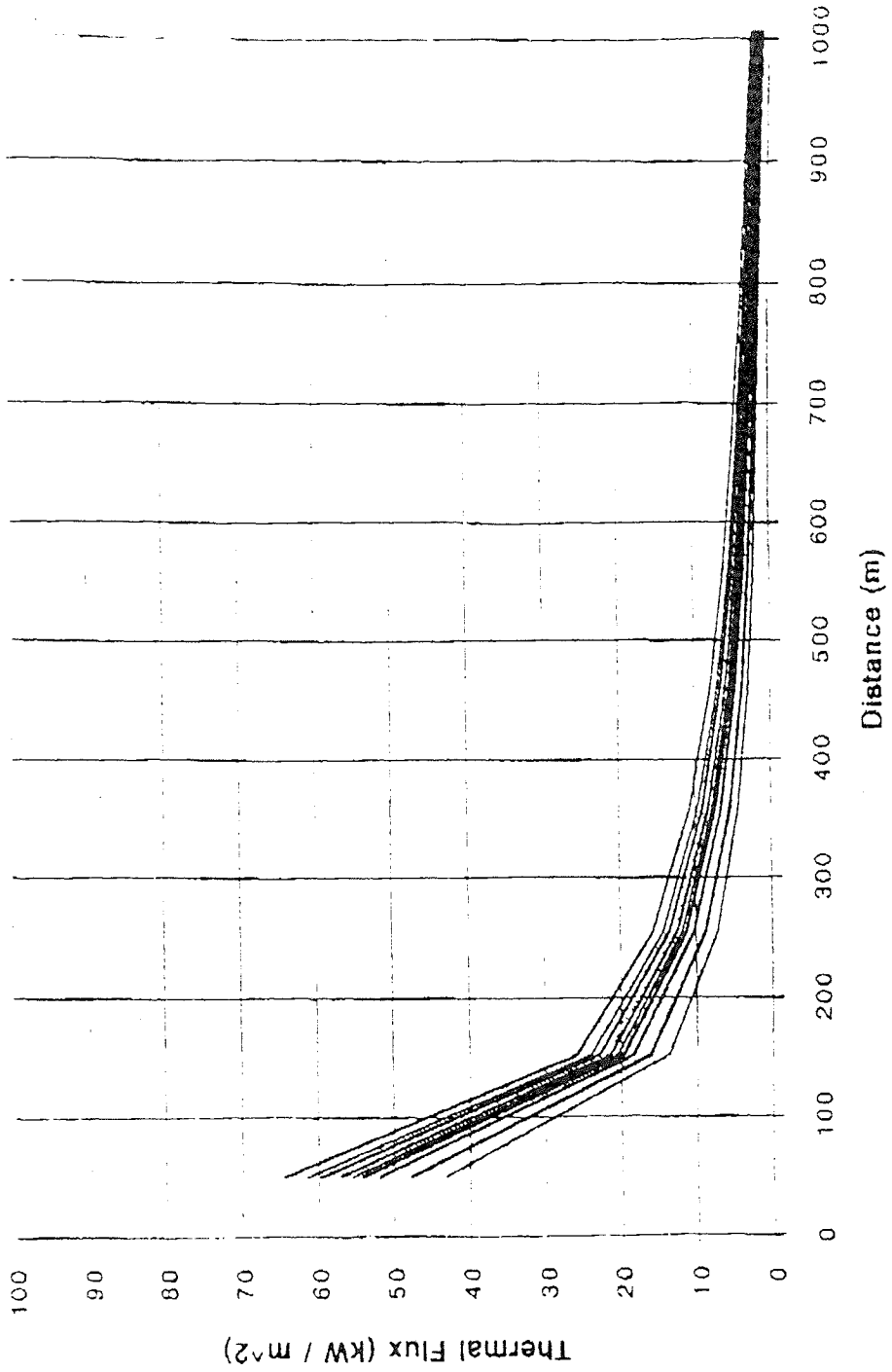NPS 36, 1000 psi, Wind Speed=10kph, Upwind Direction

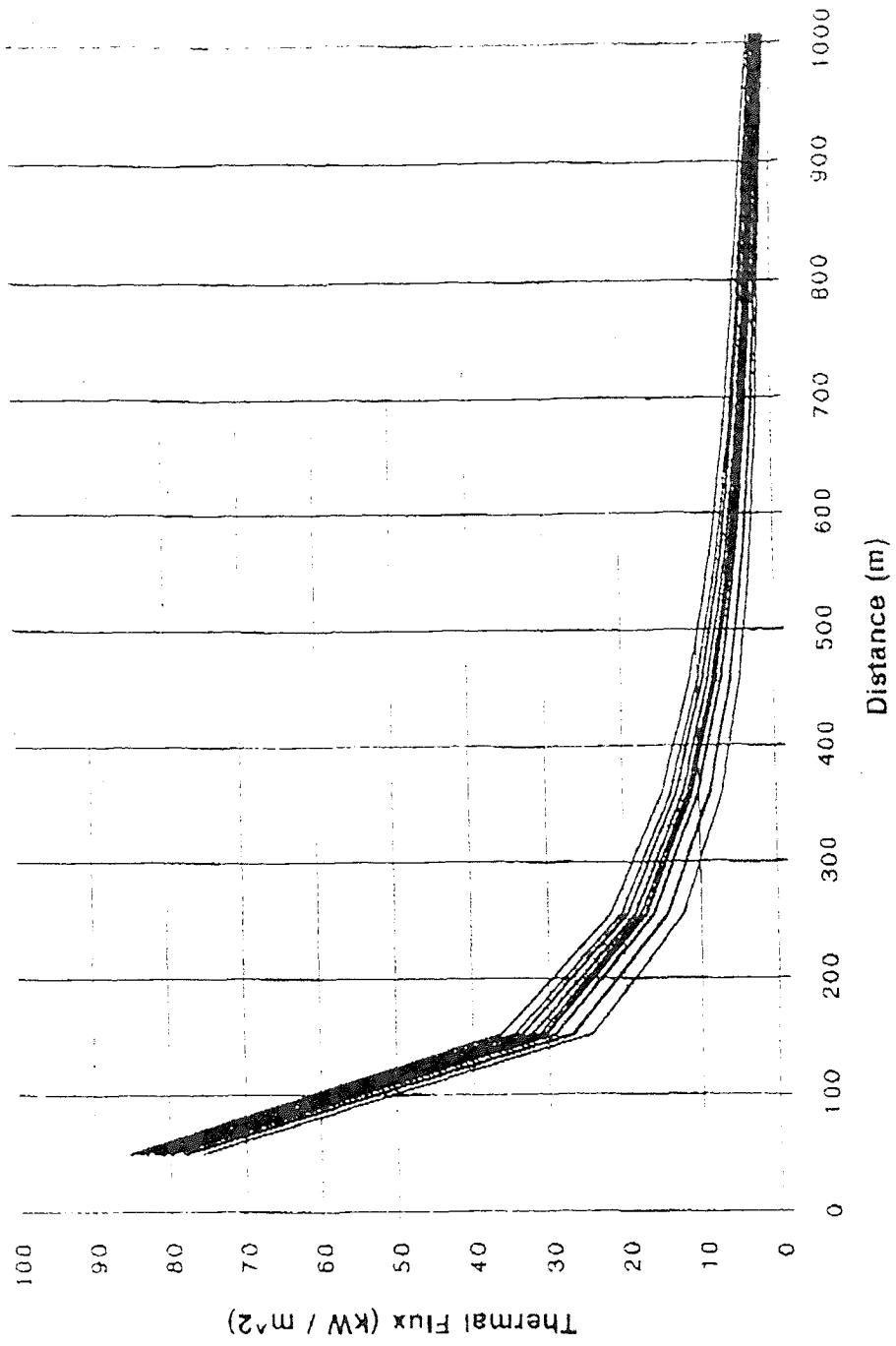NPS 36, 1000 psi, Wind Speed=10kph, Downwind Direction

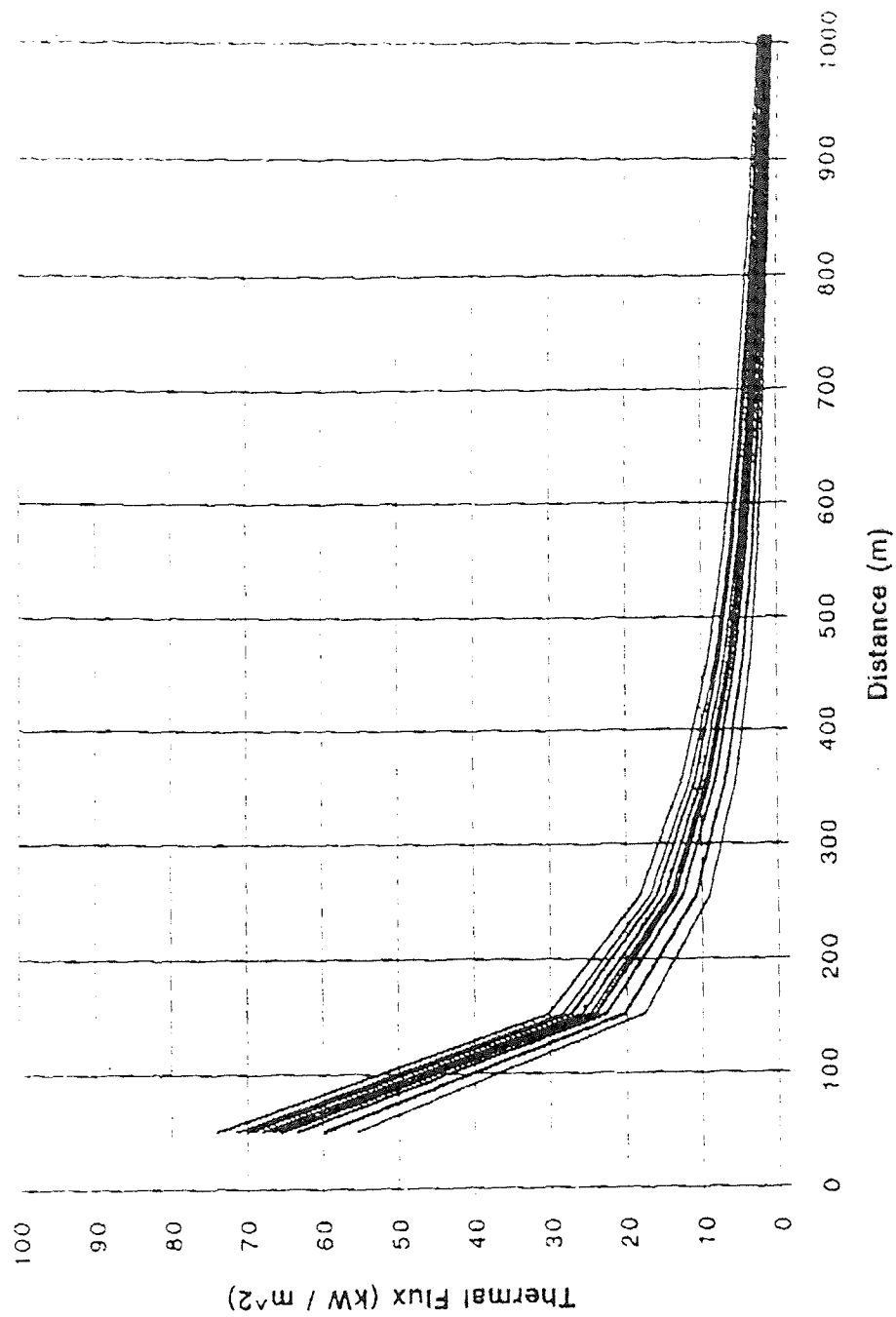NPS 36, 1000 psi, Wind Speed=10kph, Crosswind Direction

NPS 36, 1000 psi, Wind Speed = 20kph, Upwind Direction

NPS 36, 1000 psi, Wind Speed = 20kph, Downwind Direction

NPS 36, 1000psi, Wind Speed = 20kph, Crosswind Direction

REFERENCES

1. Transportation Research Board. *Special Report 219 Pipelines and Public Safety.* Washington, DC: Transportation Research Board.

2. National Transportation Safety Board. *Texas Eastern Gas Pipeline Company Ruptures and Fires at Beaumont, Kentucky on April 27, 1985 and Lancaster, Kentucky on February 21, 1986.* Washington, DC: National Transportation Safety Board (1987).

3. National Transportation Safety Board. *Texas Eastern Transmission Corporation Natural Gas Pipeline Explosion and Fire Edison, New Jersey March 23, 1994.* Washington, DC: National Transportation Safety Board (1995).

4. U.S. Department of Transportation, Research and Special Programs Administration. *Pipeline Safety Regulations.* Washington, DC: U.S. Department of Transportation (1993).

5. Griffis, F.H., R. Dresnack, S. Evans, E. Golub, J. Greenfeld, L.J. Pignataro, and L. Vega. *Pipeline Industry: Comparison of U.S. with Foreign Pipeline Land Use and Siting Standards Maintenance, Rehabilitation and Retrofitting Policies and Practices.* Final report prepared by NJIT under Contract No. DTRS 56-94-C-0006 for the U.S. Department of Transportation (April 1996).

6. Health & Safety Executive. *Risk Criteria for Land-Use Planning in the Vicinity of Major Industrial Hazards.* London, England: Her Majesty's Stationery Office (1989).

7. Groves, T.K., P.R. Bishnoi, and J.M.E. Wallbridge. "Decompression Wave Velocities in Natural Gases in Pipe Lines." *The Canadian Journal of Chemical Engineering* 56 (1978): 664-668.

8. McAllister, E.W. *Pipe Line Rules of Thumb Handbook.* Houston, TX: Gulf Publishing Company (1993).

9. Picard, D.J., and P.R. Bishnoi. "The Importance of Real-Fluid Behavior in Predicting Release Rates Resulting from High-Pressure Sour-Gas Pipeline Ruptures." *The Canadian Journal of Chemical Engineering* 67 (1989): 3-9.

10. Vennard, J.K., and R.L. Street. *Elementary Fluid Mechanics.* New York, NY: John Wiley & Sons (1982).

REFERENCES
(Continued)

11.   Wilson, D.J. *The Release and Dispersion of Gas from Pipeline Ruptures.* Edmonton, Alberta, Canada: Alberta Environment (1979).

12.   Wilson, D.J. *Expansion and Plume Rise of Gas Jets from High Pressure Pipeline Ruptures.* Edmonton, Alberta, Canada: Alberta Environment (1981).

13.   Wilson, D.J. *Predicting Risk of Exposure to Peak Concentrations in Fluctuating Plumes.* Edmonton, Alberta, Canada: Alberta Environment (1982).

14.   Fannelop, T.K., and I.L. Ryhming. "Massive Release of Gas from Long Pipelines." *J. Energy* 6 (1982): 132-140.

15.   Flatt, R. "A Singly-Iterative Second-Order Method of Characteristics for Unsteady Compressible One-Dimensional Flows." *Communications in Applied Numerical Methods* 1 (1985): 269-274.

16.   ----. "Unsteady Compressible Flow in Long Pipelines Following a Rupture." *International Journal for Numerical Methods in Fluids* 6 (1986): 83-100.

17.   Lang, E., and T.K. Fannelop. "Efficient Computation of the Pipeline Break Problem." *3rd Symposium on Fluid Transients in Fluid Structure Interaction.* ASME 56 (1987): 115-123.

18.   Ryhming, I. "On the Expansion Wave Problem in a Long Pipe with Wall Friction." *Journal of Applied Mathematics and Physics* 38 (1987): 378-390.

19.   Olorunmaiye, J.A., and N.E. Imide. "Computation of Natural Gas Pipeline Rupture Problems Using the Method of Characteristics." *Journal of Hazardous Materials.* 34 (1993): 81-98.

20.   National Fire Protection Association and Society of Fire Protection Engineers. *SFPE Handbook of Fire Protection Engineering.* Quincy, MA: National Fire Protection Association (1988).

21.   Hawthorne, W.R., D.S. Weddell, and H.C. Hottell. "Mixing and Combustion in Turbulent Gas Jets." *Third Symposium on Combustion, Flame and Explosion Phenomena.* Combustion Institute (1949): 266-288.

REFERENCES
(Continued)

22.   Gollahalli, S.R., T.A. Brzustowski, and H.F. Sullivan. "Characteristics of a Turbulent Propane Diffusion Flame in a Cross-Wind." *Transactions of the CSME* 3 (1975): 205-214.

23.   Kalghatgi, G.T. "The Visible Shape and Size of a Turbulent Hydrocarbon Jet Diffusion Flame in a Cross-wind." *Combustion and Flame* 52 (1983): 91-106.

24.   Oenbring, P.R., and T.R. Sifferman. "Flare Design...Are Current Methods Too Conservative?" *Hydrocarbon Processing* (May 1980): 124-129.

25.   Fumarola, G., D.M. De Faveri, R. Pastorino, and G. Ferraiolo. "Determining Safety Zones for Exposure to Flare Radiation." *I. Chem. E. Symposium Series No. 82* (1983): G23-G30.

26.   U.S. Environmental Protection Agency and the National Oceanic and Atmospheric Administration. *ALOHA User's Manual*. Washington, DC: U.S. Environmental Protection Agency (1992).

27.   Bakke, J.R., Dag Bjerketvedt, and Magne Bjorkhaug. "FLACS as a Tool for Safe Design Against Accidental Gas Explosions." *I. Chem. E. Symposium Series No. 122* (1990): 141-152.

28.   Raj, P.K., and J.A. Morris. "Computerized Spill Hazard Evaluation Models." *Journal of Hazardous Materials* 25 (1990): 77-92.

29.   Drivas, P.J., J.S. Sabnis, and L.H. Teuscher. "Model Simulates Pipeline, Tank-Storage Failures." *Oil & Gas Journal* (September 12, 1983): 162-169.

30.   Technica International Ltd. *WHAZAN User Guide*. March 1988.

31.   Hill, R.T., and J.R. Catmur. "Risks from Hazardous Pipelines in the United Kingdom." *HSE Contract Research Report No. 82/1994* (1995).

32   Hockey, S.M., and P.J. Rew. "Review of Human Response to Thermal Radiation." *HSE Contract Research Report No. 97/1996* (1996).

33.   Golub. E., J. Greenfeld, R. Dresnack, F.H. Griffis, and L.J. Pignataro. *Pipeline Accident Consequences for Natural Gas and Hazardous Liquid Transmission*. Draft report prepared by NJIT under Contract No. DTRS 56-94-C-0006 for the U.S. Department of Transportation (November 1995).

REFERENCES
(Continued)

34.   Center for Chemical Process Safety of the American Institute of Chemical
       Engineers. *Guidelines for Evaluating the Characteristics of Vapor Cloud
       Explosions, Flash Fires, and BLEVEs*. New York, NY: American Institute of
       Chemical Engineers (1994).

35.   American Petroleum Institute. *Guide for Pressure-Relieving and Depressuring
       Systems*. API Recommended Practice 521. Washington, DC: American
       Petroleum Institute (1990).

36.   Brzustowski, T.A., and E.C. Sommer, Jr. "Predicting Radiant Heating from
       Flares." From *Proceedings - Division of Refining*. Washington, DC: American
       Petroleum Institute 53 (1973): 865-893.

37.   Technica International Ltd. *WHAZAN Theory Manual*. March 1988.

38.   Crawley, F.K. "The Effects of the Ignition of a Major Fuel Spillage." *I. Chem. E.
       Symposium Series No. 71* (1982): 125-145.

39.   Lees, F.P. *Loss Prevention in the Process Industries*. Boston, MA: Butterworth
       Inc. (1980).

40.   Department of Housing and Urban Development. *Safety Considerations in Siting
       Housing Projects*. Washington, DC: Department of Housing and Urban
       Development (December 1975).

41.   Transportation Safety Board of Canada. *Transcanada Pipelines Limited Line
       300-1, Natural Gas Pipeline Rupture Kilometre Post MLV 302-1 +2.849 KM
       Marionville,Ontario 1705 EDT, 06 June 1990*. Hull, Quebec, Canada:
       Transportation Safety Board of Canada (1992).

42.   National Transportation Safety Board. *Northern Natural Gas Company Pipeline
       Puncture, Explosion and Fire Hudson, Iowa November 4, 1982*. Washington,
       DC: National Transportation Safety Board (1983).

43.   Transportation Safety Board of Canada. *Transcanada Pipelines Limited Natural
       Gas Pipeline Ruptures Main Line Valve 144-1 + 19.261 km Cardinal, Ontario 08
       December 1991*. Hull, Quebec, Canada: Transportation Safety Board of Canada
       (1994).

REFERENCES
(Continued)

44. National Transportation Safety Board. *Factual Pipeline Accident Report Basic Report (AR-01) FTW-79-F-P006 United Texas Transmission Co.* Washington, DC: National Transportation Safety Board (1979).

45. Transportation Safety Board of Canada. *Westcoast Energy Inc. 30-Inch Fort Nelson Main Line Natural Gas Pipeline Rupture Mile Post 102.6 Pink Mountain, British Columbia 1545 PDT, 06 October 1990.* Hull, Quebec, Canada: Transportation Safety Board of Canada (1993).

46. Transportation Safety Board of Canada. *Transcanada Pipelines Limited Natural Gas Pipeline Rupture Line 100-2, 914-Millimetre (36-Inch) Mainline Kilometre Post Main Line Valve 110-2 + 22.098 Kilometres Latchford, Ontario 23 July 1994.* Hull, Quebec, Canada: Transportation Safety Board of Canada (1995).

47. Transportation Safety Board of Canada. *Natural Gas Pipeline Rupture Foothills Pipe Lines (Sask.) Ltd. 1,067-Millimetre (42-Inch) Eastern Main Line Kilometre Post 66 + 041 Maple Creek, Saskatchewan 15 February 1994.* Hull, Quebec, Canada: Transportation Safety Board of Canada (1995).

48. Felder, R.M., and R.W. Rousseau. *Elementary Principles of Chemical Processes.* New York, NY: John Wiley & Sons (1978).

49. National Transportation Safety Board. *Arkla Energy Resources Pipeline Rupture & Fire Near Cale, Arkansas 02-24-86.* Washington, DC: National Transportation Safety Board accident file.

50. National Transportation Safety Board. *United Gas Pipe Line Company 20-Inch Pipeline Rupture and Fire Cartwright, Louisiana August 9, 1976.* Washington, DC: National Transportation Safety Board (1977).

51. National Transportation Safety Board. *Mobile Oil Corporation High-Pressure Natural Gas Pipeline, Near Houston, Texas September 9, 1969.* Washington, DC: National Transportation Safety Board (1971).

52. National Transportation Safety Board. *In the Matter of the Investigation of the Rupture and Fire Involving the Texas Eastern Gas Pipeline Company in Lancaster, Kentucky, on February 21, 1986.* Washington, DC: from the National Transportation Safety Board accident file (1986).

REFERENCES
(Continued)

53. National Transportation Safety Board. *Transcontinental Gas Pipe Line Corporation, 30-Inch Gas Transmission Pipeline Failure Near Bealeton, Virginia, June 9, 1974.* Washington, DC: National Transportation Safety Board (1975).

54. National Transportation Safety Board. *Pipeline Accident/Incident Summary Reports.* Washington, DC: National Transportation Safety Board (1986).

55. Bair, F.E. *The Weather Almanac.* Detroit, MI: Gale Research Inc. (1992).

56. Bagster, D.F., and R.M. Pitblado. "Thermal Hazards in the Process Industry." *Chemical Engineering Progress* (July 1989): 69-75.

57. Schwartz, R., and M. Keller. "Environmental Factors Vs. Flare Application." *CEP* (September 1977): 41-44.

58. Roberts, A.F. "The Effect of Conditions Prior to Loss of Containment on Fireball Behavior." I. *Chem. E. Symposium Series No. 71* (1982): 181-190.